Universidade do Porto

Faculdade de Engenharia

An injectable Sr-releasing hybrid system to promote bone regeneration

PhD Thesis

Ana Filipa Henriques Ferreira Lourenço

2018

Ana Filipa Henriques Ferreira Lourenço

An injectable Sr-releasing hybrid system to promote bone regeneration

Dissertação submetida à Faculdade de Engenharia da Universidade do Porto para obtenção do grau de Doutor em Engenharia Biomédica.

Supervisor: Maria Cristina de Castro Ribeiro

Categoria: Professor adjunto

Afiliação: Instituto de investigação e Inovação em Saúde/Instituto de Engenharia Biomédica (i3S/INEB); Instituto Superior de Engenharia do Porto (ISEP)

Co-supervisor: Cristina Maria Santos Alves de Carvalho Barrias

Categoria: Investigador principal

Afiliação: Instituto de investigação e Inovação em Saúde/Instituto de Engenharia Biomédica (i3S/INEB)

Funding

Thesis performed at INEB – Instituto de Engenharia Biomédica/ i3s – Instituto de Investigação e Inovação em Saúde.

This work was financed by FEDER - Fundo Europeu de Desenvolvimento Regional funds through the COMPETE 2020 - Operacional Programme for Competitiveness and Internationalisation (POCI), Portugal 2020, and by Portuguese funds through FCT - Fundação para a Ciência e a Tecnologia/ Ministério da Ciência, Tecnologia e Inovação in the framework of the project "Institute for Research and Innovation in Health Sciences" (POCI-01-0145-FEDER-007274) and project PTDC/CTM/103181/2008. AHL acknowledges FCT for PhD grant: SFRH/BD/87192/2012.

“Nada se ganha, nada se perde, tudo se transforma.”

Lei da conservação de massa, Lavoisier

Acknowledgements

Gostaria de agradecer em primeiro lugar às instituições que me acolheram (FEUP e INEB/i3S) e permitiram que desenvolvesse o trabalho aqui presente. Ao Prof. Mário Barbosa agradeço a possibilidade de integrar uma equipa como o grupo Microenvironments for New Therapies (INEB). Agradeço ao Prof. Fernando Jorge Monteiro por toda a sua ajuda e disponibilidade.

Gostaria de agradecer às minhas orientadoras por toda a ajuda e amparo que sempre me deram. Cristina Ribeiro, o meu mais profundo agradecimento por todas as suas palavras, que foram sempre de um carinho incrível. Agradeço todas as oportunidades que me deu de crescer, e agradeço principalmente a sua paciência. O seu coração do tamanho do mundo e a sua amabilidade para com todos são uma inspiração para mim. Cristina Barrias, muito obrigada pelo seu apoio constante, tanto a nível académico como pessoal. Estarei sempre disponível para fazer uma massagem. Muito obrigada às duas por aceitarem entrar comigo neste desafio.

A todos os que de alguma maneira contribuíram para esta tese, o meu mais sincero obrigado. Foi uma tarefa difícil, mas dos maiores investimentos e aprendizagens que já fiz. A todos os amigos que fiz no INEB, obrigada pelo companheirismo e pelas gargalhadas e por me acompanharem desde sempre. Definitivamente o caminho faz-se andando e vocês ajudaram a trilhar o meu caminho.

Sílvia, Raquelita e Keila muito obrigada por tudo o que me ensinaram.

Obrigada Estrelinha, Caty, Dani V, Dani Sousa, Ana Luísa, Bia, AR Bento, Ritinha, Fred, Ké, Aidinha, Mary Valente, Ana Freire, David Gomes, Janeca, Laúndos, L. Pires, Meriem, Ricardo Vidal, Ana Paula Filipe, Vasco, João Pedro Martins, Bernardo, Joana Silva, Rui Ribeiro, Tatiana, Cátia Lopes, Inês Estevão, Ana Paula Lima, Andreia Pereira, Patrícia Henriques, Mariana Neves, Chiara, Daniel Vasconcelos.

Um agradecimento especial aos meninos do laboratório: Andreia, Zé, João Brás, Xú, Morena, Dudu, Ana João, Mafalda, João Vasco, que fazem sempre tudo parecer melhor, que dão sempre uma ajuda e a quem nunca falta um sorriso. Muito obrigada mesmo!

Um obrigado especial ao Rúben. Foste um exemplo de dedicação e trabalho.

À minha Claudete, minha pequena Bey-sister, um obrigada especial pela tua ajuda, paciência e overall glamness.

Às meninas do prof. FJ: Ângela, Marta R, Tatiana, Lili G, Catarina Coelho, Joana Barros e Eri, muito obrigada pelo apoio e companhia, em especial para a Ângela, por seres o exemplo neste final complexo.

Aos que o meu coração escolheu ao pormenor, Sara, Francisca A, Filipa Sousa, Aninhas, D. Salvador, Grace, Luís Leitão, muito muito obrigada. As vossas palavras e apoio incondicionais foram o que me manteve à tona.

Às minhas garotas, Tininha e Idália, um obrigada por se manterem perto e me ajudarem a manter a sanidade e a perspectiva. À minha Sara Neto, obrigada por seres a minha amiga de sempre.

Aos meus pais, muito obrigada por todas as oportunidades que me proporcionaram e tudo o que me permitiram ser. Ao meu irmão, ensinaste-me mais do que o que imaginas e lembra-te que podes fazer tudo o que quiseres e que gosto de ti tal como és. Às minhas primas (Clarinha e Irene), são os meus exemplos. São vocês as minhas maiores incentivadoras e não teria conseguido chegar aqui sem vocês. Obrigada! À minha avó Micas um grande obrigada pelo teu amor. Para a árvore crescer tem que fortificar as raízes.

Publications

The work performed in the frame of this thesis resulted in the following publications:

A. Henriques Lourenço, A. L. Torres, D. P. Vasconcelos, C Ribeiro-Machado, J. N. Barbosa, M. A. Barbosa, C. C. Barrias, C. C. Ribeiro, Osteoimmunomodulatory properties of a strontium-rich injectable hybrid scaffold for bone repair (submitted) – *Chapter III*

A. Henriques Lourenço*, N. Neves*, C. Ribeiro-Machado, S.R. Sousa, M. Lamghari, C.C. Barrias, A. Trigo Cabral, M.A. Barbosa, C.C. Ribeiro, Injectable hybrid system for strontium local delivery promotes bone regeneration in a rat critical-sized defect model, Scientific Reports 7(1) (2017) 5098. (*equal contribution) – *Chapter IV*

Other publications complementary to the thesis:

C. Ribeiro-Machado, **A. Henriques Lourenço**, N. Neves, N. Alexandre, M. Lamghari, M. A. Barbosa, Cristina C. Ribeiro, Evaluation of an injectable hybrid system for strontium local delivery in a sheep vertebrae model (manuscript in preparation).

AHL contributed to data interpretation and manuscript revision.

L. M. Baptista, **A. Henriques Lourenço**, M. A. Barbosa, I. C. Gonçalves, C. C. Ribeiro, Antimicrobial properties of Sr-rich microspheres for bone regeneration (manuscript in preparation).

AHL contributed with microspheres preparation and revision of the manuscript.

Abstract

Injectable bone substitutes are very attractive for bone tissue regeneration/repair strategies, since they can be applied via minimally invasive surgical procedures and can perfectly fill irregular defects created in cases of trauma, tumor resection and bone pathologies, namely osteoporosis. These materials should combine adequate injectability and mechanical properties with the ability to induce new bone formation. Incorporating strontium (Sr) in biomaterials for bone substitution stands out as a promising strategy to achieve high local Sr concentrations at lesion sites and promote new bone formation, by taking advantage of its osteoanabolic and anti-osteoclastic activity. Furthermore, recent evidences of Sr immunomodulatory properties highlight an additional benefit for its use, as these might synergistically contribute to more efficient bone repair/regeneration.

In this context, the aim of the present work was to evaluate the *in vitro* and *in vivo* performance of a designed Sr-hybrid injectable system for bone regeneration, consisting of hydroxyapatite Sr-doped microspheres combined with an *in situ* crosslinkable Sr-alginate hydrogel. The system showed to be able to release clinically relevant Sr^{2+} amounts, providing a dual delivery, owing to the incorporation of Sr in both alginate and microspheres, with different release rates due to the different degradation kinetics of the polymer network (faster) and the ceramic particles (slower). *In vitro* results showed that the developed Sr-rich hybrid system was able to support mesenchymal stem cells (MSC) survival and osteogenic differentiation, with increase in alkaline phosphatase (ALP) activity, while inhibiting monocyte adhesion and osteoclast (OC) formation, with decreased tartrate-resistant acid phosphatase (TRAP) production. For *in vivo* studies, two different rodent models were used, to evaluate both the inflammatory response and the bone regeneration potential upon material implantation. To this end, an air-pouch model and critical-sized bone defect model were used, respectively, where non Sr-doped similar materials (Ca-hybrid system) and empty defects were used as controls. In the air-pouch model, an increase in $F4/80^{+}/CD206^{+}$ cells (M2 macrophages) in inflammatory exudates was observed upon Sr-hybrid implantation, as compared to the controls. Importantly, cytokine levels upon implantation were indicative of a mild inflammatory response when compared to Ca-hybrid system, with no increase in fibrous capsule thickness. The characteristic M2 macrophage phenotype observed is known to be pro-regenerative, namely by promoting angiogenesis and tissue repair. Furthermore, in the critical-sized bone defect model, the Sr-hybrid system led to higher material degradation with increased collagen

fibers deposition and new bone formation in the center of the defect, as opposed to bone formation restricted to the periphery in the control Ca-hybrid system. Furthermore, no alterations were observed in the Sr levels in systemic organs in both *in vivo* studies, assuring the safety of the proposed system regarding recent cardiovascular concerns of SrRan products. Most importantly, the hybrid system provided a scaffold for cell migration and offered structural support for tissue ingrowth, further improving effective local bone formation.

Overall, results obtained in this thesis suggest that the proposed hybrid system is able to modulate the inflammatory response, where Sr acts as a pro-resolution mediator through M2 macrophage polarization. Combined with the osteoanabolic and anti-osteoclastic activity of Sr, this leads to increased bone formation and enhanced osteointegration of the biomaterial. Therefore, this system might provide a promising multifunctional approach for bone regeneration, especially under osteoporotic conditions.

Resumo

Os materiais injetáveis constituem uma alternativa muito interessante para utilização em regeneração/reparação de tecido ósseo pois podem ser aplicados usando procedimentos cirúrgicos minimamente invasivos, permitindo preencher perfeitamente defeitos irregulares criados em casos de trauma, ressecção tumoral e patologias ósseas, nomeadamente osteoporose. Estes materiais devem combinar injectabilidade e propriedades mecânicas adequadas com a capacidade de induzir a formação de novo osso. A incorporação de estrôncio (Sr) em biomateriais para substituição óssea destaca-se como uma estratégia promissora, que permite obter elevadas concentrações locais de Sr no local da lesão e promover a formação de novo osso, beneficiando da atividade osteoanabólica e anti-osteoclástica deste elemento metálico. Para além disso, evidências recentes de propriedades imunomodulatórias associadas ao Sr, constituem um benefício adicional para a sua utilização, podendo assim contribuir sinergisticamente para uma reparação/regeneração óssea mais eficiente.

Neste contexto, o objectivo do presente trabalho foi avaliar o desempenho *in vitro* e *in vivo* de um sistema injectável híbrido rico em Sr para regeneração óssea, consistindo em microesferas de hidroxiapatite dopadas com Sr, combinadas com um hidrogel de alginato reticulado *in situ* também com Sr. O sistema mostrou ser capaz de libertar quantidades clinicamente relevantes de Sr^{2+}, fornecendo uma dupla entrega, em consequência da incorporação de Sr tanto no alginato como nas microesferas, com diferentes taxas de libertação devido às distintas cinéticas de degradação da rede polimérica (mais rápida) e das partículas cerâmicas (mais lenta). Resultados *in vitro* mostraram que o sistema híbrido desenvolvido rico em Sr, foi capaz de suportar a sobrevivência de células estaminais mesenquimatosas (MSC) e a sua diferenciação osteogénica, com aumento de actividade da fosfatase alcalina (ALP), inibindo a adesão de monócitos e formação de osteoclastos (OC), com diminuição da produção de fosfatase ácida resistente ao tartarato (TRAP). Foram realizados estudos *in vivo*, utilizando dois modelos animais distintos (bolsa de ar e defeito ósseo de tamanho crítico), com o objectivo de avaliar respectivamente a resposta inflamatória e o potencial de regeneração óssea após implantação do material. Nos estudos *in vivo* foram usados como controlos um material similar, não dopado com Sr (sistema Ca-híbrido), e defeitos vazios. No modelo de bolsa de ar, foi observado um aumento das células $F4/80^{+}/CD206^{+}$ (macrófagos M2) em exsudados inflamatórios após implantação do híbrido de Sr, relativamente aos controlos. Os níveis de citocinas após implantação indicaram uma reduzida resposta inflamatória comparativamente ao

verificado com o sistema híbrido de Ca, sem que tenha ocorrido aumento da espessura da cápsula fibrosa. Sabe-se que o fenótipo característico de macrófagos M2 é pró-regenerativo, promovendo a angiogénese e reparação de tecidos. Verificou-se igualmente que no modelo de defeito ósseo de tamanho crítico, o sistema híbrido de Sr levou a uma maior degradação do material com maior deposição de fibras de colagénio e formação de novo osso no centro do defeito, em oposição à formação óssea restrita à periferia, verificada no sistema híbrido de Ca usado como controlo. Para além disso não foram observadas alterações nos níveis de Sr em órgãos sistémicos em ambos os estudos *in vivo*, garantindo a segurança do sistema proposto em relação a preocupações cardiovasculares recentes, associadas à utilização de fármacos de Ranelato de Sr. Mais importante ainda, é de destacar o facto de o sistema híbrido ter fornecido um suporte estrutural que viabiliza a migração celular e o crescimento de tecido, melhorando a formação de novo osso.

Concluindo, os resultados obtidos nesta tese sugerem que o sistema híbrido proposto é capaz de modular a resposta inflamatória, onde o Sr atua como um mediador pró-resolução através da polarização de macrófagos M2. Este facto, combinado com a atividade osteoanabólica e anti-osteoclástica do Sr, leva ao aumento da formação óssea e melhora a osteointegração do biomaterial. Assim sendo, o sistema híbrido injetável rico em Sr estudado pode fornecer uma abordagem multifuncional deveras promissora para a regeneração óssea, especialmente em condições osteoporóticas.

Table of Contents

List of abbreviations

3D – three-dimensional

ALP – alkaline phosphatase activity

BC – buffy coats

BM – basal medium

BMMSC - bone marrow mesenchymal stem cells

BSA – bovine serum albumin

BV - bone volume

CD – cluster of differentiation

CSLM - confocal scanning laser microscope

DMEM - Dulbecco's modified eagle medium

DNA – deoxyribonucleic acid

ECM - extracellular matrix

EDS - energy-dispersive X-ray spectroscopy

EMA - European Medicines Agency

FACS - fluorescence-activated cell sorting

FBS - fetal bovine serum

GDL - glucone delta-lactone

GPC/SEC - gel permeation chromatography/size exclusion chromatography

H&E – hematoxylin and eosin

HAp - hydroxyapatite

ICP-AES - inductively coupled plasma - atomic emission spectroscopy

IL- interleukin

LG - light green

LOD - limit of detection

LOQ - limit of quantification

M-CSF - macrophage-colony stimulating factor

MicroCT – micro computerized tomography

MIP-1gamma - macrophage inflammatory protein 1 gamma

MSC - mesenchymal stem cells

MT - masson’s trichrome

NF-κB – nuclear factor kB

OC - osteoclasts

OM - osteogenic medium

PBMC - peripheral blood mononuclear cells

PBS - phosphate buffer saline

PFA - paraformaldehyde

PMN - polymorphonuclear neutrophils

PSR - picrosirius red

RANKL - receptor activator of nuclear factor-k

RANTES - regulated upon activation normal T cell expressed and secreted

RGD - arginine-glycine-aspartic acid peptide

ROI – region of interest

RT – room temperature

SEM - scanning electron microscopy

TBS - tris-buffered saline

TCPS – tissue culture polystyrene

TNF-RI - tumor necrosis factor receptor 1

TNF- tumor necrosis factor

TRAP – tartrate-resistant acid phosphatase

TV - total volume

UP - ultra-pure

VOI - volume of interest

α-MEM - α-minimal essential medium

β-TCP – β tricalcium phosphate

Chapter I

General Introduction

1. Bone composition and dynamics

1.1. Bone structure and composition

Bone is formed by specialized cells and a mineralized collagenous extracellular matrix (ECM) containing collagen type I, non-collagenous proteins and proteoglycans (organic part), along with calcium and phosphorus, arranged as hydroxyapatite nanocrystals (inorganic part). These nanocrystals are embedded in the collagenous matrix. Morphologically, bone presents two different types of architectures, designated as trabecular bone (spongy, cancellous) and compact bone (cortical) (Figure 1) [1]. Compact bone is characterized by a dense arrangement of osteons, concentric layers of collagen fibers (lamellae) surrounding a central canal (Haversian canal) that contains blood vessels and nerves. Compact bone has only aprox. 3–5% of voids and unique mechanical properties, accounting for nearly 80% of the total bone mass. Trabecular bone has high porosity (50-90%), where interstitial spaces are filled with bone marrow. The specific and hierarchical organization of bone tissue provides adequate mechanical properties, such as rigidity and strength, but also elasticity. Bone functions include locomotion, protection of vital organs, hematopoiesis and mineral homeostasis.

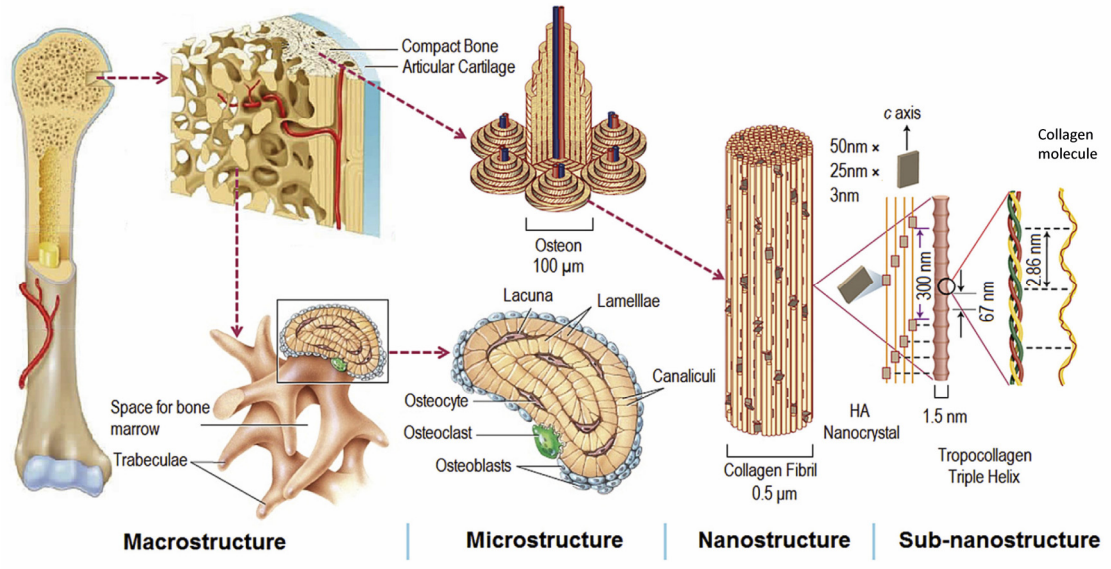

Figure 1 – Bone structure and composition [2]. At a nanostructure, bone is composed of collagen fibrils combined with hydroxyapatite nanocrystals and macrostructurally bone can be classified into trabecular bone or compact bone.

Bone structure is maintained through continuous formation and destruction of bone tissue by a balanced action of different cells that form the bone tissue. Bone cells include bone lining cells, osteoblasts, osteocytes, and osteoclasts (Figure 2). Bone

lining cells are quiescent flat-shaped osteoblastic cells covering the bone surface creating a functional barrier between bone and bone marrow. These cells also participate in bone remodeling by releasing matrix metalloproteinases that help upon osteoclastic degradation of the matrix and are thought also to deposit a thin layer of collagen before osteoblastic activity [3]. Osteoblasts are cuboidal cells located along the bone surface that secrete the osteoid, which will give raise to the bone matrix. These cells are responsible for bone formation and derive from mesenchymal stem/stromal cells (MSC). Several factors determine the commitment of MSC towards the osteoblastic lineage, in a timely programmed fashion, namely the expression of Runt-related transcription factors (Runx) 2 and osterix (Osx). Osteoblast progenitors exhibit alkaline phosphatase (ALP) activity and Osx and secrete bone matrix proteins such as osteocalcin (OCN), bone sialoprotein (BSP) I/II, and collagen type I [4]. They also initiate mineralization by secreting enzyme-rich vesicles that will accumulate inorganic ions and trigger the process [4]. During the final phase of bone remodeling, osteoblasts undergo apoptosis or become incorporated into the mineralized bone matrix as osteocytes. Osteocytes are stellate-shape cells that remain in contact with each other and with cells on the bone surface via gap junction-coupled cell processes. These cell processes pass through the matrix via small channels, the canaliculi, that connect the cell body-containing lacunae with each other and with exterior environment [5]. They are mechanosensory cells and play a pivotal role in functional adaptation of bone [5]. Osteoclasts are terminally differentiated multinucleated cells derived from pluripotent hematopoietic cells and are responsible for resorption of the mineralized bone matrix. Among the main factors influencing osteoclast differentiation are macrophage colony-stimulating factor (M-CSF), secreted by osteoprogenitor mesenchymal cells and osteoblasts, and receptor activator of nuclear factor κ B (RANK) ligand, secreted by osteoblasts, osteocytes, and stromal cells. When exposed to these factors, osteoclast precursors fuse and maturate into fully functional osteoclasts.

1.2. Bone Remodeling

Bone is a dynamic and metabolically active tissue, undergoing constant remodeling. The process of bone remodeling occurs in distinct stages, namely resorption and formation, consisting respectively on the removal of mineralized old bone and its replacement by an equivalent amount of new bone matrix, which then undergoes mineralization (Figure 2).

The removal of mineralized bone, or bone resorption, is performed by osteoclasts. These, migrate towards the bone surface to be resorbed, mainly adhering via interactions between integrin $\alpha_v\beta_3$ and bone matrix protein vitronectin. Afterwards, $\alpha_v\beta_3$ integrin-mediated binding promotes a cytoskeletal reorganization, comprising the formation of podosomes and the formation of an actin ring, which seals the area to be resorbed. Thereafter, osteoclasts develop ruffled border membranes at sites of active bone resorption [6, 7]. Ruffled borders are complex structures, rich in acidic vesicles with proton pumps and hydrolases, secreting H^+ and Cl^- ions through the ruffled border into the resorptive cavity, in order to lower the pH and dissolve the mineralized matrix. In addition, during bone resorption, osteoclasts secrete proteolytic enzymes, such as tartrate resistant acid phosphate (TRAP), cathepsin K and matrix metalloproteinase-9 (MMP-9) that digest collagen fibers and other matrix proteins, under acidic conditions. After resorption, bone debris is transported from the extracellular space under the ruffled border through the osteoclast, leaving the cell by transcytosis.

After bone has been resorbed, the process of bone formation begins, as osteoclasts stimulate osteoblasts to migrate into the area and start to produce new tissue, in order to fill the resorption pits. The resorption lacuna becomes filled with new bone (osteoid), which is gradually mineralized. As mineralization proceeds, osteoblasts become trapped within the matrix that they are producing, leading to their differentiation into osteocytes. Finally, bone formation/mineralization stops and bone lining cells remain in a quiescent state at the bone surface [8].

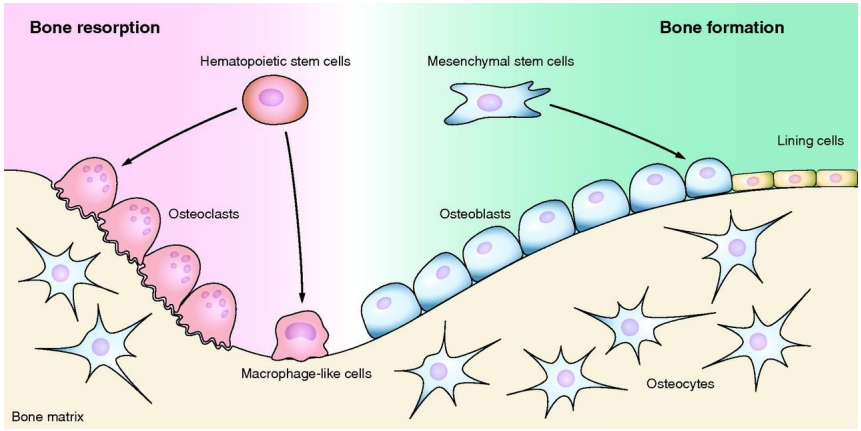

Figure 2 – Schematic representation of bone remodeling, bone cells and its precursors [9]. Bone resorption is performed by osteoclasts, derived from hematopoietic stem cells, whereas bone formation is accomplished by osteoclasts, derived from mesenchymal stem cells. Osteocytes are entrapped within the mineralized matrix with a stellate-shape and bone lining cells are present at the bone surface.

Although with distinct functions, there is a close interaction between the different bone cells and their progenitors. In particular, osteoblasts and osteoclasts activities are tightly regulated to ensure the maintenance of bone mass along remodeling [1, 10, 11]. Cells of the myeloid progenitor-macrophage-osteoclast and MSC-osteoblast differentiation axis modulate each other via different pathways, mainly paracrine. One example of these interactions is the RANKL/RANK/OPG system. RANKL is a TNF superfamily cell-surface cytokine expressed normally by osteoblasts and osteocytes and pathologically by lymphocytes. RANKL binds to RANK present in osteoclast precursors and dendritic cells, promoting osteoclasts survival and inducing their maturation and activation. Osteoprotegerin (OPG), a soluble decoy receptor produced by B cells, dendritic cells, MSCs, and osteoblasts, can block these effects through competitive binding with RANKL. Thus, the RANKL/OPG ratio is an important determinant in osteoclast activity [4].

1.3. Bone repair and regeneration

Upon injury, bone is able to heal to a certain extent without the formation of a scar, through a tightly orchestrated cascade of events (Figure 3) [12]. Immediately after trauma, a hematoma is formed and an acute inflammatory response is initiated, crucial for the regenerative process. The blood coagulation cascade is activated with the formation of a provisional fibrin matrix and activation of local macrophages [4]. The secretion of pro-inflammatory factors, such as tumor necrosis factor-α (TNF-α), interleukin-1 (IL-1), IL-6, IL-11 and IL-18, further recruits inflammatory cells and promotes angiogenesis. The acute inflammatory response peaks within the first 24 h and is completed after 7 days. Neutrophils and macrophages are recruited, the clearance of necrotic tissue occurs and a provisional matrix is formed [4]. In the second phase, MSC are recruited from the surrounding soft tissues, cortex, periosteum, bone marrow and systemic mobilization. MSC proliferate and differentiate into osteoblastic cells. Then, there is the formation of a cartilaginous soft callus, dependent on the recruitment of MSC, with production of a matrix rich in collagen-I and collagen-II, along with several signaling molecules. Afterwards, chondrocyte apoptosis and cartilaginous degradation allows for the blood vessel in-growth at the repair site, leading to proper revascularization and neoangiogenesis at the fracture site [12]. A hard callus is formed through mineralization and resorption of the soft callus, a process that combines cellular proliferation and differentiation, and increased matrix deposition. After this process, bone undergoes a remodeling process involving a balance between hard callus resorption by osteoclasts, and lamellar bone deposition by osteoblasts, a

process that is initiated after 3–4 weeks and can take up to several years to be completed [12].

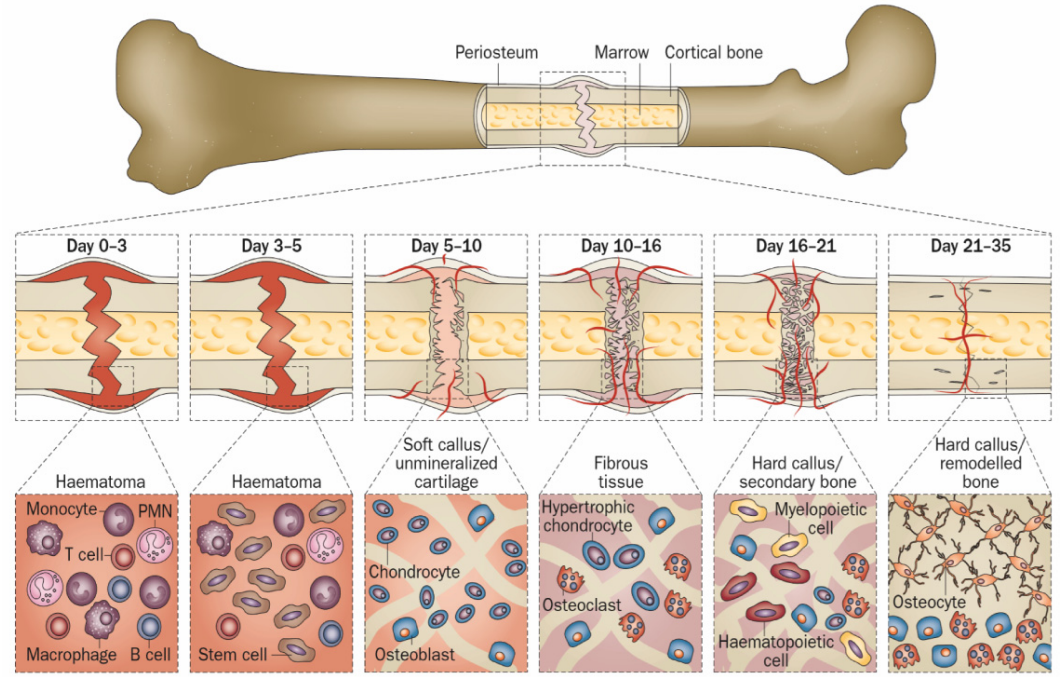

Figure 3 – Bone fracture repair [13]. Time frame and cellular players of the different phases of fracture repair.

Under normal physiological conditions, this process of bone repair and regeneration leads to the formation of new fully functional bone tissue, and to the reestablishment of bone structure and function. But the impairment of this cascade of events may lead to unsuccessful fracture healing and painful non-union fractures. Several factors can influence the success of this healing such as mechanical stability and relative proximity of the fracture ends, the influx of MSC/osteoprogenitor cells and inflammatory cells that regulate this process by secreting a repertoire of inflammatory and chemotactic mediators and growth factors [4]. Furthermore, other general conditions such as the presence of an infection, smoking, and other comorbidities such as diabetes mellitus or osteoporosis may also compromise the regeneration of the tissue, prompting medical intervention.

2. Bone repair/regeneration strategies: injectable bone substitutes

2.1. Immunomodulatory biomaterials

Current strategies for bone tissue repair/regeneration aim to achieve osteointegration of the implanted biomaterial, i.e., the complete integration of the material into the host bone tissue, without a fibrous interface, to fully restore bone architecture and functionality. For this purpose, the immune response to the material should not be overlooked, since inflammatory cellular and molecular interactions at the host-implant interface will determine the final outcome to a great extent [4]. As described previously, inflammation integrates the first stages of healing response to fractures, being also a key biological event upon biomaterial implantation. It represents a first-line protective response of the host and a favorable resolution towards tissue regeneration, dictating the final outcome and integration of the implant. A recent trend in the regenerative medicine field is the use of biomaterials that have favorable immunomodulatory properties and can shift the default response to a foreign body implant (i.e. scar tissue formation or fibrous encapsulation) towards one of tissue integration and functional remodeling. The default response to a foreign body (i.e., a biomaterial implant) commonly results in dense scar tissue formation surrounding and infiltrating the implant, limiting its interaction with the surrounding native tissue [14].

The immune response to a biomaterial implant begins with the innate immune system, which includes neutrophils and macrophages and the complex network of cytokines they release, which in turn triggers a cascade of diverse immune responders [14]. Macrophages can either reside in tissues, remnant from embryonic development, or circulate in peripheral blood as monocytes, that become activated and differentiate into macrophages following migration into inflamed tissue, where they exhibit a spectrum of transient polarization states related to their functional diversity [15]. At one end of the spectrum there is the pro-inflammatory M1 phenotype and at the other end there is the anti-inflammatory M2 phenotype.

The M1 phenotype (classically activated) emerges as a result of macrophage response to pro-inflammatory signals, such as interferon-γ (IFN-γ), and microbial products such as lipopolysaccharide (LPS). In the context of biomaterial implantation, while the initial presence of M1 macrophages promotes the necessary inflammatory response, a prolonged M1 presence leads to a severe foreign body reaction, characterized by

granuloma formation and fibrous encapsulation resulting in chronic inflammatory events and failure of biomaterial integration [15].

The M2 phenotype (alternatively activated) is the result of activation by signals (e.g., IL-4, IL-13) from basophils, mast cells and other granulocytes. M2 macrophages consistently express scavenger and mannose receptors (CD206), release anti-inflammatory cytokines such as IL-10, and encompass a range of different subsets (i.e., M2a, M2b, M2c). Within the M2 subsets, the M2a (induced by IL-4 and IL-13) and M2b (induced by immune complexes and Toll-like receptor (TLR) agonists) subsets perform immune regulatory functions by initiating Th2 lymphocyte anti-inflammatory responses (through the secretion of IL-10, IL-1ra and IL-6). Alternatively, the M2c subset is induced by IL-10 and plays a major role in tissue remodeling and suppression of inflammatory immune reactions by secreting transforming growth factor-β (TGF-β) and IL-10. The presence of such anti-inflammatory cytokines and the tissue remodeling response can aid in the vascularization of regenerative biomaterials by inhibiting fibrous tissue formation, which greatly improves the integration of the biomaterial and enables it to fulfill its intended function [15].

Therefore, the modulation of the immune response towards an M2 phenotype upon biomaterial implantation is desired, towards more efficient tissue regeneration strategies, which might be achieved using rationally designed immunomodulatory materials.

2.2. Requirements for bone substitute materials

In pathological conditions where bone repair and regeneration does not occur successfully, different strategies are being employed in the clinics, or are currently under research, to substitute the injured bone. Bone grafts and/or biomaterials are the most commonly used bone substitutes for the clinical management of bone lesions in traumatology, oncologic surgery, revision prosthetic surgery, spine surgery and dentistry [16, 17].

The available materials can be broadly categorized into natural bone-derived materials, artificial (based on ceramics, metals or polymers) or the combination of different materials (composite materials) [16]. Bone-derived materials can be autografts (same individual), allografts (cadaver, usually demineralized bone matrix) and xenografts (animal source, usually bovine or porcine bone).

The gold standard material used as bone substitute is the autologous bone graft, being osteoconductive, osteoinductive, and osteogenic (carrying osteogenic cells). The concepts of osteoconduction and osteoinduction regard the ability of a material to allow bone growth on its surface and into its pores/channels, and to stimulate the differentiation of progenitor cells into bone-forming cells, respectively [18]. Moreover, autologous grafts provide structural support without raising histocompatibility issues [17, 19]. However, bone grafting requires tissue harvesting at a secondary place, usually the iliac crest, which has associated risks, such as donor site morbidity and increased time of surgery. The shape and quantity of bone that can be harvested are also limiting factors. In addition, the harvest procedure can eventually lead to chronic pain, superficial infection, hematoma and nerve lesions, among others [19]. Other limitations of autologous bone grafts include the age, as in elderly or pediatric patients, and the presence of diseases, as in patients with malignant disease, that might lead to the failure of the autologous graft on clinical practice [20]. The problems associated with bone harvesting and the finite supply of this tissue has prompted the search for artificial materials as an alternative. The ideal bone substitute should not only provide mechanical stabilization, but also be osteoconductive, osteoinductive, osteogenic and an off-the-shelf product [16].

Bone substitutes can be synthesized in different formulations, but this thesis will focus on injectable bone substitutes, which can be used to fill-in irregular defects and be implanted via minimally invasive surgical interventions. They are particularly appealing since such procedures reduce patient discomfort and health costs, resulting also in reduced tissue damage and limited exposure to infectious agents [21, 22]. The degradation rate and biocompatibility of both the biomaterial and its degradation products should be carefully taken into account. Other requirements for these materials are sterilizability, adequate viscosity and ease of handling, and adequate setting conditions and time [22]. In general, synthetic bone substitutes show advantages over autografts and allografts in terms of unlimited supply, easy sterilization, and storage.

2.3. Ceramics

Calcium phosphate ceramics, such as hydroxyapatite (HAp) and tricalcium phosphate beta (β-TCP), have been widely studied as bone substitutes due to their similarity to the mineral phase of bone, biocompatibility, osteoconductivity and bioactivity [23]. Furthermore, these types of materials can easily be produced in large quantities at a low cost, being an off-the-shelf product. However, the main limitation of ceramic

materials is their brittle nature, relatively slow biodegradation and low mechanical strength limiting their application in bone tissue engineering, especially at load-bearing sites [23, 24]. High crystallinity, low porosity and small grain size tend to give higher stiffness, compressive and tensile strengths, and greater fracture toughness [24], achieved by sintering. Crystalline HAp exhibits the slowest degradation rate, compared with other calcium phosphates (Amorphous HAp > α-TCP>β-TCP>crystalline HAp).

For clinical use in orthopedics and dentistry, these materials are available as powders, granules, blocks and hydraulic cements, which are mixtures of calcium phosphates and water [23]. Ceramic blocks are hard and not easy to handle and to fit into irregular surgical places. The use of cements that harden *in situ* may be advantageous as injectable bone substitutes. However several parameters must be finely tuned. On one hand, pastes should have adequate rheological properties to be properly extruded by the physician through a cannula. On the other hand, the setting rate should be appropriate to allow the injection of the material, but still harden at adequate time for the surgeon to close the defect. However, the use of such pastes may lack adequate porosity for cell ingrowth and proper bone regeneration.

Particles or granules are frequently used, where the intergranular space can be rapidly invaded by newly-formed bone, and ceramic resorption can proceed fast and throughout the defect [25]. The size and shape of such particles dictate their spatial rearrangement at the implant site. Higher sphericity is associated with higher packing abilities and the use of spherical particles with uniform size leads to regular interparticular porosity (Figure 4A) [25]. This configuration is claimed to promote efficient osteoconduction. The use of particles with broader size distribution creates inhomogeneous and dense packing at the defect site, which might obstruct new tissue ingrowth and vascularization (Figure 4B). Irregular and dense particles may increase the inflammatory response [26, 27].

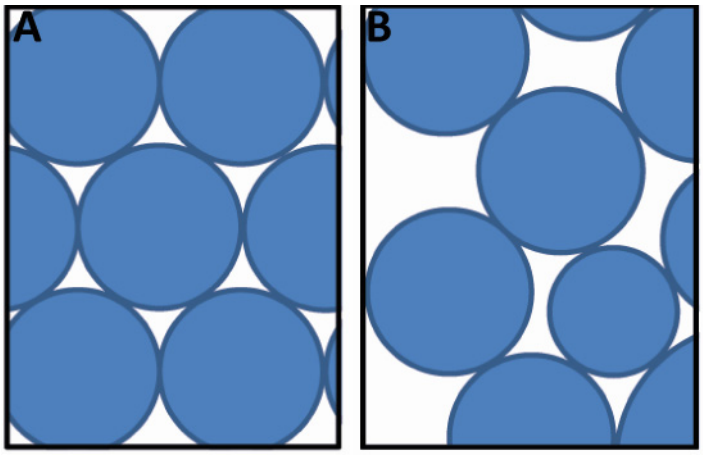

Figure 4 – Packing of spherical particles of different sizes. Adapted from [28].

The production of such spherical particles can be performed by numerous methods achieving several different ranges of diameters [25]. Importantly, the use of these microspheres in combination with hydrogels can improve cohesion of the particles. The lack of cohesion may lead to the leakage of particles to surrounding tissues, causing adverse reactions. Moreover, microspheres combined with a vehicle can be administered by injection using a narrow gauge needle, thus enabling the filling of defects of various shapes and sizes.

2.4. Hydrogels as bone substitutes

Hydrogels are polymeric materials with high water content, structured as hydrated three-dimensional (3D) networks that closely resemble the natural ECM. They can be of natural origin (e.g. alginate, chitosan, hyaluronate) or synthetic origin (e.g. poly(ethylene glycol) (PEG), poly(vinyl alcohol) (PVA)). Different strategies can be employed to obtain *in situ* crosslinking of an injectable hydrogel-precursor, through chemical or physical crosslinking mechanisms and/or different activation routes (e.g. ionic-, thermal- or photo-activation) [21]. The use of hydrogels for tissue regeneration strategies is very appealing since they act as 3D ECM-analogs that can be used as space filling agents, and delivery vehicles for bioactive molecules or even cells. Moreover, they are versatile and can be functionalized with specific bioactive cues to modulate cell behavior [29].

In the scope of this thesis, alginate hydrogels were used. Alginates are biodegradable and biocompatible natural polymers extracted from brown algae, extensively studied for biomedical applications [30, 31]. They are linear co-polymers composed of (1-4)-linked

β-D-mannuronic acid (M units) and α-L-guluronic acid (G units) monomers, arranged into M-blocks, G-blocks and/or MG-blocks, and are able to form hydrogels under mild conditions, in the presence of divalent cations through a cytocompatible physical gelation process. Cations, such as calcium (Ca) or strontium (Sr), cooperatively bind negatively-charged alginate chains, primarily between G-blocks, creating ionic interchain bridges which cause gelling of alginate solutions [31]. Alginate hydrogels are highly versatile, and different strategies can be used to modulate its biochemical and biophysical properties. While cells are not able to specifically interact with the alginate network, ‘‘bioactive’’ alginate derivatives can be easily obtained by chemical grafting of cell-instructive moieties, such as peptides. Peptide-grafted polysaccharides represent clear breakthrough alternatives for mimicking key features of the natural extracellular matrices. For instance, the grafting of arginine-glycine-aspartic acid (RGD) peptides to the polymer backbone by aqueous carbodiimide chemistry has been widely used as a strategy to provide appropriate guidance signals to promote cell adhesion and cell-matrix crosstalk [32-35].

However, as a hydrogel, alginate cannot meet the mechanical properties of bone tissue and therefore, the combination of ceramics and polymers have been used to fine tune properties such as injectability, setting time, porosity, mechanical properties and degradation time. Herein, we provide a brief overview on injectable bone substitutes based on hydrogel matrices combined with ceramic fillers.

2.5. Injectable hydrogel-ceramic hybrid materials

The combination of hydrogels and ceramics for bone regeneration strategies is a very interesting biomimetic approach since bone is, in fact, a composite material. The ceramic mimics the inorganic counterpart of bone, whilst the hydrogel creates a hydrated ECM-like matrix that acts as the organic part, permitting cell invasion and colonization. Furthermore, the use of *in situ* crosslinking hydrogels allows for the injectability of the composite material, with improved handling, while the ceramic provides mechanical reinforcement of the hydrogel properties. Several studies have used this approach, either using micro or nano-sized ceramic particles, as summarized in Table 1. In this way, ceramic particles cohesiveness is assured, during injection and after implantation in the bone defect.

A wide range of hydrogels have been considered for the production of polymer-ceramic composites, such as alginate [34, 36-42], chitosan [43-47], gelatin [48], different types

of cellulose and derivatives [49-53], hyaluronan [54-56] and fibrin [57], among others. Furthermore, different polymerization/crosslinking strategies have been used, for example to develop thermoresponsive and photosensitive hydrogels. The use of thermoresponsive hydrogels is very attractive due to sol-gel transition at body temperature, allowing gelation to occur *in situ* upon injection at the site of interest [43, 44, 47, 49, 52, 54]. Photosensitive hydrogels have also been used [48]. Although photopolymerization strategies are also interesting, by allowing for the spatial and temporal control over polymerization, with fast curing rates, there are some concerns regarding the light penetration, specially at deeper and in irregular sites.

Table 1. Injectable bone substitute based in reinforced hydrogels.

Hydrogel	Reinforcement	Size of particles	Additional bioactivity	Ref.
Alginate/ Alginate-based	Glass-reinforced HAp	granules of a 500–1000 μm size range		[40]
	microbeads of HAp, alginate + lactose-modified Chitosan/Silver Nanoparticles	average size of 990 ± 60 μm	Silver ions	[36]
	HAp and gelatin microspheres	HAp, particle size: 60 nm/ GM with drug with average size 10 um	Tetracycline hydrochloride	[42]
	HAp microspheres	500-560 um		[38]
	HAp microspheres	500-560 um	Sr ions	[34, 41]
	β-TCP	710－850 μm		[39]
	Calcium Silicate	100-150 μm	Silicon ions	[37]
Chitosan/ Chitosan-based	nanoHAp + collagen	nano-sized		[44]
	nanoHAp + collagen + Zinc	nano-sized	Zinc ions (Zinc dopped Chitosan)	[43]
	Bioactive glass nanoparticles	87±5 nm and predominant spherical shape		[45]
	tetracalcium phosphate (TTCP), dicalcium phosphate anhydrous (DCPA) and calcium sulfate hemihydrate (CSH)	1–50 μm		[47]
	HAp		MSC encapsulation	[46]

Gelatin methacryloyl	HAp and whitlochite	nanoparticles		[48]
Cellulose and derivatives	BCP	40–80 μm and 200–500 μm		[50, 53]
	CP nanoparticles	CaP NPs with a size in the range 40–50 nm		[52]
	bioceramic	1–50 μm.		[47, 49]
	BCP + Poly ε-caprolactone microspheres with vancomycin	80–200 μm granules of BCP, same for PCL	vancomycin	[51]
Hyaluronan-based	β-TCP	up to 1.4 mm	rhBMP-2 and DEX	[54]
	HAp + BMP-2	average particle size of 3.39 μm	BMP-2	[55]
	Octacalcium phosphate	diameters ranging from 300 to 500 μm		[56]
Fibrin	bTCP			[57]

The tuning of the injectability and cohesion of particles within the injectable material can also be achieved by varying the particle size and geometry. Different particle sizes have been used ranging from nano-sized up to 1.4 mm (Table 1). This aspect is of particular interest since the intergranular space should allow for blood vessel in-growth, and cellular infiltration, ultimately leading to ceramic resorption and bone ingrowth [25]. Injectability is defined as the mass of extrudate relative to the mass of the initial paste [28]. Several approaches can be used to optimize cohesion and injectability of these composite materials, namely: increase the hydrogel viscosity, since it improves the cohesion and reduces phase separation; use spherical particles and decrease its mean particle size [25]. As described in the previous section, the use of spherical particles is also particularly interesting since the uniform packing of the particles allows for the creation of adequate and defined intergranular space. Furthermore, the use of spherical particles leads to enhanced injectability compared to irregular particles [58] once smother surfaces may increase the flow of the composite.

The injectability of a composite biomaterial arises as the combination of the different parameters herein discussed, where the rheological properties of the composite should allow the injection through the cannula in a orthopedic surgery scenario with a force up to 100 N [59], limit commonly referred for manual procedures, filling the cavity without extravasation and providing adequate cohesion to prevent disintegration [28].

2.6. Injectable bone substitutes as controlled-release systems

The use of a carrier to deliver a bioactive compound has several advantages since it can downscale the dosages used, which have implications in the cost of the treatment. Moreover, the mechanical and chemical properties of the carrier may influence the release profile and bioactivity of the factor to be delivered, affecting its site-specific pharmacological action. For biodegradable materials, these properties are dynamic, changing with time, due to degradation and new tissue formation [55]. Moreover this strategy allows for *in situ*, localized delivery, reducing systemic exposure, while protecting the bioactive agent from clearance.

When using injectable hydrogel-ceramic composites both materials can be used as carriers for the delivery of bioactive agents, and different/combined release kinetics can be achieved, taking into account the properties of each material. Different strategies can be used for the incorporation of bioactive compounds in the system, namely covalent binding, physical entrapment or adsorption and incorporation into micro/nanospheres [60]. Also, hydrogels can physically slow down diffusion of both

hydrogel-entrapped and ceramic-associated drugs, therefore further modulating overall release kinetics [61]. The combination of different strategies enables better control over drug release profiles.

Combining osteoconductive materials with the delivery of osteoinductive factors is of particular interest, improving their potential for bone regeneration strategies. For instance, Petta and colleagues combined a hyaluronan-based/β-TCP composite with recombinant human bone morphogenetic protein-2 (rhBMP-2) and dexamethasone (DEX) [54]. The potency of BMP-2 in inducing bone is well recognized but, after years of clinical use, serious issues of efficacy and safety have been posed [62]. To accomplish its therapeutic action, rhBMP-2 needs to be released at the appropriate dose and time. Most of the observed issues arise from suboptimal administration, generally characterized by the use of high doses of rhBMP-2 over a short period of time. The composite presented in the above mentioned study was effective in slowing down the release of rhBMP-2 [54], increasing its therapeutic action as compared to the free compound. Stenfelt *et al* also described a study were BMP-2 was combined with an hyaluronan-based/HAp injectable bone substitute that effectively slowed down BMP-2 release [55].

Local delivery of antibiotics, such as vancomycin, using injectable bone substitutes has also been attempted to tackle infection-related problems such as osteomyelitis. Work from Iooss and coworkers have used poly(*ε*-caprolactone) encapsulated vancomycin in a biphasic calcium phosphate/hydroxypropyl methylcellulose (HPMC) injectable bone substitute. *In vitro* studies revealed that after 14 days, only 28% of vancomycin have been released showing the ability of the system to promote prolonged delivery [51]. Work from Yan and colleagues have used another antibiotic, tetracycline hydrochloride, encapsulated within gelatin microspheres, which were subsequently combined with an alginate/HAp composite to enhance bioactivity of the system. Comparing to hydrogel alone, the composite hydrogel scaffolds exhibited significantly delayed burst release behavior (46.4% released after 21days), suggesting that the combined system was more effective in modulating release kinetics [42]. In another work, the incorporation of antimicrobial Silver nanoparticles in an alginate-based/HAp material, was also evaluated as a strategy to tackle bone infection issues, with the system showing less than 6% of silver release after 1 week, *in vitro* [36].

Other works have used ion incorporation as a strategy to stimulate osteoblastogenesis, inhibiting osteoclastogenesis, such as zinc in a Chitosan-based/nanoHAp material [43]. In Dhivya et al work, the Zinc incorporation effect was not particularly studied, the focus

being made in the HAp reinforcement of chitosan injectable bone substitute. In our group, we developed a Sr rich hybrid material incorporating Sr both in alginate and HAp, in order to achieve a dual release strategy [34, 41]. The decision to incorporate Sr in the system relies on the growing evidence that this trace element has beneficial effects on bone remodeling and consequently may have potential benefits in the treatment of osteopenic disorders and osteoporosis [63]. *In vivo* studies showed that doping calcium phosphate cements and other ceramics with Sr promote bone repair [64-66].

Apart from delivering drugs, another application that raises great interest is to use injectable bone substitutes as cell delivery vehicles, namely for MSC. This might confer osteogenic capacity to the system, while improving the grafting potential of the delivered cells. In a study from Ressler et al, MSC combined with a chitosan/HAp composite were evaluated. Cells were homogeneously dispersed within the material and osteogenic differentiation of encapsulated MSC was confirmed *in vitro* [46].

In summary, different strategies can be used to achieve higher functionality of injectable biomaterials.

3. Strontium-based therapeutics and biomaterials

3.1. Sr as treatment for bone diseases

Osteoporosis is a systemic skeletal disease characterized by low bone density and microarchitectural deterioration of bone tissue. The consequent increase in bone fragility greatly increases the risk of fractures, which represent the major relevant clinical aspects of the disease. Osteoporosis affects mainly post-menopausal women but also men, in either primary or secondary forms. There are three major fracture sites in osteoporosis – the hip, the vertebrae, and the distal radius (although other sites can also be affected) [67]. Osteoporotic fractures represent an emerging medical and socioeconomic threat [68, 69]. The numbers are quite alarming and indicate that 50% of women and 20% of men with more than 50 years old are estimated to have a fragility fracture within their lifetime [68]. Women are particularly prone to this impairment due to estrogen deficiency at menopause, which induces imbalanced bone turnover with excessive bone resorption and insufficient bone formation [70, 71]. Aging is also associated with decreased bone formation relative to bone resorption, thereby

accentuating bone loss [72]. Extrinsic causes involved in the defective age-related bone formation include the decline in physical activity, insufficient protein intake, excessive alcohol and tobacco consumption and long-term glucocorticoid treatment [72].

Current therapy for osteoporosis includes dietary supplementation of calcium and vitamin D, in addition to treatments with pharmaceutical drugs [70, 73]. There are two main strategies for the treatment of osteoporosis, where the compounds can be categorized as being anti-resorptive drugs, which inhibit osteoclast differentiation or resorption efficiency, inducing their death; and anabolic agents, which will ultimately lead to an increased osteoblastogenesis [10]. Amongst the available drugs are bisphosphonates, parathyroide agonists, parathyroid antagonists, steroid hormones, selective estrogen receptor modulators (SERM), statins, monoclonal antibodies (denosumab, romosozumab, blosozumab), cathepsin K inhibitors and strontium ranelate [74].

Sr is a divalent alkaline earth metal from the second group of the periodic table, to which calcium (Ca) and magnesium (Mg) also belong. Sr is able to form divalent cations in biological fluids, having protein binding properties to serum or plasma of the same order of magnitude as Ca [75]. Sr uptake occurs mainly in food from vegetables and cereals, being however negligible when compared to Ca, and is excreted by the urine. Ca has a preferential absorption in the intestinal tract and renal tubular reabsorption than Sr (in part due to lower size of Ca) [75]. Stable Sr (^{84}Sr, ^{86}Sr, ^{87}Sr, ^{88}Sr) should not be confused with its radioactive isotopes (^{85}Sr, ^{87}mSr, ^{89}Sr, ^{90}Sr).

Administered Sr is almost exclusively deposited in bone, in small amounts [75]. Sr incorporation into the bone occurs by two mechanisms. One is the surface exchange or ionic substitution, by an initial rapid mode, where Sr, binding to pre-osteoid proteins, exchanges Ca, and the other is a slower mode involving the incorporation of Sr into the crystal lattice of the bone mineral. However, in the hydroxyapatite structure only a theoretical maximum of one Ca atom out of ten can be substituted by a Sr atom [73]. The uptake of Sr in old bone is mainly due to adsorption and exchanges at the crystal surface, whereas Sr taken up by heteroionic substitution during remodeling is more firmly linked to bone mineral substance [73]. Elimination of Sr from bone takes place by a combination of three different processes: clearance from exchangeable pools of bone, displacement of Sr, presumably by calcium, from sites within the apatite crystal, by long-term exchange processes, and volume removal from the mineral phase and the matrix by osteoclastic resorption [73].

Sr Ranelate (SrRan) has been used as a therapeutic strategy in osteoporosis due to its anti-resorptive and anabolic effect, as a dual-action drug [10, 63, 70, 74, 76-79]. SrRan is a compound with two atoms of stable Sr and ranelic acid that has been administered orally for many years. Clinical follow-ups confirmed its contribution to increase the bone mineral density and reduce the risk of fracture [67], and it has shown effectiveness in the prevention of both vertebral and non-vertebral osteoporotic fractures [80, 81]. It was found to act by dissociating bone resorption and bone formation *in vitro* through the activation of several signaling pathways in both osteoclasts and osteoblasts. These pharmacological effects were shown to translate into beneficial effects on bone mass, bone quality and bone resistance in osteopenic models and in osteoporotic patients [77].

Several *in vitro* studies have suggested that Sr, either in the form of SrRan or other Sr salts, has the potential to increase the proliferation and differentiation of osteoblasts, osteoprogenitors and MSC [82-95]. Moreover, Sr has been shown to inhibit the formation, maturation and resorptive behavior of OC [84, 96-98].

Some pre-clinical studies performed in both normal and osteopenic/osteoporotic animal models confirmed these *in vitro* results, showing the beneficial effects of SrRan on bone formation and remodeling, with an increase in bone mass and bone strength [99-103]

Although it has not yet been fully understood, several molecular targets and action mechanisms of Sr in bone have already been proposed. Due to Sr similarity to Ca it is supposed that they play a role in similar cellular targets. Sr binds to calcium-sensing receptor (CaSR, a G-protein coupled receptor) activating its downstream effectors leading to osteoblast proliferation, differentiation and survival, and inducting apoptosis in osteoclasts. Sr induces increased production of nuclear factor of activated Tc (NFATc)/Wnt signaling, prostaglandin E2 (PGE2), activation of fibroblast growth factor receptor (FGFR) in osteoblastic cells, and reduction of sclerostin expression (a Wnt antagonist produced by osteocytes) [104]. Sr also plays a role in the RANK/RANKL/OPG system. The receptor activator of nuclear factor-kappaB ligand (RANKL) binds RANK expressed on osteoclast precursor cells and thereby promotes signaling leading to increased osteoclast differentiation. Sr reduces RANKL expression and increases the expression of osteoprotegerin (OPG) by osteoblasts/stromal cells, a decoy soluble factor that antagonises the soluble RANKL, resulting in reduced pre-osteoclast differentiation into osteoclasts [72].

However, recent reports have shown a small but significant increase in non-fatal myocardial infarctions upon oral administration of SrRan [81, 105-107]. Therefore, SrRan is now contraindicated in patients with a history of cardiovascular disease, i.e. in patients with a history of ischaemic heart disease, peripheral artery disease, and/or cerebrovascular disease and in those with uncontrolled hypertension [81, 107].

3.2. Sr-based biomaterials for bone regeneration

Alternatively to the oral administration of SrRan, the use of biomaterial-based systems able to promote Sr local delivery in bone tissue may be advantageous, surpassing therefore systemic effects. Several *in vitro* studies have shown an osteoinductive effect of Sr when incorporated into different types of biomaterials [64-66, 108-112]. Also, *in vivo* studies, using mainly Sr-rich phosphate cements or Sr-doped HAp, revealed enhanced local bone formation both at the center and surface of the implant [64, 113]. Banerjee *et al* studied the effect of doping ß-TCP with MgO/SrO on bone formation in Sprague-Dawley rats [114]. Doped ß-TCP promoted more osteogenesis and faster bone formation than pure ß-TCP. In critical calvaria defects of an ovariectomized rat model, macroporous Sr-substituted scaffolds showed superior osteoinductive activity to enhance early bone formation, and could also stimulate angiogenesis compared with calcium silicate scaffolds [115]. A recent systematic review from Neves *et al*, showed that all the *in vivo* works described in the literature presented similar or increased effect of Sr in bone formation and/or regeneration, in both healthy and osteoporotic models. No study found a decreased effect [116]. This review revealed the safety and effectiveness of Sr-enriched biomaterials for stimulating bone formation and remodeling in animal models. The effect seems to increase over time and is impacted by the concentration used. In an era of rising medical and socioeconomic challenges of an aging population, where deficient bone healing is expected to occur, when native bone does not provide an optimal structure for surgical implantation procedures, osseointegration-stimulating properties of a bone substitute are of particular interest. Furthermore, the combination of Sr beneficial effects, by a sustained delivery system for local release of Sr ions, can surpass systemic complications with similar rates of bone formation at the site of implantation.

Moreover, and as already described previously, a recent area of research has been emerging in the biomaterials field, with the design of immunomodulatory materials able to regulate the host inflammatory response [117]. Although scarce, recent evidences have shown that Sr may have the potential to modulate the polarization of

macrophages towards an M2 phenotype [118-120]. In studies of Yuan and coworkers, modification of titanium surfaces with Ca and Sr, either alone or in combination at different Ca:Sr ratios, have shown that the presence of Sr was able to increase the number of M2 macrophages in an *in vivo* model, although no differences were seen between coatings of Ca and Sr alone [118]. Another work showed that a Sr-substituted sub-micron bioactive glass (SBG) significantly increased the number of M2 macrophages as compared to bare SBG, *in vivo* [119]. In studies from Zhao and colleagues, Sr in the form of Sr-substituted bioactive glass microspheres and Sr chloride (control) was shown to promote M1 to M2 polarization in a murine macrophage cell line using after 3 days of culture. An increased number of M2 macrophages ($CD206^+$ and arginase I^+) was also detected upon implantation of the Sr-substituted material at a bone augmentation model comparing to a non Sr substituted material [120].

References

[1] P.A. Downey, M.I. Siegel, Bone Biology and the Clinical Implications for Osteoporosis, Physical Therapy 86(1) (2006) 77-91.
[2] X. Wang, S. Xu, S. Zhou, W. Xu, M. Leary, P. Choong, M. Qian, M. Brandt, Y.M. Xie, Topological design and additive manufacturing of porous metals for bone scaffolds and orthopaedic implants: A review, Biomaterials 83 (2016) 127-141.
[3] M.N. Wein, Bone Lining Cells: Normal Physiology and Role in Response to Anabolic Osteoporosis Treatments, Curr Mol Bio Rep (2017) 3: 79. (2017).
[4] F. Loi, L.A. Córdova, J. Pajarinen, T.-h. Lin, Z. Yao, S.B. Goodman, Inflammation, fracture and bone repair, Bone 86 (2016) 119-130.
[5] E.M. Aarden, P.J. Nijweide, E.H. Burger, Function of osteocytes in bone, Journal of Cellular Biochemistry 55(3) (1994) 287-299.
[6] S.L. Teitelbaum, Osteoclasts: What Do They Do and How Do They Do It?, The American Journal of Pathology 170(2) (2007) 427-435.
[7] S.L. Teitelbaum, Bone Resorption by Osteoclasts, Science 289(5484) (2000) 1504-1508.
[8] L.G. Raisz, Physiology and Pathophysiology of Bone Remodeling, Clinical Chemistry 45(8) (1999) 1353-1358.
[9] Y. Imai, M.-Y. Youn, K. Inoue, I. Takada, A. Kouzmenko, S. Kato, Nuclear Receptors in Bone Physiology and Diseases, Physiological Reviews 93(2) (2013) 481-523.
[10] G. Mazziotti, J. Bilezikian, E. Canalis, D. Cocchi, A. Giustina, New understanding and treatments for osteoporosis, Endocrine 41(1) (2012) 58-69.
[11] S.C. Manolagas, R.L. Jilka, Bone marrow, cytokines, and bone remodeling. Emerging insights into the pathophysiology of osteoporosis, The New England journal of medicine 332(5) (1995) 305-311.
[12] R. Marsell, T.A. Einhorn, THE BIOLOGY OF FRACTURE HEALING, Injury 42(6) (2011) 551-555.
[13] T.A. Einhorn, L.C. Gerstenfeld, Fracture healing: mechanisms and interventions, Nature Reviews Rheumatology 11 (2014) 45.
[14] J.L. Dziki, S.F. Badylak, Immunomodulatory biomaterials, Current Opinion in Biomedical Engineering 6 (2018) 51-57.
[15] R. Sridharan, A.R. Cameron, D.J. Kelly, C.J. Kearney, F.J. O'Brien, Biomaterial based modulation of macrophage polarization: a review and suggested design principles, Materials Today 18(6) (2015) 313-325.
[16] V. Campana, G. Milano, E. Pagano, M. Barba, C. Cicione, G. Salonna, W. Lattanzi, G. Logroscino, Bone substitutes in orthopaedic surgery: from basic science to clinical practice, Journal of Materials Science. Materials in Medicine 25(10) (2014) 2445-2461.
[17] F. Y., J. J., Bone grafts and their substitutes, The Bone & Joint Journal 98-B(1_Supple_A) (2016) 6-9.
[18] T. Albrektsson, C. Johansson, Osteoinduction, osteoconduction and osseointegration, European Spine Journal 10(2) (2001) S96-S101.
[19] K. T., P.R. G., S.B. E., Bone graft substitutes currently available in orthopaedic practice, The Bone & Joint Journal 95-B(5) (2013) 583-597.
[20] P.V. Giannoudis, H. Dinopoulos, E. Tsiridis, Bone substitutes: An update, Injury 36(3, Supplement) (2005) S20-S27.
[21] J.D. Kretlow, L. Klouda, A.G. Mikos, Injectable matrices and scaffolds for drug delivery in tissue engineering, Advanced Drug Delivery Reviews 59(4) (2007) 263-273.
[22] J.S. Temenoff, A.G. Mikos, Injectable biodegradable materials for orthopedic tissue engineering, Biomaterials 21(23) (2000) 2405-2412.
[23] L.K. Ling, T.S. Huat, Z.S.H. Sharif, R.J. A., M. Viviana, B.A. R., Calcium phosphate-based composites as injectable bone substitute materials, Journal of Biomedical Materials Research Part B: Applied Biomaterials 94B(1) (2010) 273-286.

[24] K. Rezwan, Q.Z. Chen, J.J. Blaker, A.R. Boccaccini, Biodegradable and bioactive porous polymer/inorganic composite scaffolds for bone tissue engineering, Biomaterials 27(18) (2006) 3413-3431.
[25] M. Bohner, S. Tadier, N. van Garderen, A. de Gasparo, N. Döbelin, G. Baroud, Synthesis of spherical calcium phosphate particles for dental and orthopedic applications, Biomatter 3(2) (2013) e25103.
[26] D.J. Misiek, J.N. Kent, R.F. Carr, Soft tissue responses to hydroxylapatite particles of different shapes, Journal of Oral and Maxillofacial Surgery 42(3) (1984) 150-160.
[27] M.P. Ginebra, M. Espanol, E.B. Montufar, R.A. Perez, G. Mestres, New processing approaches in calcium phosphate cements and their applications in regenerative medicine, Acta Biomaterialia 6(8) (2010) 2863-2873.
[28] R. O'Neill, H.O. McCarthy, E.B. Montufar, M.P. Ginebra, D.I. Wilson, A. Lennon, N. Dunne, Critical review: Injectability of calcium phosphate pastes and cements, Acta Biomaterialia 50 (2017) 1-19.
[29] J.L. Drury, D.J. Mooney, Hydrogels for tissue engineering: Scaffold design variables and applications, Biomaterials 24(24) (2003) 4337-4351.
[30] K.Y. Lee, D.J. Mooney, Alginate: Properties and biomedical applications, Progress in Polymer Science 37(1) (2012) 106-126.
[31] J.A. Rowley, G. Madlambayan, D.J. Mooney, Alginate hydrogels as synthetic extracellular matrix materials, Biomaterials 20(1) (1999) 45-53.
[32] S.J. Bidarra, C.C. Barrias, K.B. Fonseca, M.A. Barbosa, R.A. Soares, P.L. Granja, Injectable in situ crosslinkable RGD-modified alginate matrix for endothelial cells delivery, Biomaterials 32(31) (2011) 7897-7904.
[33] M.B. Evangelista, S.X. Hsiong, R. Fernandes, P. Sampaio, H.J. Kong, C.C. Barrias, R. Salema, M.A. Barbosa, D.J. Mooney, P.L. Granja, Upregulation of bone cell differentiation through immobilization within a synthetic extracellular matrix, Biomaterials 28(25) (2007) 3644-3655.
[34] A. Henriques Lourenço, N. Neves, C. Ribeiro-Machado, S.R. Sousa, M. Lamghari, C.C. Barrias, A. Trigo Cabral, M.A. Barbosa, C.C. Ribeiro, Injectable hybrid system for strontium local delivery promotes bone regeneration in a rat critical-sized defect model, Scientific Reports 7(1) (2017) 5098.
[35] F.R. Maia, A.H. Lourenço, P.L. Granja, R.M. Gonçalves, C.C. Barrias, Effect of Cell Density on Mesenchymal Stem Cells Aggregation in RGD-Alginate 3D Matrices under Osteoinductive Conditions, Macromolecular Bioscience (2014) n/a-n/a.
[36] P. Davide, T. Andrea, T. Gianluca, C. Matteo, B. Massimiliano, D. Ivan, P. Sergio, A. Gianpiero, M. Eleonora, Antibacterial-nanocomposite bone filler based on silver nanoparticles and polysaccharides, Journal of Tissue Engineering and Regenerative Medicine 12(2) (2018) e747-e759.
[37] Y. Han, Q. Zeng, H. Li, J. Chang, The calcium silicate/alginate composite: Preparation and evaluation of its behavior as bioactive injectable hydrogels, Acta Biomaterialia 9(11) (2013) 9107-9117.
[38] O.S. M., B.C. C., A.I. F., C.P. C., F.M.R. Pena, B.M. F., B.M. A., Injectability of a bone filler system based on hydroxyapatite microspheres and a vehicle with in situ gel-forming ability, Journal of Biomedical Materials Research Part B: Applied Biomaterials 87B(1) (2008) 49-58.
[39] T. Matsuno, Y. Hashimoto, S. Adachi, K. Omata, Y. Yoshitaka, Y. Ozeki, Y. Umezu, Y. Tabata, M. Nakamura, T. Satoh, Preparation of injectable 3D-formed β-tricalcium phosphate bead/alginate composite for bone tissue engineering, Dental Materials Journal 27(6) (2008) 827-834.
[40] D.S. Morais, M.A. Rodrigues, T.I. Silva, M.A. Lopes, M. Santos, J.D. Santos, C.M. Botelho, Development and characterization of novel alginate-based hydrogels as vehicles for bone substitutes, Carbohydrate Polymers 95(1) (2013) 134-142.
[41] N. Neves, B.B. Campos, I.F. Almeida, P.C. Costa, A.T. Cabral, M.A. Barbosa, C.C. Ribeiro, Strontium-rich injectable hybrid system for bone regeneration, Materials Science and Engineering: C 59 (2016) 818-827.

[42] J. Yan, Y. Miao, H. Tan, T. Zhou, Z. Ling, Y. Chen, X. Xing, X. Hu, Injectable alginate/hydroxyapatite gel scaffold combined with gelatin microspheres for drug delivery and bone tissue engineering, Materials Science and Engineering: C 63 (2016) 274-284.
[43] S. Dhivya, S. Saravanan, T.P. Sastry, N. Selvamurugan, Nanohydroxyapatite-reinforced chitosan composite hydrogel for bone tissue repair in vitro and in vivo, Journal of Nanobiotechnology 13(1) (2015) 40.
[44] Z. Huang, J. Tian, B. Yu, Y. Xu, Q. Feng, A bone-like nano-hydroxyapatite/collagen loaded injectable scaffold, Biomedical materials (Bristol, England) 4(5) (2009) 055005.
[45] C.D.F. Moreira, S.M. Carvalho, H.S. Mansur, M.M. Pereira, Thermogelling chitosan–collagen–bioactive glass nanoparticle hybrids as potential injectable systems for tissue engineering, Materials Science and Engineering: C 58 (2016) 1207-1216.
[46] A. Ressler, J. Ródenas-Rochina, M. Ivanković, H. Ivanković, A. Rogina, G.G. Ferrer, Injectable chitosan-hydroxyapatite hydrogels promote the osteogenic differentiation of mesenchymal stem cells, Carbohydrate Polymers.
[47] H.-Y. Song, A.H.M. Esfakur Rahman, B.-T. Lee, Fabrication of calcium phosphate-calcium sulfate injectable bone substitute using chitosan and citric acid, Journal of Materials Science: Materials in Medicine 20(4) (2009) 935-941.
[48] H. Cheng, R. Chabok, X. Guan, A. Chawla, Y. Li, A. Khademhosseini, H.L. Jang, Synergistic interplay between the two major bone minerals, hydroxyapatite and whitlockite nanoparticles, for osteogenic differentiation of mesenchymal stem cells, Acta Biomaterialia 69 (2018) 342-351.
[49] E.D. Demir Oğuz Ö, Rheological and Mechanical Properties of Thermoresponsive Methylcellulose/Calcium Phosphate-Based Injectable Bone Substitutes., Materials Today 11(4):604. (2018).
[50] O. Gauthier, J.M. Bouler, P. Weiss, J. Bosco, G. Daculsi, E. Aguado, Kinetic study of bone ingrowth and ceramic resorption associated with the implantation of different injectable calcium-phosphate bone substitutes, Journal of biomedical materials research 47(1) (1999) 28-35.
[51] P. Iooss, A.M. Le Ray, G. Grimandi, G. Daculsi, C. Merle, A new injectable bone substitute combining poly(ε-caprolactone) microparticles with biphasic calcium phosphate granules, Biomaterials 22(20) (2001) 2785-2794.
[52] M.H. Kim, B.S. Kim, H. Park, J. Lee, W.H. Park, Injectable methylcellulose hydrogel containing calcium phosphate nanoparticles for bone regeneration, International Journal of Biological Macromolecules 109 (2018) 57-64.
[53] G. O., K. I., B. J., O. L., B. X., R. C., M. D., B.J. M., A. E., D. G., W. P., Noninvasive bone replacement with a new injectable calcium phosphate biomaterial, Journal of Biomedical Materials Research Part A 66A(1) (2003) 47-54.
[54] D. Petta, G. Fussell, L. Hughes, D.D. Buechter, C.M. Sprecher, M. Alini, D. Eglin, M. D'Este, Calcium phosphate/thermoresponsive hyaluronan hydrogel composite delivering hydrophilic and hydrophobic drugs, Journal of Orthopaedic Translation 5 (2016) 57-68.
[55] S. Stenfelt, G. Hulsart-Billström, L. Gedda, K. Bergman, J. Hilborn, S. Larsson, T. Bowden, Pre-incubation of chemically crosslinked hyaluronan-based hydrogels, loaded with BMP-2 and hydroxyapatite, and its effect on ectopic bone formation, Journal of Materials Science: Materials in Medicine 25(4) (2014) 1013-1023.
[56] K. Suzuki, T. Anada, T. Miyazaki, N. Miyatake, Y. Honda, K.N. Kishimoto, M. Hosaka, H. Imaizumi, E. Itoi, O. Suzuki, Effect of addition of hyaluronic acids on the osteoconductivity and biodegradability of synthetic octacalcium phosphate, Acta Biomaterialia 10(1) (2014) 531-543.
[57] S. Reppenhagen, J.C. Reichert, L. Rackwitz, M. Rudert, P. Raab, G. Daculsi, U. Nöth, Biphasic bone substitute and fibrin sealant for treatment of benign bone tumours and tumour-like lesions, International Orthopaedics 36(1) (2012) 139-148.

[58] K. Ishikawa, S. Matsuya, M. Nakagawa, K. Udoh, K. Suzuki, Basic properties of apatite cement containing spherical tetracalcium phosphate made with plasma melting method, Journal of Materials Science: Materials in Medicine 15(1) (2004) 13-17.
[59] J.K.S.J.F.M.B.G.B.T.S.P.F. Heini, Clinical Measurements of Cement Injection Pressure During Vertebroplasty, Spine. 30(5):E118-E122 (2005).
[60] T.-M. De Witte, L.E. Fratila-Apachitei, A.A. Zadpoor, N.A. Peppas, Bone tissue engineering via growth factor delivery: from scaffolds to complex matrices, Regenerative Biomaterials (2018) rby013-rby013.
[61] A. Vashist, A. Vashist, Y.K. Gupta, S. Ahmad, Recent advances in hydrogel based drug delivery systems for the human body, Journal of Materials Chemistry B 2(2) (2014) 147-166.
[62] J.W. Hustedt, D.J. Blizzard, The Controversy Surrounding Bone Morphogenetic Proteins in the Spine: A Review of Current Research, The Yale Journal of Biology and Medicine 87(4) (2014) 549-561.
[63] P.J. Marie, P. Ammann, G. Boivin, C. Rey, Mechanisms of Action and Therapeutic Potential of Strontium in Bone, Calcified Tissue International 69(3) (2001) 121-129.
[64] M. Baier, P. Staudt, R. Klein, U. Sommer, R. Wenz, I. Grafe, P.J. Meeder, P.P. Nawroth, C. Kasperk, Strontium enhances osseointegration of calcium phosphate cement: a histomorphometric pilot study in ovariectomized rats, Journal of Orthopaedic Surgery and Research 8(1) (2013) 16.
[65] G. Hulsart-Billström, W. Xia, E. Pankotai, M. Weszl, E. Carlsson, C. Forster-Horváth, S. Larsson, H. Engqvist, Z. Lacza, Osteogenic potential of Sr-doped calcium phosphate hollow spheres in vitro and in vivo, Journal of Biomedical Materials Research Part A 101A(8) (2013) 2322-2331.
[66] U. Thormann, S. Ray, U. Sommer, T. ElKhassawna, T. Rehling, M. Hundgeburth, A. Henß, M. Rohnke, J. Janek, K.S. Lips, C. Heiss, G. Schlewitz, G. Szalay, M. Schumacher, M. Gelinsky, R. Schnettler, V. Alt, Bone formation induced by strontium modified calcium phosphate cement in critical-size metaphyseal fracture defects in ovariectomized rats, Biomaterials 34(34) (2013) 8589-8598.
[67] L. Cianferotti, F. D'Asta, M.L. Brandi, A review on strontium ranelate long-term antifracture efficacy in the treatment of postmenopausal osteoporosis, Therapeutic Advances in Musculoskeletal Disease 5(3) (2013) 127-139.
[68] P. Sambrook, C. Cooper, Osteoporosis, The Lancet 367(9527) (2006) 2010-2018.
[69] T.D. Rachner, S. Khosla, L.C. Hofbauer, Osteoporosis: now and the future, The Lancet 377(9773) 1276-1287.
[70] P.J. Marie, Strontium as therapy for osteoporosis, Current Opinion in Pharmacology 5(6) (2005) 633-636.
[71] S. Roux, New treatment targets in osteoporosis, Joint Bone Spine 77(3) (2010) 222-228.
[72] Z. Saidak, P.J. Marie, Strontium signaling: Molecular mechanisms and therapeutic implications in osteoporosis, Pharmacology & Therapeutics 136(2) (2012) 216-226.
[73] S.G. Dahl, P. Allain, P.J. Marie, Y. Mauras, G. Boivin, P. Ammann, Y. Tsouderos, P.D. Delmas, C. Christiansen, Incorporation and distribution of strontium in bone, Bone 28(4) (2001) 446-53.
[74] A. Moshiri, A.M. Sharifi, A. Oryan, Current Knowledge, Drug-Based Therapeutic Options and Future Directions in Managing Osteoporosis, Clinical Reviews in Bone and Mineral Metabolism 15(1) (2017) 1-23.
[75] S. Pors Nielsen, The biological role of strontium, Bone 35(3) (2004) 583-588.
[76] P.J. Marie, Optimizing bone metabolism in osteoporosis: insight into the pharmacologic profile of strontium ranelate, Osteoporos Int 14 Suppl 3 (2003) S9-12.
[77] P.J. Marie, Strontium ranelate: a novel mode of action optimizing bone formation and resorption, Osteoporos Int 16 Suppl 1 (2005) S7-10.
[78] P.J. Marie, Strontium ranelate: a physiological approach for optimizing bone formation and resorption, Bone 38(2 Suppl 1) (2006) S10-4.

[79] P.J. Marie, Effective doses for strontium ranelate, Osteoporos Int 19(12) (2008) 1813; author reply 1815-7.
[80] P.J. Meunier, C. Roux, E. Seeman, S. Ortolani, J.E. Badurski, T.D. Spector, J. Cannata, A. Balogh, E.M. Lemmel, S. Pors-Nielsen, R. Rizzoli, H.K. Genant, J.Y. Reginster, The effects of strontium ranelate on the risk of vertebral fracture in women with postmenopausal osteoporosis, N Engl J Med 350 (2004).
[81] J.Y. Reginster, A. Neuprez, N. Dardenne, C. Beaudart, P. Emonts, O. Bruyere, Efficacy and safety of currently marketed anti-osteoporosis medications, Best Practice & Research Clinical Endocrinology & Metabolism 28(6) (2014) 809-834.
[82] G.J. Atkins, K.J. Welldon, P. Halbout, D.M. Findlay, Strontium ranelate treatment of human primary osteoblasts promotes an osteocyte-like phenotype while eliciting an osteoprotegerin response, Osteoporosis International 20(4) (2009) 653-664.
[83] A. Barbara, P. Delannoy, B.G. Denis, P.J. Marie, Normal matrix mineralization induced by strontium ranelate in MC3T3-E1 osteogenic cells, Metabolism 53(4) (2004) 532-537.
[84] E. Bonnelye, A. Chabadel, F. Saltel, P. Jurdic, Dual effect of strontium ranelate: Stimulation of osteoblast differentiation and inhibition of osteoclast formation and resorption in vitro, Bone 42(1) (2008) 129-138.
[85] T.C. Brennan, M.S. Rybchyn, W. Green, S. Atwa, A.D. Conigrave, R.S. Mason, Osteoblasts play key roles in the mechanisms of action of strontium ranelate, British Journal of Pharmacology 157(7) (2009) 1291-1300.
[86] J. Caverzasio, Strontium ranelate promotes osteoblastic cell replication through at least two different mechanisms, Bone 42(6) (2008) 1131-6.
[87] J. Caverzasio, C. Thouverey, Activation of FGF receptors is a new mechanism by which strontium ranelate induces osteoblastic cell growth, Cellular physiology and biochemistry : international journal of experimental cellular physiology, biochemistry, and pharmacology 27(3-4) (2011) 243-50.
[88] N. Chattopadhyay, S.J. Quinn, O. Kifor, C. Ye, E.M. Brown, The calcium-sensing receptor (CaR) is involved in strontium ranelate-induced osteoblast proliferation, Biochemical Pharmacology 74(3) (2007) 438-447.
[89] S. Choudhary, P. Halbout, C. Alander, L. Raisz, C. Pilbeam, Strontium Ranelate Promotes Osteoblastic Differentiation and Mineralization of Murine Bone Marrow Stromal Cells: Involvement of Prostaglandins, Journal of Bone and Mineral Research 22(7) (2007) 1002-1010.
[90] O. Fromigué, E. Haÿ, A. Barbara, P.J. Marie, Essential Role of Nuclear Factor of Activated T Cells (NFAT)-mediated Wnt Signaling in Osteoblast Differentiation Induced by Strontium Ranelate, Journal of Biological Chemistry 285(33) (2010) 25251-25258.
[91] Y. Li, J. Li, S. Zhu, E. Luo, G. Feng, Q. Chen, J. Hu, Effects of strontium on proliferation and differentiation of rat bone marrow mesenchymal stem cells, Biochemical and Biophysical Research Communications 418(4) (2012) 725-730.
[92] S. Peng, G. Zhou, K.D.K. Luk, K.M.C. Cheung, Z. Li, W.M. Lam, Z. Zhou, W.W. Lu, Strontium Promotes Osteogenic Differentiation of Mesenchymal Stem Cells Through the Ras/MAPK Signaling Pathway, Cellular Physiology and Biochemistry 23(1-3) (2009) 165-174.
[93] S.C. Verberckmoes, M.E. De Broe, P.C. D'Haese, Dose-dependent effects of strontium on osteoblast function and mineralization, Kidney Int 64(2) (2003) 534-543.
[94] F. Yang, D. Yang, J. Tu, Q. Zheng, L. Cai, L. Wang, Strontium Enhances Osteogenic Differentiation of Mesenchymal Stem Cells and In Vivo Bone Formation by Activating Wnt/Catenin Signaling, STEM CELLS 29(6) (2011) 981-991.
[95] L.-L. Zhu, S. Zaidi, Y. Peng, H. Zhou, B.S. Moonga, A. Blesius, I. Dupin-Roger, M. Zaidi, L. Sun, Induction of a program gene expression during osteoblast differentiation with strontium ranelate, Biochemical and Biophysical Research Communications 355(2) (2007) 307-311.

[96] R. Baron, Y. Tsouderos, In vitro effects of S12911-2 on osteoclast function and bone marrow macrophage differentiation, European Journal of Pharmacology 450(1) (2002) 11-17.
[97] A.S. Hurtel-Lemaire, R. Mentaverri, A. Caudrillier, F. Cournarie, A. Wattel, S. Kamel, E.F. Terwilliger, E.M. Brown, M. Brazier, The Calcium-sensing Receptor Is Involved in Strontium Ranelate-induced Osteoclast Apoptosis: NEW INSIGHTS INTO THE ASSOCIATED SIGNALING PATHWAYS, Journal of Biological Chemistry 284(1) (2009) 575-584.
[98] N. Takahashi, T. Sasaki, Y. Tsouderos, T. Suda, S 12911-2 Inhibits Osteoclastic Bone Resorption In Vitro, Journal of Bone and Mineral Research 18(6) (2003) 1082-1087.
[99] S.D. Bain, C. Jerome, V. Shen, I. Dupin-Roger, P. Ammann, Strontium ranelate improves bone strength in ovariectomized rat by positively influencing bone resistance determinants, Osteoporosis International 20(8) (2009) 1417-1428.
[100] J. Buehler, P. Chappuis, J.L. Saffar, Y. Tsouderos, A. Vignery, Strontium ranelate inhibits bone resorption while maintaining bone formation in alveolar bone in monkeys (Macaca fascicularis), Bone 29(2) (2001) 176-179.
[101] P. Delannoy, D. Bazot, P.J. Marie, Long-term treatment with strontium ranelate increases vertebral bone mass without deleterious effect in mice, Metabolism 51(7) (2002) 906-911.
[102] A. Patrick, B. Isabelle, B. Sébastien, D. Romain, R. René, Strontium Ranelate Treatment Improves Trabecular and Cortical Intrinsic Bone Tissue Quality, a Determinant of Bone Strength, Journal of Bone and Mineral Research 22(9) (2007) 1419-1425.
[103] A. Patrick, S. Victor, R. Bruno, M. Yves, B. Jean-Philippe, R. Rene, Strontium Ranelate Improves Bone Resistance by Increasing Bone Mass and Improving Architecture in Intact Female Rats, Journal of Bone and Mineral Research 19(12) (2004) 2012-2020.
[104] S. Bose, G. Fielding, S. Tarafder, A. Bandyopadhyay, Understanding of dopant-induced osteogenesis and angiogenesis in calcium phosphate ceramics, Trends in Biotechnology 31(10) (2013) 594-605.
[105] B. Abrahamsen, E.L. Grove, P. Vestergaard, Nationwide registry-based analysis of cardiovascular risk factors and adverse outcomes in patients treated with strontium ranelate, Osteoporosis International 25(2) (2014) 757-762.
[106] C. Cooper, K.M. Fox, J.S. Borer, Ischaemic cardiac events and use of strontium ranelate in postmenopausal osteoporosis: a nested case–control study in the CPRD, Osteoporosis International 25(2) (2014) 737-745.
[107] A.F. Donneau, J.Y. Reginster, Cardiovascular safety of strontium ranelate: real-life assessment in clinical practice, Osteoporosis International 25(2) (2014) 397-398.
[108] J. Hao, A. Acharya, K. Chen, J. Chou, S. Kasugai, N.P. Lang, Novel bioresorbable strontium hydroxyapatite membrane for guided bone regeneration, Clinical Oral Implants Research 26(1) (2015) 1-7.
[109] V. Nardone, S. Fabbri, F. Marini, R. Zonefrati, G. Galli, A. Carossino, A. Tanini, M.L. Brandi, Osteodifferentiation of Human Preadipocytes Induced by Strontium Released from Hydrogels, International Journal of Biomaterials 2012 (2012) 10.
[110] M. Raucci, D. Giugliano, M.A. Alvarez-Perez, L. Ambrosio, Effects on growth and osteogenic differentiation of mesenchymal stem cells by the strontium-added sol–gel hydroxyapatite gel materials, Journal of Materials Science: Materials in Medicine 26(2) (2015) 1-11.
[111] K. Sariibrahimoglu, W. Yang, S.C.G. Leeuwenburgh, F. Yang, J.G.C. Wolke, Y. Zuo, Y. Li, J.A. Jansen, Development of porous polyurethane/strontium-substituted hydroxyapatite composites for bone regeneration, Journal of Biomedical Materials Research Part A (2014) n/a-n/a.
[112] Y. Zhu, Y. Ouyang, Y. Chang, C. Luo, J. Xu, C. Zhang, W. Huang, Evaluation of the proliferation and differentiation behaviors of mesenchymal stem cells with partially

converted borate glass containing different amounts of strontium in vitro, Molecular medicine reports 7(4) (2013) 1129-36.
[113] C.T. Wong, W.W. Lu, W.K. Chan, K.M.C. Cheung, K.D.K. Luk, D.S. Lu, A.B.M. Rabie, L.F. Deng, J.C.Y. Leong, In vivo cancellous bone remodeling on a strontium-containing hydroxyapatite (sr-HA) bioactive cement, Journal of Biomedical Materials Research Part A 68A(3) (2004) 513-521.
[114] S.S. Banerjee, S. Tarafder, N.M. Davies, A. Bandyopadhyay, S. Bose, Understanding the influence of MgO and SrO binary doping on the mechanical and biological properties of β-TCP ceramics, Acta Biomaterialia 6(10) (2010) 4167-4174.
[115] K. Lin, L. Xia, H. Li, X. Jiang, H. Pan, Y. Xu, W.W. Lu, Z. Zhang, J. Chang, Enhanced osteoporotic bone regeneration by strontium-substituted calcium silicate bioactive ceramics, Biomaterials 34(38) (2013) 10028-10042.
[116] N. Neves, D. Linhares, G. Costa, C.C. Ribeiro, M.A. Barbosa, In vivo and clinical application of strontium-enriched biomaterials for bone regeneration: A systematic review, Bone & Joint Research 6(6) (2017) 366-375.
[117] A. Vishwakarma, N.S. Bhise, M.B. Evangelista, J. Rouwkema, M.R. Dokmeci, A.M. Ghaemmaghami, N.E. Vrana, A. Khademhosseini, Engineering Immunomodulatory Biomaterials To Tune the Inflammatory Response, Trends in Biotechnology 34(6) (2016) 470-482.
[118] X. Yuan, H. Cao, J. Wang, K. Tang, B. Li, Y. Zhao, M. Cheng, H. Qin, X. Liu, X. Zhang, Immunomodulatory Effects of Calcium and Strontium Co-Doped Titanium Oxides on Osteogenesis, Frontiers in Immunology 8 (2017) 1196.
[119] W. Zhang, F. Zhao, D. Huang, X. Fu, X. Li, X. Chen, Strontium-Substituted Submicrometer Bioactive Glasses Modulate Macrophage Responses for Improved Bone Regeneration, ACS Applied Materials & Interfaces 8(45) (2016) 30747-30758.
[120] F. Zhao, B. Lei, X. Li, Y. Mo, R. Wang, D. Chen, X. Chen, Promoting in vivo early angiogenesis with sub-micrometer strontium-contained bioactive microspheres through modulating macrophage phenotypes, Biomaterials 178 (2018) 36-47.

Chapter II

Aim of the thesis

Motivation

In bone tissue repair/regeneration therapeutic strategies, the use of injectable bone substitutes is very attractive since these can be applied with minimally invasive surgical procedures and can perfectly fill irregular defects resulting from trauma, disease, infection or tumor resection. Bone substitute materials should ideally combine adequate mechanical properties with the ability to induce/support new bone formation. Incorporating Sr in injectable biomaterials stands out as a promising strategy to achieve high local concentrations of this element, which exhibits both osteoanabolic and anti-osteoclastic activities, for the enhancement of new bone formation. Recent evidences also suggest that Sr may induce a more pro-regenerative immune response, important upon biomaterial implantation.

Objectives

The aim of the present work was to evaluate the biological response to a Sr-hybrid injectable system for bone regeneration, designed by our group, consisting of hydroxyapatite microspheres doped with Sr and an alginate vehicle crosslinked *in situ* with Sr ions. A similar Sr-free system (Ca-hybrid) was used as a control. The main tasks of this work consisted of:

- Study the release profile of Sr^{2+} from the designed system and the *in vitro* effect of different Sr^{2+} concentrations on bone marrow MSC and OC derived from peripheral blood derived monocytes, within the range of the expected values of Sr^{2+} to be released from the hybrid system (Chapter III).

- Study the *in vitro* potential of the system to drive MSC differentiation into osteoblasts and inhibit OC formation and activity (Chapter III).

- Evaluate the *in vivo* inflammatory response to the developed system in a rodent air-pouch model, focusing on tissue histology, flow cytometry analyses of the cellular infiltrate and cytokine analysis (Chapter III).

- Evaluate the *in vivo* response to the Sr-hybrid system in a rat critical-sized defect model, regarding bone tissue formation by radiological techniques (X-ray and MicroCT) and methylmethacrylate histological study (Chapter IV).

Chapter III

Osteoimmunomodulatory properties of a strontium-rich injectable hybrid scaffold for bone repair

Ana Henriques Lourenço, Ana Luísa Torres, Daniela P. Vasconcelos, Cláudia Ribeiro-Machado, Judite N. Barbosa, Mário A. Barbosa, Cristina C. Barrias, Cristina C. Ribeiro

Submitted

Osteoimmunomodulatory properties of a strontium-rich injectable hybrid scaffold for bone repair

Ana Henriques Lourenço[1,2,3] , Ana Luísa Torres[1,2,4] , Daniela P. Vasconcelos[1,2,4], Cláudia Ribeiro-Machado[1,2], Judite N. Barbosa[1,2,4], Mário A. Barbosa[1,2,4], Cristina C. Barrias[1,2,4], Cristina C. Ribeiro[1,2,5, *]

[1]i3S - Instituto de Investigação e Inovação em Saúde, Universidade do Porto, Rua Alfredo Allen, 208, 4200 - 135 Porto, Portugal
[2]INEB - Instituto de Engenharia Biomédica, Universidade do Porto, Rua Alfredo Allen, 208, 4200 - 135 Porto, Portugal
[3]Faculdade de Engenharia, Universidade do Porto, Rua Dr. Roberto Frias, s/n, 4200-465 Porto, Portugal
[4]ICBAS - Instituto de Ciências Biomédicas de Abel Salazar, Universidade do Porto, Rua de Jorge Viterbo Ferreira n. 228, 4050-313 Porto, Portugal
[5]ISEP – Instituto Superior de Engenharia do Porto, Instituto Politécnico do Porto, Rua Dr. António Bernardino de Almeida 431, 4249-015, Porto, Portugal

[*] Corresponding author:
Cristina C. Ribeiro (cribeiro@ineb.up.pt)
Address: i3S – Instituto de Investigação e Inovação em Saúde da Universidade do Porto
Rua Alfredo Allen, 208
4200 – 135 Porto

Abstract

Strontium (Sr) is known to stimulate osteogenesis, while inhibiting osteoclastogenesis, thus encouraging research on its application as a therapeutic agent for bone repair/regeneration. It has been suggested that it may possess immunomodulatory properties, which might act synergistically in bone repair/regeneration. To further explore this hypothesis we have designed a Sr-hybrid system composed of an *in situ* forming Sr-crosslinked RGD-alginate hydrogel reinforced with Sr-doped hydroxyapatite (HAp) microspheres and studied its *in vitro* osteoinductive behaviour and *in vivo* inflammatory response. The Sr-hybrid scaffold acts as a dual Sr^{2+} delivery system, showing a cumulative Sr^{2+} release of ca. 0.3 mM after 15 days. *In vitro* studies using Sr^{2+} concentrations within this range (0 to 3 mM Sr^{2+}) confirmed its ability to induce osteogenic differentiation of mesenchymal stem/stromal cells (MSC), as well as to reduce osteoclastogenesis and osteoclasts (OC) functionality. In comparison with a similar Sr-free system, the Sr-hybrid system stimulated osteogenic differentiation of MSC, while inhibiting the formation of OC. Implantation in an *in vivo* model of inflammation, revealed an increase in $F4/80^{+}/CD206^{+}$ cells, highlighting its ability to modulate the inflammatory response as a pro-resolution mediator, through M2 macrophage polarization. Therefore, the Sr-hybrid system is potentially an appealing biomaterial for future clinical applications.

Keywords

Strontium, Hydroxyapatite, Alginate, Osteoclasts, Mesenchymal Stem/Stromal Cells, Immune response modulation

1. *Introduction*

Bone is a complex and highly dynamic tissue, and the maintenance of its mass is ensured by a proper balance between bone resorption and bone formation. The deregulation of this equilibrium may lead to severe pathological conditions, such as osteoporosis, cancer and Paget's disease, as well as inflammatory disorders like rheumatoid arthritis and periodontal disease [1, 2]. These pathological situations are frequently associated with multiple morbidities, especially in an increasingly older population, and often lead to non-healing fractures. Autologous bone grafts remain the gold standard material for the treatment of this kind of fractures, though they present critical drawbacks, including low tissue availability and high morbidity of the secondary harvest place. Thus, the development of synthetic bone grafts that support and stimulate bone repair and regeneration is a major need in clinics [3]. Among those, injectable bone substitutes are attractive options, as they can be implanted through minimally invasive surgery and can easily fit into irregular bone defects, providing local support for bone repair [4]. Synthetic hydroxyapatite (HAp) has been widely used as bone-like ceramic owing to its biocompatibility and resemblance to the mineral phase of natural bone [5]. Injectable systems are often composed of ceramic particles embedded within hydrogels, somehow mimicking the composite nature of bone tissue [6]. Ceramic materials also provide strength and improve the mechanical properties of the system, as compared to hydrogels alone [7]. In turn, the hydrogel phase provides a hydrated three-dimensional (3D) environment, that may allow the entrapment of bioactive factors or even cells, and may also support host cell colonization and new tissue ingrowth [8]. Gel-precursor solutions can act as vehicles for the ceramic particles, facilitating their injection, and preferably reticulating *in situ*.

Strontium (Sr) ranelate has been administered orally as an anti-osteoporotic drug for many years, and clinical follow-ups confirmed its contribution to increase the bone mineral density and reduce the risk of fracture [9]. Several *in vitro* studies have

suggested that Sr, either in the form of Sr ranelate or other Sr salts, has the potential to increase the proliferation and differentiation of osteoblasts, osteoprogenitors and mesenchymal stem/stromal cells (MSC) [10-15]. Moreover, Sr has been shown to inhibit the formation, maturation and resorptive behavior of osteoclasts (OC) [16-18]. However, oral administration of Sr ranelate in patients with osteoporosis and osteoarthritis has been recently associated with myocardial infarction, due to a significant increase in the number of non-fatal occurrences [19-21]. Currently, the prescription of Sr ranelate is restricted to patients with no history of ischemic heart disease, peripheral arterial disease and/or cerebrovascular disease or uncontrolled hypertension (European Medicines Agency, EMEA, 2014).

Alternatively to the oral administration of Sr ranelate, the use of biomaterial-based systems able to promote Sr local delivery in bone tissue may be advantageous, surpassing therefore systemic effects. Several *in vitro* studies have shown an osteoinductive effect of Sr when incorporated into different type of biomaterials [22-26]. Also, *in vivo* studies, using mainly Sr-rich phosphate cements or Sr-doped HAp, revealed enhanced local bone formation both at the center and surface of the implant [27, 28].

Growing evidence of the importance of inflammation in the regulation of bone healing [29] highlights the need to consider a global approach for an effective therapy. Inflammation is a natural process following injury, where macrophages play a key role. Upon implantation of a material, monocytes differentiate into macrophages that can polarize into two phenotypes (M1 and M2). M1 macrophages (classically activated/inflammatory) are pro-inflammatory exerting an immunostimulatory effect, whereas M2 macrophages (alternatively activated/regenerative) are anti-inflammatory and promote tissue repair [30-32]. Therefore, the modulation of the immune response towards an M2 phenotype may lead to more efficient tissue regeneration strategies and immunomodulatory materials [33-35].

In our group we have designed an injectable, viscoelastic hybrid system for bone regeneration consisting of Sr-rich HAp microspheres and an RGD (arginine-glycine-aspartic acid)-modified alginate hydrogel that crosslinks *in situ* at body temperature when mixed with Sr carbonate, which acts as crosslinking agent. The incorporation of cell-adhesive RGD peptides is key to promote cell attachment to the hydrogel and also to enhance the viability and function of osteoblastic cells, as already reported [36, 37]. In a previous work, we have demonstrated that the incorporation of HAp microspheres at 35% w/v represented the best compromise between system injectability and compression strength, and also resulted in a homogeneous distribution of microspheres throughout the hydrogel phase [38]. Moreover, it was able to promote bone regeneration in a critical-sized bone defect [39].

The main goals of the present study were to assess the ability of the Sr-hybrid system to promote sustained release of Sr^{2+}, analyze the effect of Sr^{2+} in osteogenesis and osteoclastogenesis as well as to evaluate the *in vivo* inflammatory response to the designed material, using a rodent air-pouch model of inflammation.

2. Materials and Methods

2.1. Preparation of Sr-HAp microspheres

Sr-HAp or HAp microspheres (control) were obtained as described elsewhere [40]. Briefly, HAp was dispersed in a 3% w/v alginate (Protanal 10/60, FMC BioPolymer) solution in deionized water, under gentle stirring until a homogeneous paste was obtained. The paste was extruded dropwise and crosslinked in solutions of Sr chloride ($SrCl_2$, 0.1 M, Sigma) or calcium (Ca) chloride ($CaCl_2$, 0.1 M, Merck), and allowed to harden for 30 minutes (min). The size was controlled by regulating the extrusion flow rate using a syringe pump (Cole-Parmer), and by applying a coaxial air stream (Encapsulation Unit Var J1–Nisco). Afterwards, microspheres were recovered and rinsed in deionized water, in order to remove the excess of crosslinking ions and dried overnight at 60 °C. Microspheres were subsequently sintered at 1200 ºC to burn-off the polymer and aggregate the ceramic granules. Microspheres were washed with deionized water, dried and finally sieved to obtain particles with a uniform spherical shape with 500-560 μm diameter. Sr-enriched and Sr-free microspheres will be hereafter designated as Sr-HAp microspheres and HAp microspheres, respectively. Sr-HAp microspheres were imaged by scanning electron microscopy (SEM) and analysed by SEM/Energy-dispersive X-ray spectroscopy (SEM/EDS).

2.2. Synthesis of RGD-alginate

Ultra-pure sodium alginate with high content of guluronic acid units (>60%, NovaMatrix, FMC Biopolymers) and molecular weight of 131±13 kDa (determined by Gel Permeation Chromatography/size exclusion chromatography (GPC/SEC)) [38] was used for hydrogel preparation. The cell-adhesion peptide sequence (glycine)-4-arginine-glycine-aspartic acid-serine-proline (G4RGDSP, GenScript), hereafter abbreviated as RGD, was coupled to alginate using carbodiimide chemistry, as

described in detail in previous studies [41, 42]. Briefly, a 1% w/v alginate solution in 0.1 M MES buffer (Sigma) was prepared and stirred overnight. Thereafter, sulfo-NHS (Thermo Scientific) and EDC (Sigma) at a molar ratio of 1:2, and RGD peptides (17 mg/g alginate) were sequentially added. After stirring for 24 hours (h), the reaction was quenched with hydroxylamine (NH_2OH, Sigma). Non-reacted species were removed by dialysis (MWCO 3500 membrane, Spectrum Lab) against solutions of decreasing concentration of sodium chloride (NaCl, Merck) and finally deionized water. The recovered solution was lyophilized, sterile filtered and the RGD-alginate was stored at -20 ºC until further use. The conjugation yield was determined using the BCA Protein Assay (Pierce), as previously described [43].

Endotoxin levels were measured in RGD-modified alginate using the Food and Drug Administration (FDA) approved Endosafe™-PTS system (Charles River). The analysis was performed and certified by an external entity (Analytical Services Unit, IBET/ITQB), indicating endotoxin levels below 0.1 EU/mL (EU - unit of measurement for endotoxin activity).

2.3. Preparation of Sr-hybrid system

For the hybrid system, RGD-alginate was combined with Sr-HAp or HAp microspheres and crosslinked by internal gelation with Sr^{2+} or Ca^{2+}, respectively (hereafter designated as Sr-hybrid or Ca-hybrid). The used methodology [38] was adapted and optimized from previous works using Ca-crosslinked alginate hydrogels [37, 40, 42, 43]. Briefly, RGD-alginate was thoroughly mixed with an aqueous suspension of Sr carbonate ($SrCO_3$, Sigma) or Ca carbonate ($CaCO_3$, Fluka) at a $SrCO_3$/COOH or $CaCO_3$/COOH molar ratio of 1.6. A fresh solution of glucone delta-lactone (GDL, Sigma) was added to trigger gel formation. The $SrCO_3$/GDL or $CaCO_3$/GDL molar ratio was set at 0.125 and the total polymer concentration was 3.5% w/v in deionized water, with a final RGD concentration of 235 μM in the hydrogel. Microspheres were homogeneously mixed with the alginate solution at

35% w/v. The final mixture was allowed to polymerize in a mold, yielding a cylindrical shape with 5.96 mm diameter and 2.5 mm height. For cell culture studies, Sr- or Ca-hybrid systems were placed in 96-well plates with 200 µL of cell culture medium.

2.4. Quantification of Sr^{2+} released from Sr-hybrid and Sr-HAp microspheres

Sr^{2+} levels released to cell culture medium were quantified by Inductively Coupled Plasma - Atomic Emission Spectroscopy (ICP-AES, Horiba Jobin-Yvon, Ultima spectrometer, generator RF of 40,68 MHz). Sr-hybrid system or Sr-HAp microspheres alone were maintained for up to 15 days in Dulbecco's Modified Eagle Medium with glutamax (DMEM, Gibco), at 37 ºC under a humidified atmosphere of 5% v/v CO_2 in air. A ratio of 200 µL of medium *per* disc (Sr-hybrid system with 35% w/v Sr-HAp microspheres, corresponding to a total amount of 40.35 mg) or 40.35 mg Sr-HAp microspheres was maintained, in order to simulate the conditions subsequently used for cell culture studies. Three replicate readings from each material per time point were analysed. Cell culture medium was renewed every three days and stored at -20 ºC until further analysis.

2.5. Cell Culture Procedures

2.5.1. Cultures of human MSC

Human MSC were purchased from Lonza (PT-2501, Lot no. 0F3825, 22Y, female) and routinely cultured in a basal medium (hereafter designated as BM) composed of low-glucose DMEM supplemented with 10% v/v fetal bovine serum (FBS, MSC-qualified, HyClone, GE Healthcare Life Sciences) and 1% v/v penicillin/streptomycin (Pen/Strep, Gibco). Cultures were maintained at 37 ºC under a humidified atmosphere of 5% v/v CO_2 in air, with culture medium being changed twice a week. Cells were trypsinized when reaching ca. 70% confluence. Osteogenic differentiation was induced by culturing cells (passage 6-7) in an osteogenic medium (OM)

composed by low-glucose DMEM with 10% v/v FBS (pre-selected batch from PAA), 1%v/v Pen/Strep, 100 nM dexamethasone (Sigma), 10mM β-glycerophosphate (Sigma) and 0.05 mM 2-phospho-L-ascorbic acid (Fluka) [44], for up to 21 days. In monoculture studies, $SrCl_2$ was added to cell cultures at different concentrations (0.5, 1 and 3 mM of Sr^{2+}) and renewed in every culture medium replacement, every 2 to 3 days. Cells cultured in the absence of Sr^{2+} (untreated cells) and in BM were used as controls. In studies with Sr-hybrid materials, cells were cultured in direct contact and medium was replaced every 2 to 3 days. Ca-hybrid materials were used as controls.

2.5.2. Human monocyte isolation and OC differentiation

Buffy coats (BC, kindly donated by Hospital S. João, Porto) from healthy blood donors, were used to isolate monocytes by negative selection, using RosetteSep isolation kit (Stem Cell Technologies SARL) and a method adapted from the manufacturer's instructions [45]. Briefly, BC were centrifuged at 1200xg, for 20 min, without brake and peripheral blood mononuclear cells (PBMC) collected. Cells were incubated for 20 min with RosetteSep human monocyte enrichment isolation kit. The mixture was then diluted at a 1:1 ratio with phosphate buffer saline (PBS): 2% FBS (Lonza), layered over Histopaque (Sigma Aldrich, System Histopaque 1077) and centrifuged as previously. The enriched monocyte fraction was carefully collected from the gradient formed and washed with PBS. Washes were performed at 100xg for 17 min, to ensure platelet removal. Cells were then resuspended in α-minimal essential medium (α-MEM, Gibco), supplemented with 10% FBS and 1% Pen/Strep. Monocyte purity was routinely checked by flow cytometry, as described previously [45]. Finally, cells were plated on TCPS at $0.63x10^6$ cells/cm^2 and allowed to differentiate into OC in the presence of 50 ng/mL of receptor activator of nuclear factor-k (RANKL) combined with 30 ng/mL of macrophage-colony stimulating factor (M-CSF) for up to 21 days at 37 ºC, 5%CO_2, as previously described [46]. For cells cultured in monolayer, culture medium supplemented with cytokines and Sr^{2+} was

replaced every 3 to 4 days, where no Sr^{2+} addition was used as a control. In studies with Sr-hybrid materials, cells were cultured in direct contact and media was replaced every 3 to 4 days. Ca-hybrid materials were used as controls.

2.6. Effect of Sr^{2+} on human MSC

2.6.1. Metabolic activity and viability

Cell metabolic activity of monolayer cultures was assessed using the resazurin assay. Cells were incubated with 20% v/v of the stock resazurin solution (0.1 mg/mL resazurin (Sigma) in PBS) in medium for 2 h at 37 ºC. The supernatant was then transferred to a 96-well plate black with clear bottom (Greiner) and fluorescence measurements (Ex 530 nm / Em 590 nm) were carried out using a microplate reader (Biotek Synergy MX).

Live/Dead assay was used to assess viability of cells cultured on hybrid systems, according to the manufacturer's instructions. Briefly, cells were washed three times with serum-free DMEM without phenol red (Gibco), to remove/dilute esterases, and then incubated with 1 μM Calcein AM and 2.5 μM ethidium homodimer-1 (EthD-1) for 45 min at 37 ºC, protected from light. Afterwards, the supernatant was removed and fresh serum-free DMEM without phenol red was added. Calcein AM (Ex 485 nm/ Em 530 nm) stains live cells green and EthD-1 (Ex 530 nm/Em 645 nm) stains dead cells red. Samples were imaged with confocal scanning laser microscope (CSLM, Leica SP2 AOBS) using LCS software (Leica). Further image treatment was performed using ImageJ 1.43u software (Wayne Rasband).

2.6.2. Osteogenic differentiation: ALP and Von Kossa stainings

ALP staining was performed on cells either in monolayer or on the hybrid systems. Cells were washed three times with tris-buffered saline (TBS) and fixed with 4% v/v

PFA in TBS for 20 min at RT, followed by another washing step, and incubated for 30 min in Naphthol AS-MX phosphate/Fast Violet B salt (Sigma) at 37 ºC, protected from light. For Von Kossa staining, cells in monolayer were washed with PBS, fixed with 4% PFA v/v in PBS and further washed with deionized water. Afterwards, cells were incubated in 2.5 wt % silver nitrate (Sigma) for 30 min under UV light, followed by incubation in 5 wt % sodium thiosulfate (Aldrich) for 3 min, and finally washed in deionized water. Images were obtained using a stereoscope (SZX10, Olympus) with a digital camera (DP21, Olympus) or with a Zeiss Axiovert 200M fluorescence microscope.

2.6.3. Morphology

The morphology of MSC on the hybrid system was observed by CSLM, after F-actin and nuclei staining. First, culture medium was removed from the wells, cells washed with TBS and fixed for 20 min with 4% v/v paraformaldehyde (PFA, Sigma) in TBS at RT. After washing in TBS, cells were permeabilized using 0.1% Triton X-100 in TBS for 5 min and further washed. Samples were incubated for 1 h with 1% w/v bovine serum albumin (BSA, Merck) in TBS for blocking, and then incubated for 1 h in 6.6 µM Alexa Fluor 488 Phalloidin (Ex 495 nm/Em 518 nm, Molecular Probes, Invitrogen) and 2.5 µM EthD-1 in 1% w/v BSA solution. After a final washing step, samples were kept at -20 ºC and protected from light until being imaged by CSLM.

2.7. Human OC biofunctionality tests and Sr^{2+} effect

2.7.1. Analysis of multinucleated OC formation

To analyse the formation of multinucleated OC in monolayer and on the hybrid systems, the cell cytoskeleton and nuclei were stained as previously described (section 2.6.3). 3D samples were visualized by CLSM and monolayer samples were

observed in a fluorescence microscope. For cells cultured in monolayer, quantitative analysis was performed in 3 independent experiments (3 different individuals). For each experiment, 4 images per time point were acquired, with an AxioCam MRm (Zeiss), using the AxioVision Rel. 4.8 software. The analysed area was of 0.357 mm^2 per image. Image analysis and nuclei per cell counting were performed with Cell Note software [47]. For a more comprehensive analysis of the quantified results, multinucleated cells were divided into three categories based on the number of nuclei per cell: 2 nuclei, 3 to 9 nuclei and more than 10 nuclei per cell. This division was intended to distinguish binucleated cells from truly multinucleated ones and within the multinucleated cells, the smaller osteoclasts, with up to 9 nuclei, from the very large ones [46].

2.7.2. TRAP staining and quantification of TRAP Release

The TRAP assay (Sigma-Aldrich) was performed according to the manufacturer's instructions. OC at days 7, 14 and 21 of differentiation were fixed in citrate/acetone solution, washed in deionized water and dried. Afterwards, samples were incubated with a solution containing water, acetate, naphthol and 1 capsule of fast garnet GBC salt for 1 h, at 37 ºC, in the dark. At the end of the incubation period, cells were washed in deionized water, counter-stained with acid hematoxylin solution, washed and finally allowed to air dry. Cells were then analysed with a stereomicroscope, coupled to a digital camera, or with an inverted fluorescence microscope. Images (0.357 mm^2 per image) were acquired with AxioCam HRc (Zeiss) and using AxioVision Rel. 4.8 software. This was performed for 3 independent experiments.

Released TRAP was quantified as previously described [48]. At day 20, fresh complete culture medium was added to the cells and, after 24 h of incubation, supernatants were removed for analysis. Cell lysates were prepared by washing cells with PBS, incubating in 100 µL 0.1% v/v Triton X-100 in water, for 10 min. To quantify the activity of TRAP, the conversion of p-nitrophenyl phosphate

(phosphatase substrate, Sigma-Aldrich) into p-nitrophenol, in the presence of sodium tartrate, was measured. 80 µL of the supernatant or the lysate of each condition was transferred to a 96-well plate, containing 80 µL of 0.09 M citrate buffer, 20 mM phosphatase substrate and 80 mM tartaric acid and incubated at RT for 40 min. In order to stop the reaction, 40 µL of 0.5 M NaOH was added to each well. Serial dilutions of p-nitrophenol (Sigma-Aldrich) were performed, to create a standard curve, and the absorbance of all samples was measured at 405 nm on a microplate reader. The activity of TRAP was measured in the supernatant and lysate of cells and enzyme activity released into the supernatant was calculated as a percentage of total enzyme activity [48, 49]. For each condition, 5 replicates were prepared and from each well triplicate readings were performed.

2.7.3. Resorption assay with dentine slices

To evaluate the effect of Sr^{2+} in OC resorption activity, cells were cultured on top of dentine slices and treated with $SrCl_2$ as previously described. Commercially available sterile dentine slices, with approximately 5 mm of diameter and 0.3 mm of thickness (IDS, Lucron, Benelux) were placed in a 96-well plate and incubated for 1 h with PBS prior to cell culture. Cells were seeded, at a density of $0.5x10^6$ cells per slice and cultured in the presence of 50 ng/mL of RANKL and 30 ng/mL of M-CSF. Cell culture medium was changed every 3 to 4 days. After 21 days of culture, samples were prepared for SEM analysis. Cells were washed with PBS at RT and a 2.5% v/v glutaraldehyde in 0.1 M sodium cacodylate solution was added to each well. Fixation was performed at RT, for 30 min, under gentle shaking (50 rpm), on an orbital shaker. Samples were then washed 3 times with cacodylate buffer. Finally, cells were incubated for 10 min in each of a graded series of ethanol solutions (50, 60, 70, 80, 90 and 99% v/v), in order to dehydrate them, and stored in absolute ethanol, at 4 ºC, until being subjected to critical point drying, mounted onto appropriate supports with Araldite glue, sputtered-coated with gold and examined by SEM, using a FEI

Quanta 400FEG ESEM / EDAX Genesis X4M microscope, at 15.00 kV.

2.8. In vivo inflammatory response

2.8.1. Rodent air-pouch model of inflammation

All animal experiments were conducted following protocols approved by the Ethics Committee of the Portuguese Official Authority on Animal Welfare and Experimentation (DGAV). The air-pouch model of inflammation was used [34, 35, 50, 51] in 7-9 weeks old, male BALB/c mice. The formation of an air-pouch was achieved by subcutaneous injection of 5 mL of sterile air in the dorsal area. The air-pouch was reinforced with a 3 mL sterile air injection after 5 days. After 24h, mice were anaesthetized by intraperitoneal injection of ketamine and medetomidine (75 mg/kg and 1mg/kg, respectively) and the dorsal area shaved and cleaned. A surgical incision was performed and the material was placed inside the air-pouch followed by wound suture. Anaesthetic reverser, atipamezole, was administered intraperitoneally. Three experimental groups were performed: animals implanted with Sr-hybrid material, animals implanted with Ca-hybrid material and Sham-operated animals. For each experimental group 6 (Sham-operated) or 7(Sr-hybrid and Ca-hybrid) animals were used. Two different time-points, 3 and 15 days post-surgery, were analysed. For inflammatory exudates recovery, after 3 days, animals were anesthetised as previously described and 4 mL of PBS were injected in the air-pouch cavity. The cavity was gently shaken and the lavage fluid recovered. For both time-points, animals were sacrificed and organs (skin, heart, liver, spleen, kidneys) and implanted materials were recovered.

2.8.2. Flow cytometry analysis

The recovered inflammatory exudates at day 3 were filtered through a 40 μm nylon mesh and centrifuged at 1200 rpm for 5 min at 4 ºC. Supernatants were stored at -80

ºC until further process. Cells recovered were re-suspended in FACS buffer (PBS, 0.5% BSA, 0.1 % Sodium Azide). Cells were counted in a Neubauer chamber. Cells were incubated with Fc-receptor-blocking antibody (Miltenyi Biotech) for 15 min at RT. Labelling was performed incubating cells with antibodies for 30 min, 4 ºC in the dark. The following antibodies from R&D systems were used: Phycoeryhrin (PE)-conjugated rat monoclonal anti-mouse F4/80/EMR1 (clone 521204, 10µl/10^6 cells), Alexa Fluor 488-conjugated polyclonal goat anti-mouse MMR/CD206 (5µl/10^6 cells), Allophycocyanin (APC)-conjugated rat monoclonal anti-mouse CCR7 (clone 4B12, 10µl/10^6 cells). The isotype controls PE-labelled IgG_{2A}, Alexa Fluor 488-conjugated goat IgG, APC-conjugated Rat IgG_{2A} (clone 54447) were used as negative controls. A FACS Calibur flow cytometer (BD Biosciences) was used with Cell Quest software. Analysis was performed using FlowJo software.

2.8.3. Cytokine production

Supernatants recovered from inflammatory exudates at day 3 were analyzed using a commercially available 62-mouse cytokine array (RayBiotech), according to manufacturer instructions. A pool of the inflammatory exudates of 6 animals per group was used, reaching a final volume of 1 mL. Membranes were exposed in a Chemidoc XRS+ (BioRad). Quantification of the results was generated by quantifying the mean spot pixel density from the array using image software analyses (ImageLab 4.1; BioRad), and results are shown in comparison to control (Sham-operated animals).

2.8.4. Histological evaluation

Skin, implanted materials and adjacent tissues were retrieved at days 3 and 15 for histological evaluation. Samples were fixed in 10% Formalin for 24 to 48 h and decalcified in formic acid 10% for 3 days, to allow for the sectioning of HAp microspheres. Heart, spleen, kidneys and liver were also retrieved. All samples were

processed and paraffin embedded. Paraffin sections of 3 μm thickness were sequentially obtained and stained with H&E. Liver and heart samples were also stained with Masson's Thricrome (MT) staining. Skin and materials samples were sequentially sectioned with 5 μm and stained for H&E and MT stainings. Briefly, H&E sections were stained 3 min in Gill III Hematoxilin and 1 min in alcoholic Eosin. For MT staining, sections were stained 5 min in Celestine Blue and 5 min Gill III Hematoxylin, 10 min running water, incubated 1h in Bouin solution at RT, washed with deionized water, stained with Biebrich Scarlet-Acid Fuchsin solution for 5 min, washed with deionized water, incubated in fresh phosphomolybdic acid/phosphotungstic acid solution for 5 min, removed excess, stained with Anilin Blue for 5 min, differentiated with acetic acid 1% for 2 min, washed in deionized water, allowed to air dry and mounted in Entellan.

2.9. Statistical Analysis

Statistical analysis was performed using Prism5 software, vs. 5.0a. The D'Agostino&Pearson omnibus normality test was performed to determine if data was normally distributed. For normally distributed data One Way ANOVA was used, followed by the Bonferroni's Multiple Comparison Test to compare selected pairs of columns. For non-parametric data, the Mann-Whitney test was used to compare two samples, whereas comparison between more than two samples was performed using the Kruskal-Wallis followed by Dunns test. Asterisks indicate statistical significance: * $p < 0.05$; ** $p<0.01$; *** $p<0.001$.

3. Results

3.1. Sr-hybrid system promotes sustained Sr^{2+} release

By design, the Sr-hybrid system has two Sr^{2+} sources in order to promote sequential Sr^{2+} release. In the hybrid system, Sr carbonate was mixed with the alginate solution, as crosslinking agent, at 0.6 mg Sr^{2+} per disc, while Sr-HAp microspheres contained Sr^{2+} at approximately 4.12 % w/w, as shown by SEM/EDS semi-quantitative elemental analysis (Fig. 1A). Sr-hybrid discs were incubated for up to 15 days in cell culture media, at the same volume ratio of medium-to-disc subsequently used in cell culture studies. Sr-HAp microspheres alone (same amount present in one disc) were also analyzed. Under these conditions, the total amount of Sr^{2+} available per disc was 112.4 mM (20.3 mM in the hydrogel, 92.1 mM in the microspheres). The delivery of Sr^{2+} from the hybrid system and the microspheres alone is depicted in Fig. 1B, showing a continuous release along 15 days of incubation. At day 15, the Sr-hybrid showed a cumulative release of ca. 0.3 mM, representing 0.3% of the total available amount, while microspheres showed a cumulative release of ca. 0.05 mM, representing 0.054% of the total available amount, which suggests that a sustained release over longer periods of time is to be expected. The slower release kinetics observed for the microspheres alone suggests that Sr^{2+} is more easily released from the hydrogel crosslinks. The release of Sr^{2+} along the first 72 h was analyzed in more detail (Fig. 1C), showing that in both cases there is an initial burst followed by a sustained release. Altogether these results showed that the system effectively promotes Sr^{2+} release, where the alginate hydrogel acts as a faster delivery source when compared to the Sr-HAp microspheres.

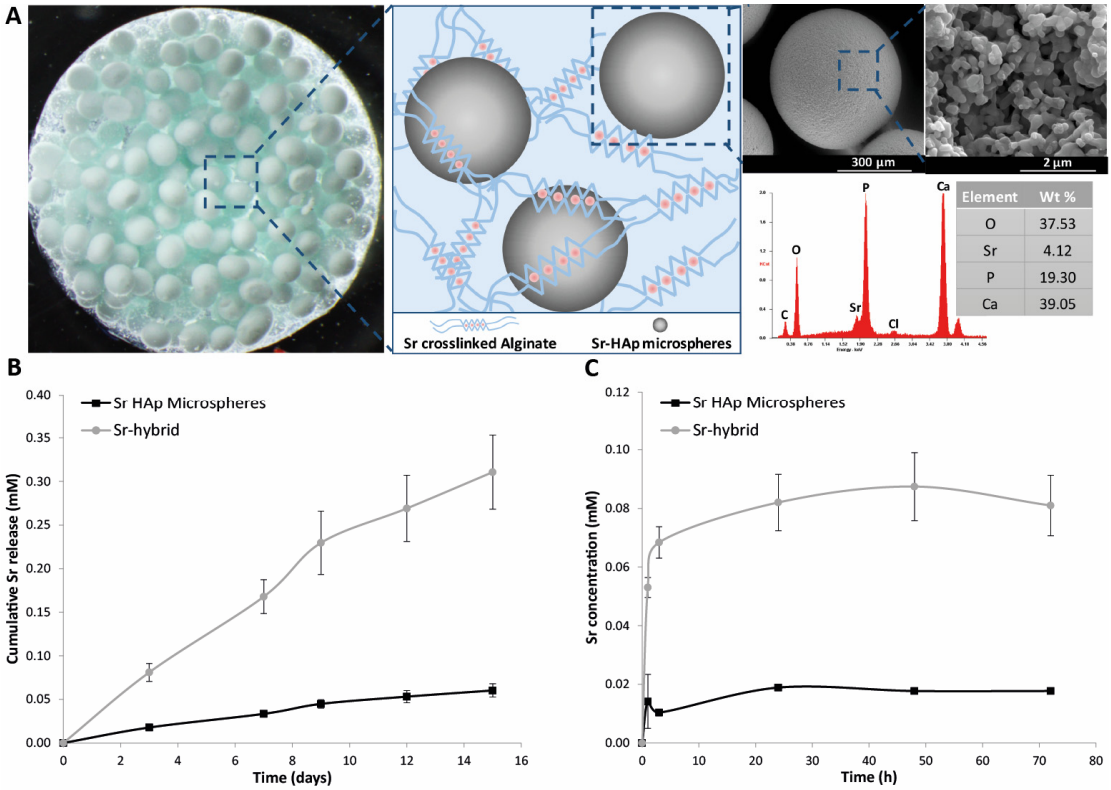

Figure 1. Representation of the Sr-hybrid system and Sr^{2+} release profile of the material. (A) Image of Sr-hybrid disc with schematic representation of its components - Sr crosslinked alginate and Sr-HAp microspheres. Highlight of a Sr HAp microsphere with SEM images and EDS spectra analysis and elemental quantification. (B) Cumulative Sr released from Sr-HAp microspheres and Sr-hybrid system along 15 days, mimicking cell culture conditions. (C) Sr concentration released from Sr-HAp microspheres and Sr-hybrid along 72 h in cell culture medium.

3.2. Sr^{2+} enhances MSC osteogenic differentiation in monolayer culture

Considering the total amount of Sr^{2+} present and released from the Sr-hybrid system, under simulated cell culture conditions, the effect of relevant concentrations of soluble Sr on human MSC was evaluated. MSC were cultured in the absence or presence of Sr^{2+} ($SrCl_2$) in the range of 0 to 3 mM (Fig. 2). MSC were cultured in monolayer, under basal and osteogenic conditions, and untreated cells (without Sr^{2+}) were used as control. Metabolic activity and proliferation were evaluated along time (Fig. 2A and 2B). Under basal conditions, the addition of 3 mM Sr^{2+} significantly increased MSC metabolic activity from day 7 and up to day 21 ($p<0.001$), as compared to the control group (0 mM Sr^{2+}). Cell proliferation also increased in the presence of Sr^{2+}.

Under osteogenic conditions, a significant increase in metabolic activity was also observed in the presence of Sr^{2+}, since day 7, with a 5-fold increase in relation to control at day 21. Regarding MSC proliferation, a decrease at day 7 was observed for Sr^{2+} concentrations of 1 mM ($p<0.05$) and 3 mM ($p<0.01$). At days 14 and 21 a significant increase in DNA content was seen in the presence of 0.5 and 1 mM Sr^{2+} ($p<0.001$), reaching a 4-fold increase at day 21 upon addition of 0.5 mM Sr^{2+}. Therefore, although the addition of Sr^{2+}increased metabolic activity, independently of the concentration used, cell proliferation under osteogenic conditions was shown to increase in the presence of low Sr^{2+} doses.

MSC osteogenic differentiation was analysed by measuring ALP activity, an early osteogenic marker. Quantitatively (Fig. 2C), higher ALP activity (normalized to the total DNA content) was observed under osteoinductive conditions, compared to basal conditions, as expected. Under basal conditions, higher ALP activity was detected in Sr-treated cultures as compared to the control (0 mM Sr^{2+}) at days 14 and 21, with a significant increase ($p<0.05$) for 1 mM Sr^{2+}. Under osteogenic conditions, a dose-dependent increase in ALP activity was observed with increasing Sr^{2+} concentrations, with statistical differences observed at all time-points for 1 mM and 3 mM Sr^{2+}. MSC monolayers were stained for ALP activity (pink staining, Fig. 2D). From day 14 onwards, higher expression of ALP activity was obtained in Sr-treated cultures, especially at 3 mM Sr^{2+}, whereas in basal conditions a less intense staining was observed without evident differences among the tested concentrations (data not shown). The formation of mineralized deposits was assessed by Von Kossa staining (Fig. 2E). Matrix mineralization, a hallmark of osteogenic differentiation, was detected under osteoinductive conditions at day 21, being much more evident for the highest Sr^{2+} concentrations used (1 and 3 mM).

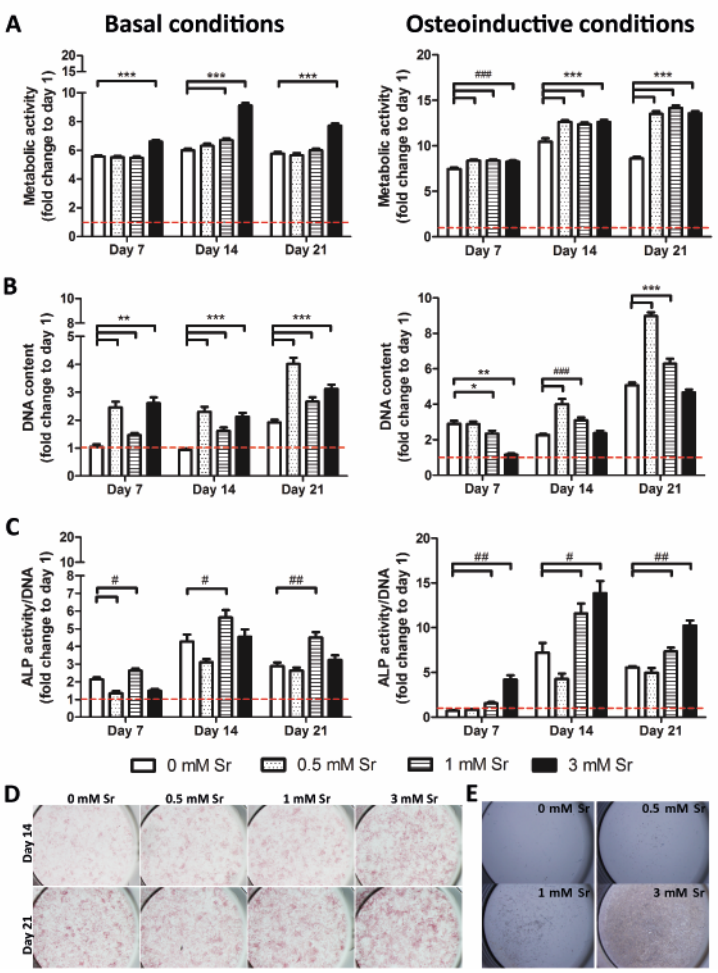

Figure 2. Sr^{2+} effect on MSC proliferation and osteogenic differentiation. Human MSC cultured on TCPS in the absence (0 mM Sr) or presence of different strontium (Sr^{2+}) concentrations (0.5, 1 and 3 mM) under basal (left) or osteoinductive conditions (right), along 21 days of culture: (A) Metabolic activity, (B) DNA content and (C) ALP activity normalized by DNA, all shown as fold change to day 1 (dashed red line as 1-fold). Results are shown as mean±(standard error of the mean, SE). Asterisks indicate statistical significance performed using parametric unpaired t test: *p< 0.05; **p< 0.01; ***p< 0.001. Hashtags indicate statistical significance performed using non-parametric Mann Whitney U test: # p< 0.05; ## p< 0.01; ### p< 0.001. (D) ALP staining images at days 14 and 21 under osteogenic induction conditions (Magnification 10x). (E) Von Kossa staining images at day 21 of MSC cultured under osteogenic induction conditions (Magnification 10x).

3.3. Sr^{2+} decreases OC adhesion and fusion with decreased functionality

Human PBMC were allowed to differentiate into OC in monolayer cultures, and the effect of Sr^{2+} on the formation of large and multinucleated OC was evaluated (Fig. 3). As depicted in Fig. 3A, treatment with Sr^{2+} had a major effect on OC adhesion, which was higher in the control condition (0 mM Sr^{2+}) and decreased in Sr^{2+}-treated cultures, in a dose-dependent manner. Along differentiation, cells were able to merge, originating large and multinucleated OC (Fig. 3B). An increase in OC size

throughout the culture time was observed, for all tested conditions, especially in the absence of Sr^{2+} or at the lowest Sr^{2+} concentration (0.5 mM). However, when higher Sr^{2+} concentrations were used, the increase in cell size was not so evident. These differences were categorized/grouped according to the number of nuclei (2, 3-to-9 or 10+ nuclei), a measure of osteoclastogenesis (Fig. C a to c). As shown, in the absence of Sr^{2+}, the number of multinucleated OC increased along the culture time. At day 7 (Fig. 3C a), the number of OC with 2 nuclei and 3-9 nuclei, for 0 mM Sr^{2}, was significantly higher than the number of OC (within the same categories), cultured with 3 mM of Sr^{2+}. By day 21 (Fig.3C c), the number of multinucleated OC in all categories was significantly higher in control cultures compared to those with 3 mM of Sr^{2+}. Also, there were significantly more OC with 10 or more nuclei in Sr^{2+}-free control cultures than in those with 1 mM of Sr^{2+}.

OC are described as TRAP-producing cells and the only cells able to resorb mineralized substrates. As shown in Fig. 3D, OC cultured without Sr^{2+} for 21 days were able to produce TRAP, with a typical “brownish” staining resulting from TRAP enzymatic hydrolysis of tartrate substrate. In presence of Sr^{2+} concentrations, especially at 3 mM, the amount of TRAP produced by OC decreased, which is in accordance with the results obtained in the osteoclastogenesis studies. TRAP quantification results (Fig. 3E), confirmed that OC released a significantly higher amount of TRAP when cultured without Sr^{2+}. OC were also cultured for 21 days on top of dentine slices, and their ability to resorb mineralized substrates was evaluated. As illustrated in Fig. 3F, OC were able to adhere to dentine and degrade its surface, in all the tested conditions, forming typical resorption pits. However, SEM images suggest that Sr^{2+} may have an inhibitory effect on OC resorbing activity, as there is a clear decrease in the number and size of resorption pits when Sr^{2+} is present, which is particularly evident for the higher concentration tested (3 mM).

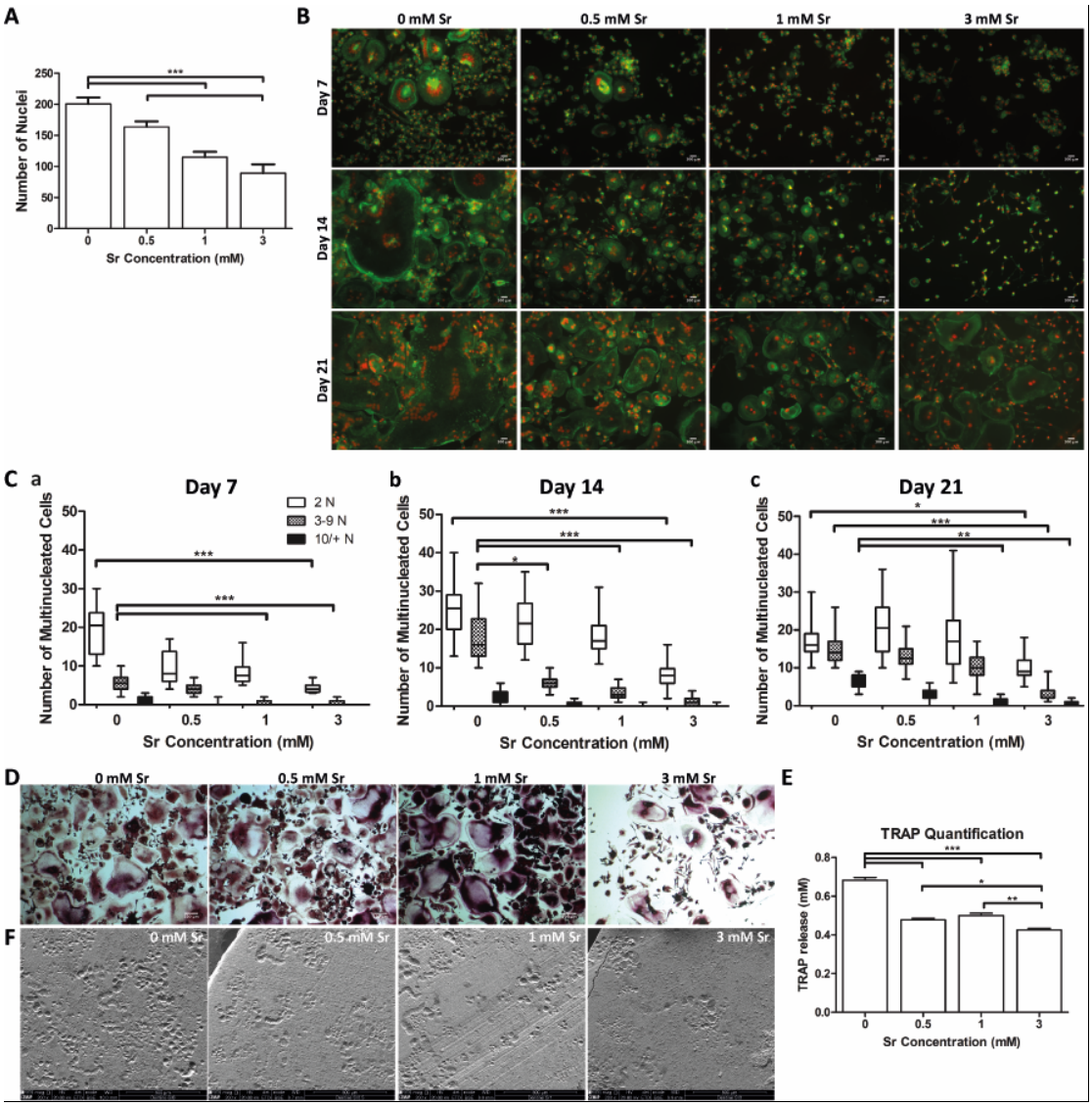

Figure 3. Sr^{2+} effect on PBMC adhesion and OC formation, TRAP production and resorption capacity. Monocytes were differentiated into OC, in the presence of M-CSF and RANKL, on TCPS without or with different strontium (Sr) concentrations (0.5, 1 and 3 mM) for up to 21 days. (A) Number of nuclei of monocytes adherent to TCPS after 7 days. (B) Staining for the actin cytoskeleton (green) and nuclei (red) at days 7, 14 and 21 and (C) quantification of number of nuclei per cell, at days: 7 (a), 14 (b) and 21 (c). Boxes represent the median and min-max percentiles and whiskers represent 5–95 percentiles. (D) TRAP staining of OC differentiated for 21 days and (E) quantification of TRAP production in 24h, measured in the supernatant and lysate of cells. Statistical significance: *p < 0.05; **p < 0.01; ***p < 0.001. (F) SEM images of resorption pits in the surface of dentine slices created by functional OC.

3.4. The Sr-hybrid system supports MSC and OC adhesion

After establishing the effect of relevant Sr^{2+} concentrations on MSC and OC response, the effect of the Sr-hybrid system on osteogenesis and osteoclastogenesis was evaluated. Combined brightfield/fluorescence imaging of the system with f-

actin/nuclei stained MSC and OC, cultured for 21 days on Sr-hybrid system, allowed for the spatial localization of the microspheres (more opaque within the hydrogel) and labeled cells (Fig. 4). As shown, both cell types could be cultured in contact with Sr-hybrid system, being preferably located in the vicinities of the microspheres.

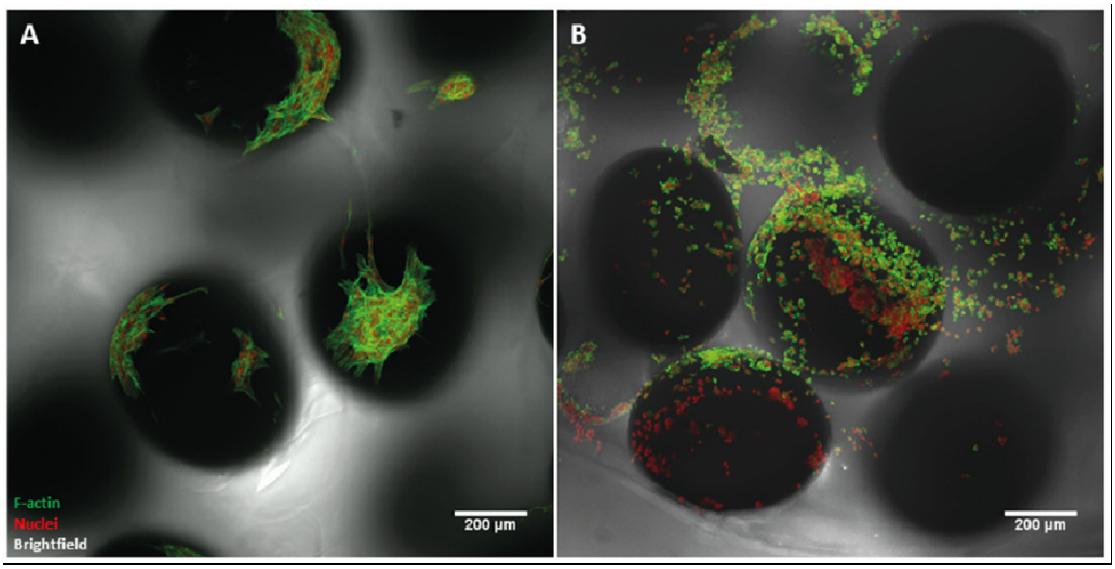

Figure 4 – Cells located in the vicinity of microspheres in Sr-hybrid system. Cells cultured on Sr-hybrid system at day 14, stained for f-actin (in green) and nuclei (in red) and brightfield chanel (showing contour of microspheres, more opaque), imaged by CLSM (Z projection). MSC under osteogenic conditions (A) and OC (B).

3.5. The Sr-hybrid system promotes osteogenic differentiation of MSC

MSC were cultured on Sr-hybrid system, under basal and osteoinductive conditions. Ca-hybrid was used as control. Live/Dead assay images (Fig. 5A) of MSC cultured under basal conditions in Ca- or Sr-hybrid at days 1, 7 and 14, show that the viability was not compromised during the time of culture. Moreover, in both systems, a progressive increase in the number of cells was observed, suggesting that MSC were able to proliferate. ALP activity was also evaluated in both systems for MSC cultured under osteogenic conditions (Fig. 5B). Higher ALP activity was observed for the Sr-hybrid, as compared to the control, at day 7. As shown in Fig. 5C, when cultured under osteogenic conditions, MSC adopted a spread shape with polygonal osteoblast-like morphology. While no differences were observed in MSC viability or

morphology in the Sr-hybrid, as compared to Ca-hybrid, increased ALP expression suggested enhanced osteogenic differentiation.

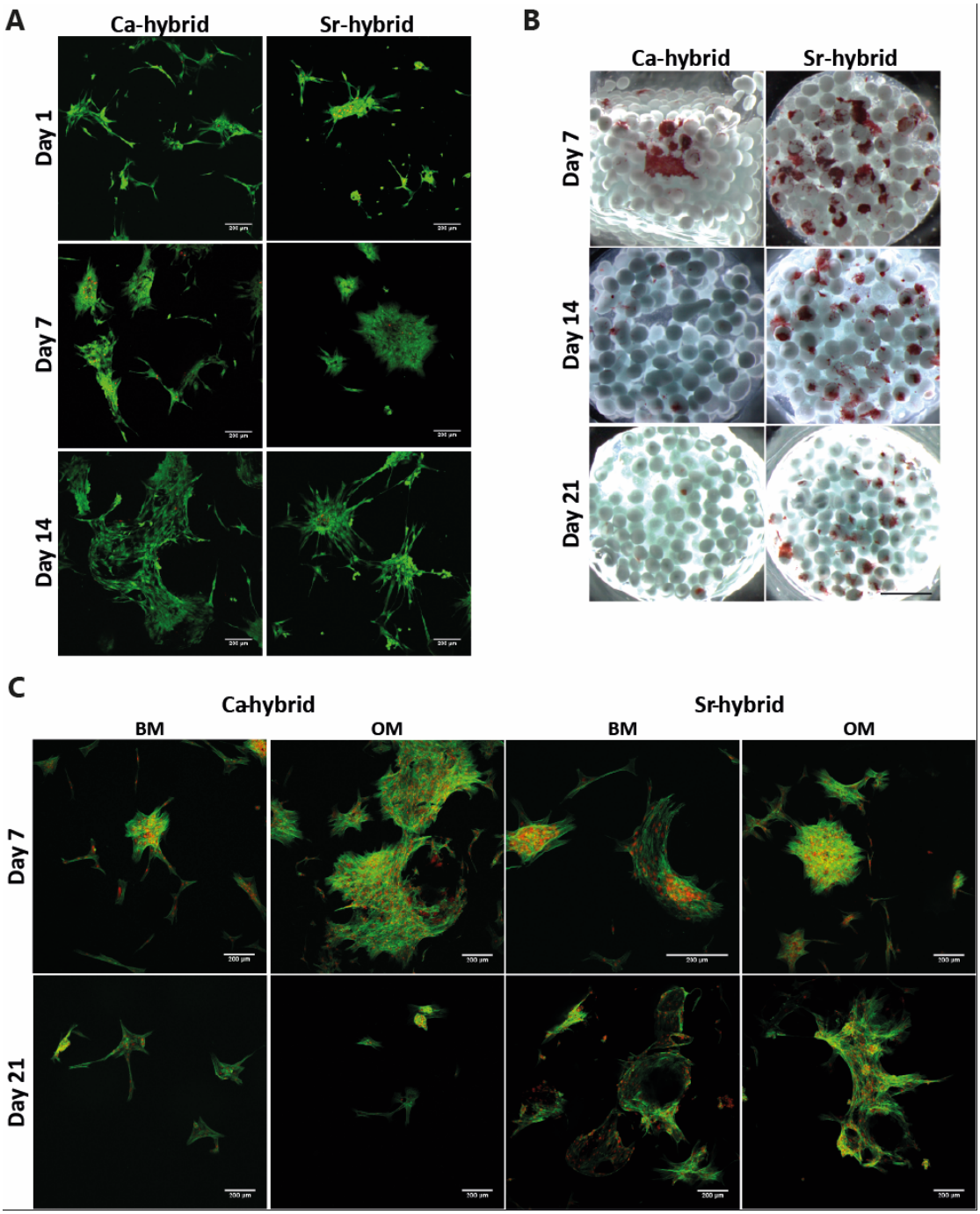

Figure 5 – Sr-Hybrid effect on MSC survival and osteogenic differentiation. (A) Viability of MSC cultured on Sr-hybrid or Ca-hybrid systems after 1,7 and 14 days imaged by CLSM (Z projection, live cells in green, dead cells in red, scale bars: 200 µm). (B) ALP staining images of MSC cultured on Sr- or Ca-hybrid systems under osteogenic conditions at days 7, 14 and 21 (Scale bar 1 mm). (C) F-actin staining of MSC cultured on Sr- or Ca-hybrid, under basal (BM) or osteogenic conditions (OM), at days 7 and 21, imaged by CLSM (Z-projection, F-actin in green, nuclei in red, scale bars: 200 µm).

3.6. Sr-hybrid system decreases OC adhesion, fusion and activity

Human PBMC were allowed to differentiate into OC on Sr-hybrid and Ca-hybrid systems for 21 days, and both osteoclastogenesis and OC functionality were evaluated (Fig. 6). Images of f-actin stained OC cultured on both systems at days 7 and 21 are depicted in Fig. 6A, showing that cells were able to adhere and merge to form multinucleated OC in both systems. Already at day 7, it was possible to detect more adherent cells in the Ca-hybrid system. The extent of osteoclastogenesis was decreased in the Sr-hybrid, as compared to the control, where the presence of larger and multinucleated OC was more evident, especially at day 21. OC functionality was assessed by TRAP staining, at days 7, 14 and 21 (Fig. 6B). The Sr-hybrid apparently inhibited the ability of OC to secrete TRAP after 7 days of culture, which was not observed for the Ca-hybrid system. During the culture period, it was also possible to observe the presence of “brownish” agglomerates on the Ca-hybrid system, indicating that OC maintained their functionality when cultured for 21 days in the absence of Sr^{2+}. These results were further confirmed by quantification of released TRAP (Fig. 6C), which was significantly lower in Sr-hybrid ($p<0.001$), suggesting that OC were more functional on Ca-hybrid than on Sr-hybrid system.

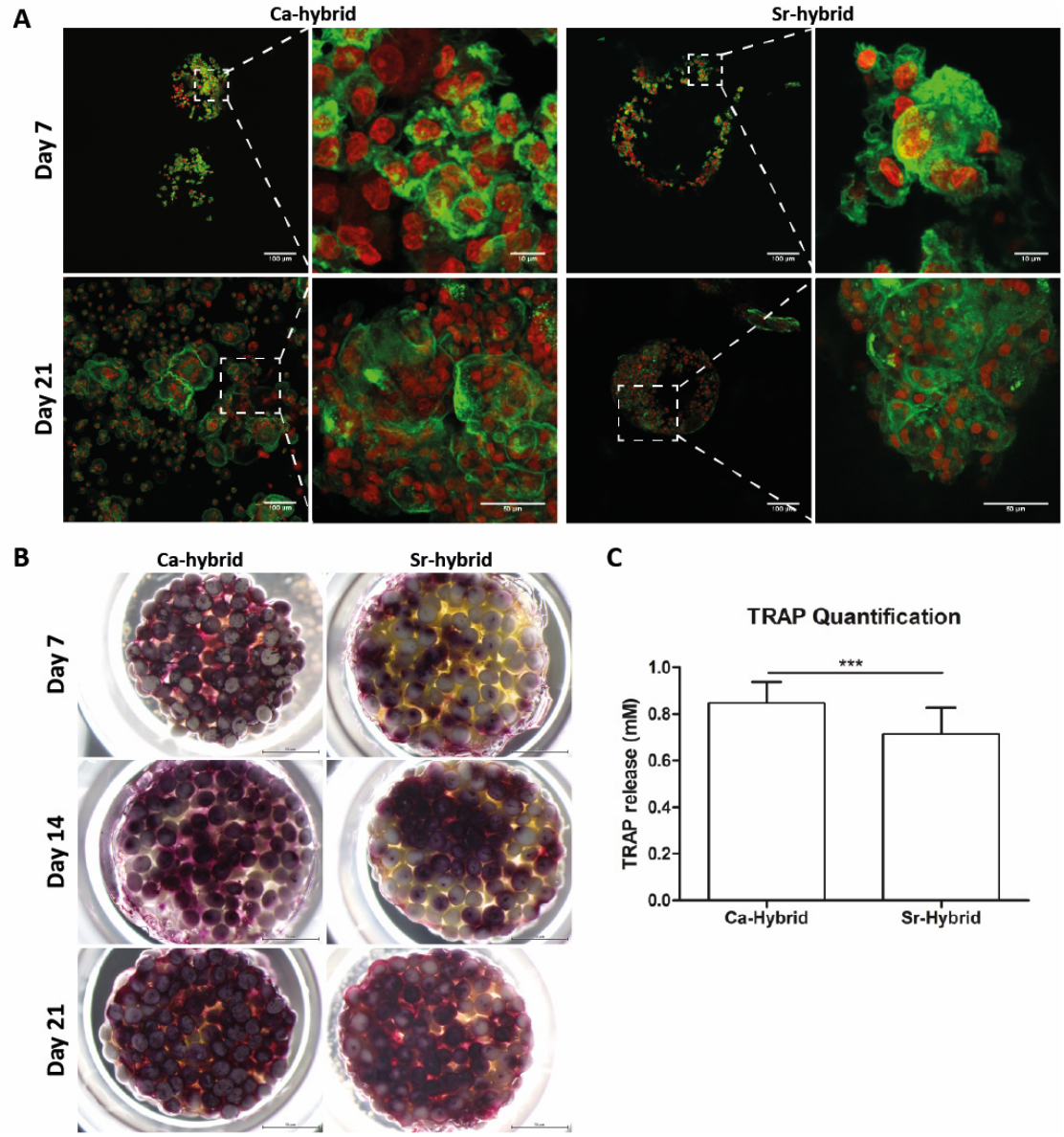

Figure 6 - Sr-hybrid system effect on OC formation and TRAP production. PBMC were allowed to differentiate into OC in the presence of M-CSF and RANKL for up to 21 days, on Sr-hybrid or Ca-hybrid systems. (A) OC cytoskeleton (green) and nuclei (red) staining at days 7 and 21 imaged by CLSM (Z projection). (B) TRAP staining and (C) quantification of its production after 24h. Statistical significance: *p < 0.05; **p < 0.01; ***p < 0.001.

3.7. Sr-hybrid system promotes M2 macrophage polarization *in vivo*

An *in vivo* air-pouch model of inflammation was used to evaluate the inflammatory response to the developed Sr-hybrid system, in comparison to Ca-hybrid. Three different animal groups were performed: Sham-operated, Ca-hybrid-implanted and Sr-hybrid-implanted animals. Three days after implantation, the inflammatory cells

present in the inflammatory exudates retrieved from the air-pouches were analysed by flow cytometry (Fig. 7A) and in addition, the exudates were evaluated using a cytokine array (Fig. 7B). The average number of cells recovered from the air-pouches was higher in the sham-operated animals, with a statistically significant ($p<0.05$) decrease for cells retrieved from the Ca-hybrid group (Fig. 7A a). Macrophages were identified using F4/80, a commonly used murine macrophage marker, and CCR7 and CD206 were used as specific M1 and M2 markers, respectively. As depicted in Fig. 7A b, the percentage of F4/80+/CCR7+ cells, marking M1 macrophages, was low and showed no significant differences between groups. However, regarding M2 macrophages, in the Sr-hybrid group, a statistically significant increase ($p<0.05$) in the percentage of F4/80+/CD206+ cells was observed when compared to the control (Sham-operated, Fig. 7A c).

The cytokine production by the inflammatory cells was analyzed by a cytokine array (Supplementary Fig. 1) and the cytokines with at least a 1.5 fold-change to the control (Sham-operated group) are depicted in Fig. 7B. Sr-hybrid implantation caused a decrease in inflammatory cytokines, such us TNF-RI, MIP-1gamma and RANTES, compared to Ca-hybrid. Similar levels of TNF-α were observed for the two experimental groups and a decrease in IL-6 was also seen in both groups. Importantly, in the Sr-hybrid group, the cytokine levels were indicative of a mild inflammatory response, as opposed to Ca-hybrid group, where higher range variations were observed, from -4 to 2 times fold-change to control in Sr-hybrid group as opposed to variations from -12 to 15 times fold-change to control in Ca-hybrid system. These results seem to corroborate the flow cytometry analysis, where the overall evidences point out to an M2 macrophage response after Sr-hybrid implantation.

Histological analysis of materials and surrounding tissues at day 3 was performed and representative H&E stained sections are shown in Fig. 7 C. In sham-operated animals, normal skin structures can be observed as well as the presence of the

collapsed air-pouch surrounding fibroblastic-like cells (Fig. 7C a and b). In the experimental groups (Fig. 7C c to h), this structure was also present, surrounding the materials with high cell infiltration in the nearby tissue. These tissues were also analyzed after 15 days of implantation and Masson's Trichrome (MT) stained sections are shown in Fig. 7D, where collagen is stained in blue. A thin fibrous capsule with low infiltration of inflammatory cells within the scaffolds was observed in both materials. The thickness of this capsule was measured and results are shown in Fig. 7E. An average thickness of 150 μm was measured and no statistically significant differences were observed between Sr-hybrid and Ca-hybrid groups. Furthermore, histological analysis of liver, kidneys, spleen (Supplementary Fig. 2), and heart of animals were also performed to assess possible detrimental systemic effects of the designed system, especially regarding cardiovascular safety due to the recent restrictions in Sr Ranelate prescription. As shown in Fig. 7F, MT stained sections of hearts do not show any deposition of collagen in the myocardium or any noteworthy alterations in the Sr-hybrid implanted group after 15 days, as compared to the Ca-hybrid group and Sham-operated animals.

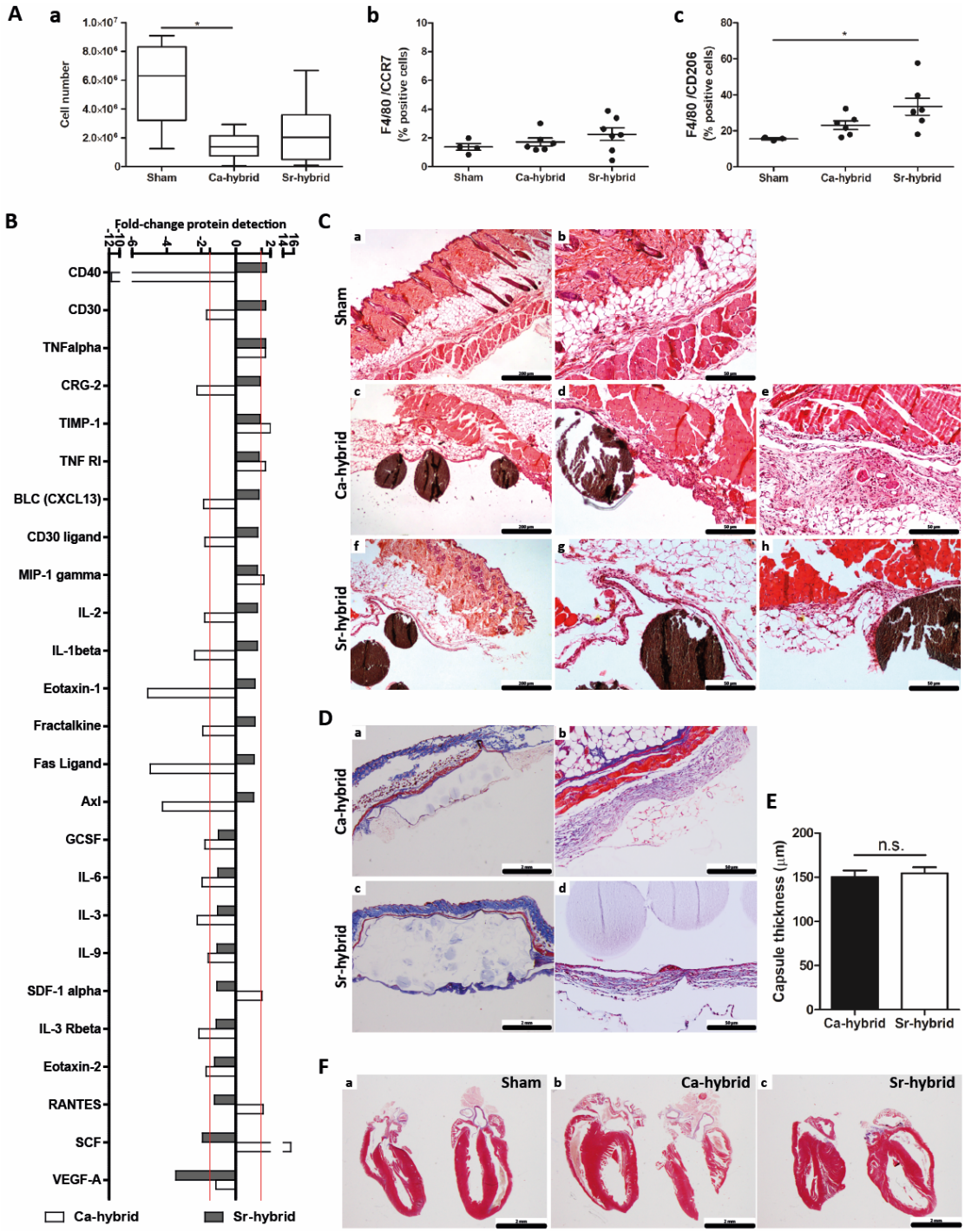

Figure 7 – Characterization of the *in vivo* inflammatory response to the implantation of the Sr-hybrid system. (A) Flow cytometry analysis after 3 days of implantation regarding (a) total cell number, (b) percentage of F4/80+/CCR7+ (M1 macrophages) and (c) percentage of F4/80+/CD206+ (M2 macrophages) cells. Results are shown as mean±SE, statistical significance: *p < 0.05. **(B)** Cytokine production by inflammatory cells present on the retrieved inflammatory exudates evaluated using a cytokine array. Results are shown as fold-change to control (sham-operated animals) of exudates retrieved from Ca-hybrid and Sr-hybrid animal groups. **(C)** H&E stained sections of the surrounding tissues and implanted materials after 3 days of implantation of sham animals (a, b), Ca-hybrid (c, d ,e) and Sr-hybrid (f, g, h) group. **(D)** MT stained sections of the surrounding tissues and implanted materials after 15 days of implantation of Ca-hybrid (a, b) and Sr-hybrid (c, d) group. Collagen - blue **(E)** Thickness of the fibrous capsule found surrounding the implants after 15 days of implantation. n.s. – not statistically significant. **(F)** MT stained sections of the hearts of the animals retrieved after 15 days (collagen – blue).

4. Discussion

We have designed a hybrid polymeric-ceramic material, here designated as Sr-hybrid system, for bone regeneration applications. The system is highly enriched in Sr, being composed of Sr-HAp microspheres embedded in an RGD-modified alginate hydrogel that crosslinks *in situ* in the presence of Sr carbonate, where Sr^{2+} acts as the crosslinking agent. This Sr-hybrid system is expected to have a dual role, acting on one hand as a Sr^{2+} delivery system and, on the other hand, as a bone-defect injectable filler for repair/regeneration strategies. In this system, alginate hydrogels were chemically modified with RGD peptides, providing a more physiologically relevant microenvironment, which better mimics the natural extracellular matrix (ECM). The incorporation of RGD is important to promote cell anchorage, in otherwise non-adhesive hydrogels, and to improve cell survival and function, as we previously demonstrated using osteoblastic cell lines and MSC, and also other relevant cell types such as endothelial cells [36, 37, 52]. The alginate hydrogel can be crosslinked *in situ*, using a previously described internal gelation strategy [36, 37, 42, 43, 52], enabling the injectability of the system, which is an important advantage in clinical use. HAp microspheres, embedded within the hydrogel, act as mechanical reinforcement of the system [38]. Microspheres with a diameter of around 500 μm were used, as this size results in sufficient interstitial space within packed microspheres, which is expected to provide an adequate porosity for new tissue ingrowth upon implantation [38, 53]. Microspheres prepared by the same methodology were previously studied [40, 54, 55]. MG63 osteoblast-like cells and human MSC were shown to be able to spread on their surface, produce their own ECM and even bridge adjacent microspheres [54]. The composite nature of bone has previously inspired the development of other biomimetic materials for bone regeneration [5], where hydrogels were combined with calcium phosphates [8]. Apart from Ca^{2+}, the incorporation of additional metal ions in calcium phosphate ceramics, such as Sr^{2+} or Mg^{2+}, is of particular interest, due to their high affinity for HAp and

demonstrated bioactivity [56, 57]. Several studies, as systematically reviewed in [58], have shown increased *in vivo* bone formation and bone remodelling upon Sr addition to biomaterials. Particularly, the addition of Sr to HAp in different HAp/alginate materials has shown to lead to increase *in vitro* bioactivity [22] and *in vivo* bone formation [26, 39, 57].

The hybrid system has two Sr^{2+} sources, the hydrogel and the microspheres. Results showed that after 15 days of incubation in cell culture medium, only 0.3% (corresponding to 0.3 mM) of the total amount of Sr^{2+} initially present in the Sr-hybrid had been released. This suggests that the system is able to provide a sustained release of Sr^{2+} over long periods of time, which is very appealing for clinical applications. A more detailed analysis along the first 72 h of incubation, showed that Sr^{2+} release profile is characterized by an initial burst, followed by a plateau. By studying the behavior of the microspheres alone, we were able to conclude that they release Sr^{2+} at a slower rate, presumably due to the rather stable nature of Sr-HAp, while the hydrogel releases Sr^{2+} at a faster rate, mainly due to ionic exchange with non-gelling ions present in the medium. The magnitude of the values observed is in the same range of clinically relevant Sr concentrations, since upon oral administration of Sr Ranelate therapeutic (2g/day/3 years), serum concentrations of 0.12 mM Sr were found [59].

After establishing the Sr^{2+} release kinetics profile of our system, we set out to check the effect of relevant Sr^{2+} concentrations on MSC and OC response, first by using a simpler *in vitro* model of monolayer cultures, and then by testing the system itself.

The presence of Sr^{2+} in the MSC culture medium showed that under basal conditions the addition of a concentration of 3 mM led to increased metabolic activity and an increase in cell proliferation for all concentrations tested. Under osteogenic conditions, the presence of Sr^{2+} led to increased metabolic activity and cell proliferation only for low Sr^{2+} doses (0.5 and 1 mM Sr^{2+}), after 21 days of culture.

Some controversy can be found in the literature regarding the effect of different Sr^{2+} concentrations on different cell types. For example, Li and colleagues reported that proliferation of rat bone marrow MSC (BMMSC) was inhibited in the presence of Sr^{2+}concentrations between 0.1 and 1 mM after 15 days of culture under basal conditions [11]. In contrast, our results show that 0.5 and 1 mM Sr^{2+} increase cell proliferation after 14 days under basal conditions. In another study using human MSC, and Sr^{2+} concentrations ranging from 0.001 to 10 mM, an increase in cell proliferation after 21 days under osteogenic conditions was observed for concentrations up to 0.1 mM, and the opposite effect was observed for higher concentrations, from 1 to 10 mM. Similar results were seen in basal conditions, however, for 1 mM Sr^{2+} only a slight decrease in cell number was observed [60]. Our results did not show a decrease in cell proliferation, however a similar trend of higher proliferation at lower concentrations was also observed.

In terms of MSC osteogenic differentiation, the expression of ALP activity increased in Sr-treated cultures, particularly under osteogenic conditions and at higher Sr^{2+} concentrations (1 and 3 mM Sr^{2+}). A similar positive effect was also observed for the Sr-hybrid system. MSC were able to adhere and spread on the hybrid scaffolds and remained viable along the culture, showing increased expression of ALP activity from early time points on the Sr-hybrid system, as compared to the control Ca-hybrid system. The effect of Sr^{2+} on MSC and osteoblastic cells has been described in several studies. For example, Peng and colleagues treated primary murine BMMSC cultures with Sr^{2+} concentrations similar to the ones tested herein (1 and 3 mM Sr^{2+}), showing that both dosages promoted osteogenic differentiation with an increase in Runx2 (day 7), ALP activity (day 14) and calcium nodules (day 21, Alizarin red staining), in a dose-dependent manner [15]. Also, studies using human umbilical cord-derived MSC treated with 2 mM Sr^{2+} showed a significant increase in ALP activity (day 10) and mineralization nodules (4 weeks, Von Kossa), as compared to osteoinductive media without the addition of Sr^{2+} [10]. This effect was shown to be

mainly dose-dependent. Studies from Li *et al* also demonstrated that rat BMMSC treated with 0.1 and 1 mM Sr^{2+} exhibited higher ALP activity after 2 weeks of culture, as compared to untreated cells [11]. On the other hand, Verberckmoes and co-workers showed a multiphasic effect of Sr^{2+} on *in vitro* bone formation, using primary cultures of rat calvaria osteoblasts treated with Sr^{2+} at concentrations ranging from 0.00625 to 1 mM [13]. At low Sr^{2+} concentrations an inhibitory effect on osteoblastic differentiation was observed with a decrease in mineralized nodule formation [13]. These results were also supported by studies from Wornham and coworkers that showed a decrease in mineralization nodules when primary osteoblast cells retrieved from Sprague Dawly calvaria were cultured in the presence of Sr concentrations of 0.1 and 1 mM [61]. Studies from Schumacher *et al* showed a deleterious effect in human MSC osteogenic differentiation for Sr^{2+} concentrations above 0.1 mM, with a decrease in ALP activity (day 14) for Sr^{2+} concentrations of 1 and 5 mM [60].

Regarding OC response, our results showed the inhibitory effect of Sr^{2+} on the ability of OC to attach to a substrate and merge. The number of large, multinucleated OC decreased in the presence of Sr^{2+}, in a dose-dependent manner. OC treated with higher Sr^{2+} concentrations also showed decreased functionality, with lower expression of TRAP activity and impaired ability to resorb mineralized substrates. Likewise, osteoclastogenesis occurred to a lower extent on Sr-hybrid scaffolds, as compared to Ca-hybrid control. Although human PBMC could be cultured on both types of materials and successfully differentiate into OC, more adherent cells were detected in the Ca-hybrid system, with higher number of multinucleated and larger OC. The ability of OC to secrete TRAP also decreased in the Sr-hybrid, as compared to the Ca-hybrid where OC seemed to be more functional. Similar effects of Sr on OC activity were reported by Schumacher *et al*, in which higher Sr^{2+} concentrations of 5 mM and 10 mM Sr^{2+} promoted a decrease in the number of adherent cells, while 1 mM did not show significant alterations in cell behavior [62]. Similarly, in another study, 1 mM only exerted a modest reduction on OC number and resorption area

[61]. Moreover, the analysis of the enzymatic activities of TRAP and carbonic anhydrase type II, and gene expressions of denditric cell-specific transmembrane protein and CD44, did not show any effect of Sr in osteoclastogenesis besides the observation of actin disruption in some cells at 0.1 mM Sr^{2+} concentration [62]. Interestingly, it has been previously demonstrated that 1 mM of Sr^{2+} was sufficient to decrease the expression of functional osteoclast markers such as integrin $\alpha_v\beta_3$, a vitronectin receptor that has a prominent role in osteoclast adhesion, being involved in podosomes formation and cytoskeleton re-organization, and is also implicated in OC motility and in the maintenance of the sealing zone [18]. Accordingly, 1 mM of Sr^{2+} was previously found to inhibit the ability of mouse and chicken OC to resorb the surface of dentine slices [16] and to decrease the number of OC expressing carbonic anhydrase II, an enzyme that dissolves bone matrix [18]. Importantly, the loss of OC functionality when cultured in the presence of Sr^{2+} might be explained by its ability to disrupt the OC actin-containing sealing zone and the ruffled border, essential for the OC resorbing activity *in vitro* and bone resorption [15-17]. Another study demonstrated that Sr impaired osteoclastogenesis by blocking RANKL-induced activation of the NF-κB pathway [63].

Evidence in recent years has been shifting concepts in the bone regeneration field, where inflammatory cells and their mediators are being nowadays considered crucial players for proper bone healing [29]. Therefore, current strategies include the design of immunomodulatory biomaterials able to establish a pro-regenerative *milieu* [34, 35]. Upon biomaterial implantation, macrophages are amongst the first cells to arrive to the injury site and their polarization and M2/M1 increased ratio may be beneficial to improve tissue regeneration. Some studies suggested that Sr may have immunomodulatory properties [63-65], however the information in the literature concerning the influence of Sr-rich biomaterials in the host immune response is very scarce, being the present work a significant contribution to the field.

Our results show a decrease in the number of inflammatory cells recruited to the implant site in both materials compared to sham-operated animals, but most importantly, an increase in the number of M2 macrophages was observed in the Sr-hybrid group. These results are in agreement with others where Sr has been shown to promote an M2 polarization of macrophages. In studies of Yuan and coworkers, surface modification of titanium surfaces with Ca and Sr, either alone or in different Ca:Sr ratios, have shown that the presence of Sr was able to increase the number of M2 macrophages in a similar *in vivo* model, although no differences were seen between coatings of Ca and Sr alone [64]. Another work using the air-pouch model of inflammation showed that a Sr-substituted sub-micron bioactive glass (SBG) significantly increased the number of M2 macrophages as compared to bare SBG [65]. The cytokine analysis of the inflammatory exudates revealed a mild inflammatory reaction to Sr-hybrid, when compared to Ca-hybrid system. In Sr-hybrid system, increased levels of both TNF-α and IL-1β were observed, shown to correlate with an increase in MSC mineralization potential [66]. Although a decrease in RANTES and SDF-1α, both known to recruit MSC [67-69], was observed in Sr-hybrid implanted animals, the material did not show a decreased capacity to promote bone regeneration. In an *in vivo* model, Sr-hybrid was seen to promote, 60 days after implantation, an increase in cell recruitment and in new bone formation at both center and periphery of the defect, as opposed to Ca-hybrid where new bone formation was limited to the periphery of the defect [39].

The histological analysis revealed a thin fibrous capsule, with a non-significant difference between groups, and low numbers of inflammatory cells were observed in the implanted materials groups. Although neither system induced a massive M1-like inflammatory response, our results indicate that Sr-hybrid system was able to promote an M2 regenerative response when compared to the Ca-hybrid system.

Recent concerns regarding Sr ranelate oral administration also highlight the importance of the use of Sr-releasing materials for local delivery. In this study, the

histological evaluation of organs and particularly the hearts of animals did not show any alteration after 15 days. Furthermore, in an *in vivo* critical-sized bone defect model, no alterations were observed in peripheral organs (liver, kidneys, spleen) or in Sr serum levels of animals implanted with Sr-hybrid [39].

Taken together, our results demonstrate that the Sr-hybrid scaffold promotes long-term Sr^{2+} release and exhibits both osteoinductive and anti-osteoclastogenesis properties. Moreover, it was able to modulate the immune response towards the M2 macrophage phenotype. These results highlight the potential of this injectable biomaterial for bone repair/regeneration, particularly for the treatment of pathological conditions where bone remodelling is impaired, namely osteoporosis.

5. Conclusions

Our findings confirmed that the proposed Sr-hybrid, which acted as Sr^{2+} release system, has the ability to drive the differentiation of MSC towards the osteoblastic lineage, while inhibiting OC adhesion/fusion, activity and resorptive behaviour. This dual effect of Sr^{2+} is of major interest for the therapeutic management of bone pathologies characterized by abnormal bone remodelling such as osteoporosis. The Sr-hybrid also showed to be able to modulate the immune response, inducing macrophage polarization towards a pro-regenerative M2 phenotype. Moreover, the system exhibits some unique properties, such as injectability for minimally invasive surgery, mechanical reinforcement with HAp microspheres, and sustained Sr^{2+} release over extended periods of time, which are appealing for future clinical applications.

Acknowledgments

The authors would like to thank Hospital S. João, for kindly donating the buffy coats. This work was financed by FEDER funds, through the Programa Operacional

Factores de Competitividade — COMPETE and by Portuguese funds through FCT — Fundação para a Ciência e a Tecnologia in the framework of the project PTDC/CTM/103181/2008. A.H. Lourenço is recipient of a doctoral fellowship from FCT, ref. SFRH/BD/87192/2012. ALT thanks FCT for the doctoral grant SFRH/BD/94306/2013 and the BiotechHealth PhD Programme. Daniela P. Vasconcelos is funded by FCT - Fundação para a Ciência e Tecnologia through the FCT PhD Programmes and by Programa Operacional Potencial Humano (POCH), specifically by the BiotechHealth Programme (Doctoral Programme on Cellular and Molecular Biotechnology Applied to Health Sciences – reference *PD/00016/2012*), and through the PhD studentship *PD/BD/114011/2015.* CB acknowledges her research position (IF/00296/2015) funded by FCT and POPH/ESF (EC).

Disclosures

The authors declare no conflict of interest.

References

[1] X. Feng, J.M. McDonald, Disorders of Bone Remodeling, Annual review of pathology 6 (2011) 121-145.
[2] G.A. Rodan, T.J. Martin, Therapeutic Approaches to Bone Diseases, Science 289(5484) (2000) 1508-1514.
[3] E.M.M. Van Lieshout, V. Alt, Bone graft substitutes and bone morphogenetic proteins for osteoporotic fractures: what is the evidence?, Injury 47, Supplement 1 (2016) S43-S46.
[4] K.L. Low, S.H. Tan, S.H.S. Zein, J.A. Roether, V. Mouriño, A.R. Boccaccini, Calcium phosphate-based composites as injectable bone substitute materials, Journal of Biomedical Materials Research Part B: Applied Biomaterials 94B(1) (2010) 273-286.
[5] A.R. Amini, C.T. Laurencin, S.P. Nukavarapu, Bone Tissue Engineering: Recent Advances and Challenges, Critical reviews in biomedical engineering 40(5) (2012) 363-408.
[6] M.M. Stevens, Biomaterials for bone tissue engineering, Materials Today 11(5) (2008) 18-25.
[7] F. Barrere, C.A. van Blitterswijk, K. de Groot, Bone regeneration: molecular and cellular interactions with calcium phosphate ceramics, Int J Nanomedicine 1(3) (2006) 317-32.
[8] M. D'Este, D. Eglin, Hydrogels in calcium phosphate moldable and injectable bone substitutes: Sticky excipients or advanced 3-D carriers?, Acta Biomaterialia 9(3) (2013) 5421-5430.
[9] L. Cianferotti, F. D'Asta, M.L. Brandi, A review on strontium ranelate long-term antifracture efficacy in the treatment of postmenopausal osteoporosis, Therapeutic Advances in Musculoskeletal Disease 5(3) (2013) 127-139.
[10] F. Yang, D. Yang, J. Tu, Q. Zheng, L. Cai, L. Wang, Strontium Enhances Osteogenic Differentiation of Mesenchymal Stem Cells and In Vivo Bone Formation by Activating Wnt/Catenin Signaling, STEM CELLS 29(6) (2011) 981-991.
[11] Y. Li, J. Li, S. Zhu, E. Luo, G. Feng, Q. Chen, J. Hu, Effects of strontium on proliferation and differentiation of rat bone marrow mesenchymal stem cells, Biochemical and Biophysical Research Communications 418(4) (2012) 725-730.
[12] J. Caverzasio, C. Thouverey, Activation of FGF receptors is a new mechanism by which strontium ranelate induces osteoblastic cell growth, Cellular physiology and biochemistry : international journal of experimental cellular physiology, biochemistry, and pharmacology 27(3-4) (2011) 243-50.
[13] S.C. Verberckmoes, M.E. De Broe, P.C. D'Haese, Dose-dependent effects of strontium on osteoblast function and mineralization, Kidney Int 64(2) (2003) 534-543.
[14] Z. Saidak, E. Haÿ, C. Marty, A. Barbara, P.J. Marie, Strontium ranelate rebalances bone marrow adipogenesis and osteoblastogenesis in senescent osteopenic mice through NFATc/Maf and Wnt signaling, Aging Cell 11(3) (2012) 467-474.
[15] S. Peng, G. Zhou, K.D.K. Luk, K.M.C. Cheung, Z. Li, W.M. Lam, Z. Zhou, W.W. Lu, Strontium Promotes Osteogenic Differentiation of Mesenchymal Stem Cells Through the Ras/MAPK Signaling Pathway, Cellular Physiology and Biochemistry 23(1-3) (2009) 165-174.
[16] N. Takahashi, T. Sasaki, Y. Tsouderos, T. Suda, S 12911-2 Inhibits Osteoclastic Bone Resorption In Vitro, Journal of Bone and Mineral Research 18(6) (2003) 1082-1087.
[17] E. Bonnelye, A. Chabadel, F. Saltel, P. Jurdic, Dual effect of strontium ranelate: Stimulation of osteoblast differentiation and inhibition of osteoclast formation and resorption in vitro, Bone 42(1) (2008) 129-138.

[18] R. Baron, Y. Tsouderos, In vitro effects of S12911-2 on osteoclast function and bone marrow macrophage differentiation, European Journal of Pharmacology 450(1) (2002) 11-17.
[19] J.Y. Reginster, A. Neuprez, N. Dardenne, C. Beaudart, P. Emonts, O. Bruyere, Efficacy and safety of currently marketed anti-osteoporosis medications, Best Practice & Research Clinical Endocrinology & Metabolism 28(6) (2014) 809-834.
[20] C. Cooper, K.M. Fox, J.S. Borer, Ischaemic cardiac events and use of strontium ranelate in postmenopausal osteoporosis: a nested case–control study in the CPRD, Osteoporosis International 25(2) (2014) 737-745.
[21] B. Abrahamsen, E.L. Grove, P. Vestergaard, Nationwide registry-based analysis of cardiovascular risk factors and adverse outcomes in patients treated with strontium ranelate, Osteoporosis International 25(2) (2014) 757-762.
[22] M. Raucci, D. Giugliano, M.A. Alvarez-Perez, L. Ambrosio, Effects on growth and osteogenic differentiation of mesenchymal stem cells by the strontium-added sol–gel hydroxyapatite gel materials, J Mater Sci: Mater Med 26(2) (2015) 1-11.
[23] V. Nardone, S. Fabbri, F. Marini, R. Zonefrati, G. Galli, A. Carossino, A. Tanini, M.L. Brandi, Osteodifferentiation of Human Preadipocytes Induced by Strontium Released from Hydrogels, International Journal of Biomaterials 2012 (2012) 10.
[24] Y. Zhu, Y. Ouyang, Y. Chang, C. Luo, J. Xu, C. Zhang, W. Huang, Evaluation of the proliferation and differentiation behaviors of mesenchymal stem cells with partially converted borate glass containing different amounts of strontium in vitro, Molecular medicine reports 7(4) (2013) 1129-36.
[25] K. Sariibrahimoglu, W. Yang, S.C.G. Leeuwenburgh, F. Yang, J.G.C. Wolke, Y. Zuo, Y. Li, J.A. Jansen, Development of porous polyurethane/strontium-substituted hydroxyapatite composites for bone regeneration, Journal of Biomedical Materials Research Part A (2014) n/a-n/a.
[26] J. Hao, A. Acharya, K. Chen, J. Chou, S. Kasugai, N.P. Lang, Novel bioresorbable strontium hydroxyapatite membrane for guided bone regeneration, Clinical Oral Implants Research 26(1) (2015) 1-7.
[27] C.T. Wong, W.W. Lu, W.K. Chan, K.M.C. Cheung, K.D.K. Luk, D.S. Lu, A.B.M. Rabie, L.F. Deng, J.C.Y. Leong, In vivo cancellous bone remodeling on a strontium-containing hydroxyapatite (sr-HA) bioactive cement, Journal of Biomedical Materials Research Part A 68A(3) (2004) 513-521.
[28] M. Baier, P. Staudt, R. Klein, U. Sommer, R. Wenz, I. Grafe, P. Meeder, P. Nawroth, C. Kasperk, Strontium enhances osseointegration of calcium phosphate cement: a histomorphometric pilot study in ovariectomized rats, Journal of Orthopaedic Surgery and Research 8(1) (2013) 16.
[29] F. Loi, L.A. Córdova, J. Pajarinen, T.-h. Lin, Z. Yao, S.B. Goodman, Inflammation, fracture and bone repair, Bone 86(Supplement C) (2016) 119-130.
[30] A. Mantovani, A. Sica, S. Sozzani, P. Allavena, A. Vecchi, M. Locati, The chemokine system in diverse forms of macrophage activation and polarization, Trends in Immunology 25(12) 677-686.
[31] B.N. Brown, B.M. Sicari, S.F. Badylak, Rethinking Regenerative Medicine: A Macrophage-Centered Approach, Frontiers in Immunology 5 (2014) 510.
[32] F.O. Martinez, S. Gordon, The M1 and M2 paradigm of macrophage activation: time for reassessment, F1000Prime Reports 6 (2014) 13.
[33] D.P. Vasconcelos, A.C. Fonseca, M. Costa, I.F. Amaral, M.A. Barbosa, A.P. Águas, J.N. Barbosa, Macrophage polarization following chitosan implantation, Biomaterials 34(38) (2013) 9952-9959.
[34] D.P. Vasconcelos, M. Costa, I.F. Amaral, M.A. Barbosa, A.P. Águas, J.N. Barbosa, Modulation of the inflammatory response to chitosan through M2 macrophage polarization using pro-resolution mediators, Biomaterials 37(Supplement C) (2015) 116-123.

[35] D.P. Vasconcelos, M. Costa, I.F. Amaral, M.A. Barbosa, A.P. Águas, J.N. Barbosa, Development of an immunomodulatory biomaterial: Using resolvin D1 to modulate inflammation, Biomaterials 53(Supplement C) (2015) 566-573.
[36] S.I.J. Bidarra, C.C. Barrias, M.r.A. Barbosa, R. Soares, P.L. Granja, Immobilization of Human Mesenchymal Stem Cells within RGD-Grafted Alginate Microspheres and Assessment of Their Angiogenic Potential, Biomacromolecules 11(8) (2010) 1956-1964.
[37] S.J. Bidarra, C.C. Barrias, K.B. Fonseca, M.A. Barbosa, R.A. Soares, P.L. Granja, Injectable in situ crosslinkable RGD-modified alginate matrix for endothelial cells delivery, Biomaterials 32(31) (2011) 7897-7904.
[38] N. Neves, B.B. Campos, I.F. Almeida, P.C. Costa, A.T. Cabral, M.A. Barbosa, C.C. Ribeiro, Strontium-rich injectable hybrid system for bone regeneration, Materials Science and Engineering: C 59 (2016) 818-827.
[39] A. Henriques Lourenço, N. Neves, C. Ribeiro-Machado, S.R. Sousa, M. Lamghari, C.C. Barrias, A. Trigo Cabral, M.A. Barbosa, C.C. Ribeiro, Injectable hybrid system for strontium local delivery promotes bone regeneration in a rat critical-sized defect model, Scientific Reports 7(1) (2017) 5098.
[40] C.C. Ribeiro, C.C. Barrias, M.A. Barbosa, Calcium phosphate-alginate microspheres as enzyme delivery matrices, Biomaterials 25(18) (2004) 4363-4373.
[41] J.A. Rowley, G. Madlambayan, D.J. Mooney, Alginate hydrogels as synthetic extracellular matrix materials, Biomaterials 20(1) (1999) 45-53.
[42] F.R. Maia, A.H. Lourenço, P.L. Granja, R.M. Gonçalves, C.C. Barrias, Effect of Cell Density on Mesenchymal Stem Cells Aggregation in RGD-Alginate 3D Matrices under Osteoinductive Conditions, Macromolecular Bioscience (2014) n/a-n/a.
[43] K.B. Fonseca, S.J. Bidarra, M.J. Oliveira, P.L. Granja, C.C. Barrias, Molecularly designed alginate hydrogels susceptible to local proteolysis as three-dimensional cellular microenvironments, Acta Biomaterialia 7(4) (2011) 1674-1682.
[44] N. Jaiswal, S.E. Haynesworth, A.I. Caplan, S.P. Bruder, Osteogenic differentiation of purified, culture-expanded human mesenchymal stem cells in vitro, Journal of Cellular Biochemistry 64(2) (1997) 295-312.
[45] M.I. Oliveira, S.G. Santos, M.J. Oliveira, A.L. Torres, M.A. Barbosa, Chitosan drives anti-inflammatory macrophage polarisation and pro-inflammatory dendritic cell stimulation, European cells & materials 24 (2012) 136-52; discussion 152-3.
[46] A.L. Torres, S.G. Santos, M.I. Oliveira, M.A. Barbosa, Fibrinogen promotes resorption of chitosan by human osteoclasts, Acta Biomaterialia 9(5) (2013) 6553-6562.
[47] B.A.C. Lopes, Cell Note: Plataforma para a análise escrita de imagens, University of Porto, Porto, 2010.
[48] K. Fuller, J.L. Ross, K.A. Szewczyk, R. Moss, T.J. Chambers, Bone Is Not Essential for Osteoclast Activation, PLOS ONE 5(9) (2010) e12837.
[49] B. Kirstein, U. Grabowska, B. Samuelsson, M. Shiroo, T.J. Chambers, K. Fuller, A novel assay for analysis of the regulation of the function of human osteoclasts, Journal of Translational Medicine 4 (2006) 45-45.
[50] A.G. Castro, N. Esaguy, P.M. Macedo, A.P. Aguas, M.T. Silva, Live but not heat-killed mycobacteria cause rapid chemotaxis of large numbers of eosinophils in vivo and are ingested by the attracted granulocytes, Infection and Immunity 59(9) (1991) 3009-3014.
[51] A.D. Sedgwick, P. Lees, Studies of eicosanoid production in the air pouch model of synovial inflammation, Agents and Actions 18(3) (1986) 429-438.
[52] M.B. Evangelista, S.X. Hsiong, R. Fernandes, P. Sampaio, H.J. Kong, C.C. Barrias, R. Salema, M.A. Barbosa, D.J. Mooney, P.L. Granja, Upregulation of bone cell differentiation through immobilization within a synthetic extracellular matrix, Biomaterials 28(25) (2007) 3644-3655.

[53] M. Bohner, S. Tadier, N. van Garderen, A. de Gasparo, N. Döbelin, G. Baroud, Synthesis of spherical calcium phosphate particles for dental and orthopedic applications, Biomatter 3(2) (2013) e25103.
[54] C.C. Barrias, C.C. Ribeiro, M. Lamghari, C.S. Miranda, M.A. Barbosa, Proliferation, activity, and osteogenic differentiation of bone marrow stromal cells cultured on calcium titanium phosphate microspheres, Journal of Biomedical Materials Research Part A 72A(1) (2005) 57-66.
[55] C.C. Barrias, M. Lamghari, P.L. Granja, M.C. Sá Miranda, M.A. Barbosa, Biological evaluation of calcium alginate microspheres as a vehicle for the localized delivery of a therapeutic enzyme, Journal of Biomedical Materials Research Part A 74A(4) (2005) 545-552.
[56] F. Jiang, D.P. Wang, S. Ye, X. Zhao, Strontium-substituted, luminescent and mesoporous hydroxyapatite microspheres for sustained drug release, Journal of materials science. Materials in medicine 25(2) (2014) 391-400.
[57] J. Hao, J. Chou, S. Kuroda, M. Otsuka, S. Kasugai, N.P. Lang, Strontium hydroxyapatite in situ gel-forming system – a new approach for minimally invasive bone augmentation, Clinical Oral Implants Research (2014) n/a-n/a.
[58] N. Neves, D. Linhares, G. Costa, C.C. Ribeiro, M.A. Barbosa, In vivo and clinical application of strontium-enriched biomaterials for bone regeneration: A systematic review, Bone & Joint Research 6(6) (2017) 366-375.
[59] P.J. Meunier , C. Roux , E. Seeman , S. Ortolani , J.E. Badurski , T.D. Spector , J. Cannata , A. Balogh , E.-M. Lemmel , S. Pors-Nielsen , R. Rizzoli , H.K. Genant , J.-Y. Reginster The Effects of Strontium Ranelate on the Risk of Vertebral Fracture in Women with Postmenopausal Osteoporosis, New England Journal of Medicine 350(5) (2004) 459-468.
[60] M. Schumacher, A. Lode, A. Helth, M. Gelinsky, A novel strontium(II)-modified calcium phosphate bone cement stimulates human-bone-marrow-derived mesenchymal stem cell proliferation and osteogenic differentiation in vitro, Acta Biomaterialia 9(12) (2013) 9547-9557.
[61] D.P. Wornham, M.O. Hajjawi, I.R. Orriss, T.R. Arnett, Strontium potently inhibits mineralisation in bone-forming primary rat osteoblast cultures and reduces numbers of osteoclasts in mouse marrow cultures, Osteoporosis International 25(10) (2014) 2477-2484.
[62] M. Schumacher, A.S. Wagner, J. Kokesch-Himmelreich, A. Bernhardt, M. Rohnke, S. Wenisch, M. Gelinsky, Strontium substitution in apatitic CaP cements effectively attenuates osteoclastic resorption but does not inhibit osteoclastogenesis, Acta Biomaterialia 37 (2016) 184-194.
[63] S. Zhu, X. Hu, Y. Tao, Z. Ping, L. Wang, J. Shi, X. Wu, W. Zhang, H. Yang, Z. Nie, Y. Xu, Z. Wang, D. Geng, Strontium inhibits titanium particle-induced osteoclast activation and chronic inflammation via suppression of NF-κB pathway, Scientific Reports 6 (2016) 36251.
[64] X. Yuan, H. Cao, J. Wang, K. Tang, B. Li, Y. Zhao, M. Cheng, H. Qin, X. Liu, X. Zhang, Immunomodulatory Effects of Calcium and Strontium Co-Doped Titanium Oxides on Osteogenesis, Frontiers in Immunology 8 (2017) 1196.
[65] W. Zhang, F. Zhao, D. Huang, X. Fu, X. Li, X. Chen, Strontium-Substituted Submicrometer Bioactive Glasses Modulate Macrophage Responses for Improved Bone Regeneration, ACS Applied Materials & Interfaces 8(45) (2016) 30747-30758.
[66] N. Charatcharoenwitthaya, S. Khosla, E.J. Atkinson, L.K. McCready, B.L. Riggs, Effect of Blockade of TNF-α and Interleukin-1 Action on Bone Resorption in Early Postmenopausal Women, Journal of Bone and Mineral Research 22(5) (2007) 724-729.
[67] B. Zhou, Z.C. Han, M.-C. Poon, W. Pu, Mesenchymal stem/stromal cells (MSC) transfected with stromal derived factor 1 (SDF-1) for therapeutic neovascularization: Enhancement of cell recruitment and entrapment, Medical Hypotheses 68(6) 1268-1271.

[68] T.T. Lau, D.-A. Wang, Stromal cell-derived factor-1 (SDF-1): homing factor for engineered regenerative medicine, Expert Opinion on Biological Therapy 11(2) (2011) 189-197.
[69] K. Anton, D. Banerjee, J. Glod, Macrophage-Associated Mesenchymal Stem Cells Assume an Activated, Migratory, Pro-Inflammatory Phenotype with Increased IL-6 and CXCL10 Secretion, PLOS ONE 7(4) (2012) e35036.

Supplementary figures

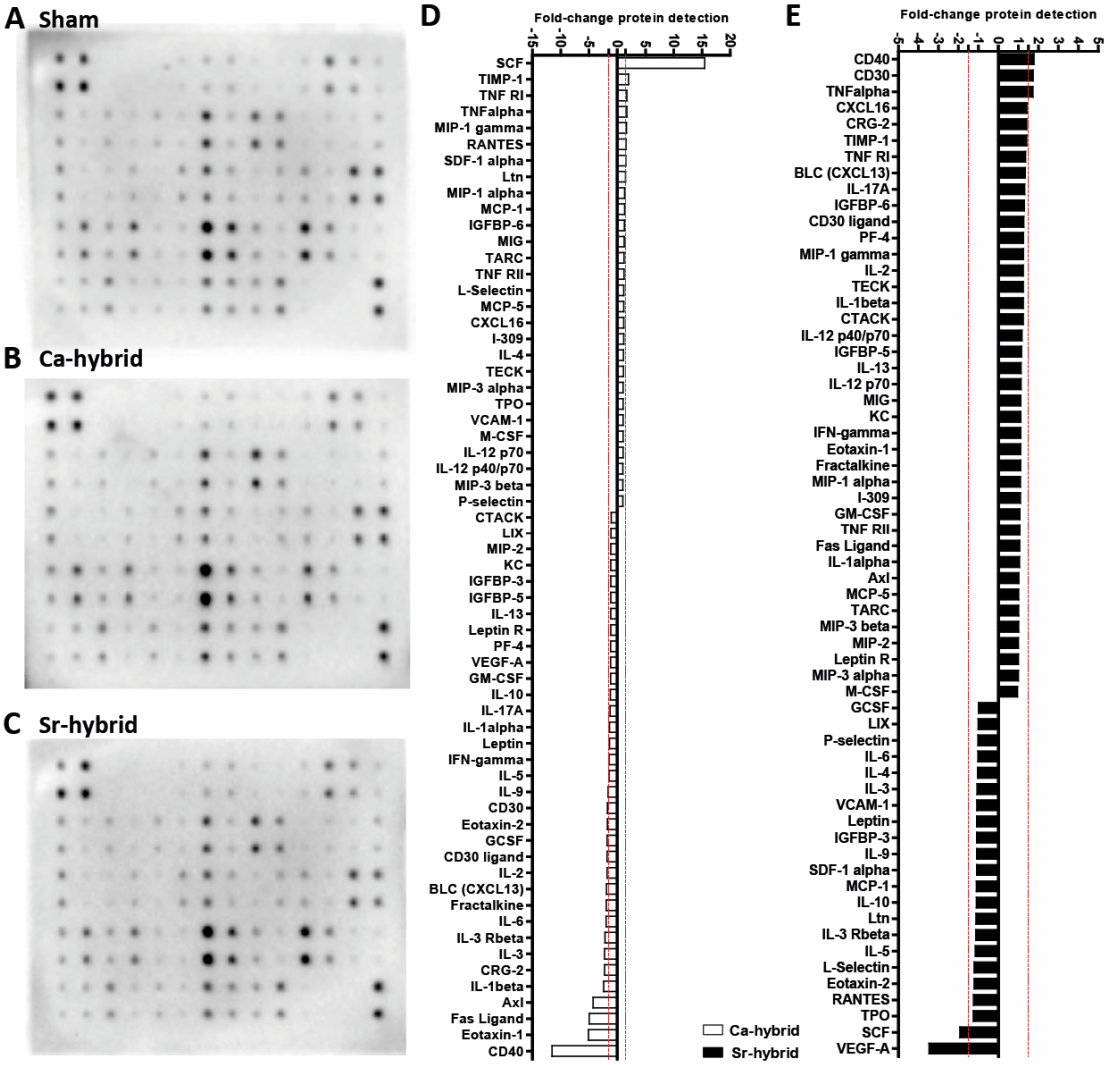

Supplementary Figure 1 –Cytokine production by inflammatory cells exudates after 3 days of implantation. A, B, C - Membranes obtained from the cytokine array for the different groups: (A) Sham, (B) Ca-hybrid and (C) Sr-hybrid. **D, E-** Total results of the array organized as fold change to the control (Sham) of Ca-hybrid (D) and Sr-hybrid (E).

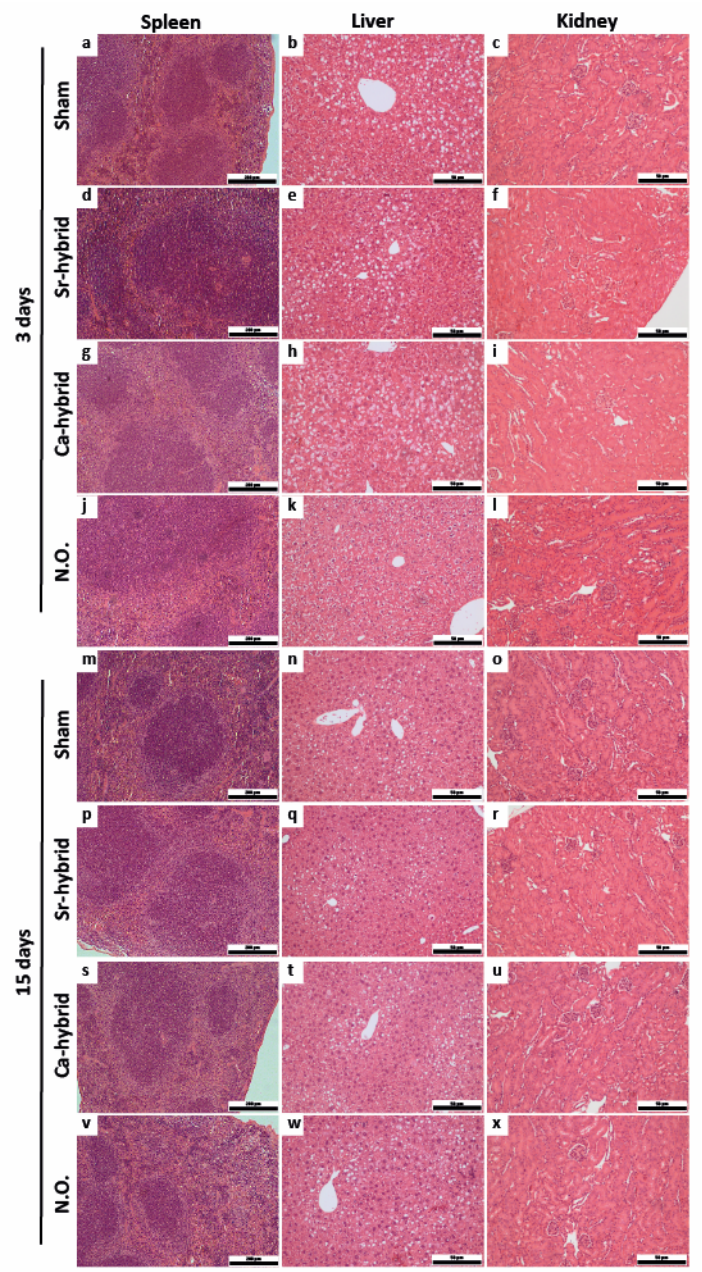

Supplementary Figure 2 – Strontium systemic evaluation. Representative H&E stained sections of spleen (1st column), liver (2nd column) and kidney (3rd column) of sham (a,b,c,m,n,o), Sr-hybrid (d,e,f,p,q,r), Ca-hybrid (g,h,i,s,t,u) and Non-operated (N.O., j,k,l,v,w,x), at 3 days (a to l) and 15 days (m to x) post-surgery. No alterations were observed in the spleen and kidney. All liver samples showed areas of microvesicular and macrovesicular steatosis with similar degree of extension.

Chapter IV

Injectable hybrid system for strontium local delivery promotes bone regeneration in a rat critical-sized defect model

Ana Henriques Lourenço[*], Nuno Neves[*], Cláudia Ribeiro-Machado, Susana R. Sousa, Meriem Lamghari, Cristina C. Barrias, Abel Trigo Cabral, Mário A. Barbosa and Cristina C. Ribeiro

[*] *These authors contributed equally to this work.*

Published in *Scientific Reports 7(1) (2017) 5098.*

Injectable hybrid system for strontium local delivery promotes bone regeneration in a rat critical-sized defect model

Ana Henriques Lourenço[1,2,3] [*], Nuno Neves[1,2,4] [*], Cláudia Ribeiro-Machado [1,2], Susana R. Sousa[1,2,5], Meriem Lamghari[1,2], Cristina C. Barrias[1,2], Abel Trigo Cabral[4], Mário A. Barbosa[1,2,6] and Cristina C. Ribeiro[1,2,5]

[1]i3S - Instituto de Investigação e Inovação em Saúde, Universidade do Porto, Rua Alfredo Allen, 208, 4200 - 135 Porto, Portugal

[2]INEB - Instituto de Engenharia Biomédica, Universidade do Porto, Rua Alfredo Allen, 208, 4200 - 135 Porto, Portugal

[3]Faculdade de Engenharia, Universidade do Porto, Rua Dr. Roberto Frias, s/n, 4200-465 Porto, Portugal

[4]Faculdade de Medicina, Universidade do Porto, Serviço de Ortopedia, Alameda Prof. Hernâni Monteiro, 4200-319 Porto, Portugal

[5]ISEP – Instituto Superior de Engenharia do Porto, Instituto Politécnico do Porto, Rua Dr. António Bernardino de Almeida 431, 4249-015, Porto, Portugal

[6]ICBAS - Instituto de Ciências Biomédicas de Abel Salazar, Universidade do Porto, Rua de Jorge Viterbo Ferreira n. 228, 4050-313 Porto, Portugal

[*] *These authors contributed equally to this work.*

Abstract

Strontium (Sr) has been described as having beneficial influence in bone strength and architecture. However, negative systemic effects have been reported on oral administration of Sr ranelate, leading to strict restrictions in clinical application. We hypothesized that local delivery of Sr improves osteogenesis without eliciting detrimental side effects. Therefore, the *in vivo* response to an injectable Sr-hybrid system composed of RGD-alginate hydrogel cross-linked *in situ* with Sr and reinforced with Sr-doped hydroxyapatite microspheres, was investigated. The system was injected in a critical-size bone defect model and compared to a similar Sr-free material. Micro-CT results show a trend towards higher new bone formed in Sr-hybrid group and major histological differences were observed between groups. Higher cell invasion was detected at the center of the defect of Sr-hybrid group after 15 days with earlier bone formation. Higher material degradation with increase of collagen fibers and bone formation in the center of the defect after 60 days was observed as opposed to bone formation restricted to the periphery of the defect in the control. These histological findings support the evidence of an improved response with the Sr enriched material. Importantly, no alterations were observed in the Sr levels in systemic organs or serum.

Keywords: *strontium, bone regeneration, injectable bone substitute, alginate, hydroxyapatite, ionic delivery system*

1. Introduction

The management of fractures and bone defects remains a significant challenge, and there is the need for improved therapeutic strategies [1]. Biological (autografts, allografts and xenografts) and synthetic bone grafts are currently used in clinical practice for bone repair. Because of their osteogenic potential and the absence of risks of immune rejection or disease transfer, autografts are clinically preferred. However, they are limited in supply, imply the additional morbidity of a harvest surgery and their properties and shape do not match exactly those of the bone to be replaced [2]. Intensive investigation is being carried out to produce synthetic bone grafts in order to overcome these problems. The use of injectable materials in bone regeneration, especially calcium phosphate based materials, presents several advantages, namely due to their adequate biological responses, osteoconductivity and mechanical properties [3-6]. These materials can be applied by minimally invasive surgical procedures, to efficiently fill-in cavities of non-uniform shapes, with no tissue damage and limited exposure to infectious agents, thus reducing patient discomfort and procedure-associated health costs. The addition of osteoinductive factors or osteoprogenitor/stem cells may improve bone repair, particularly in osteoporotic conditions, characterized by an impaired healing response [7-10].

Oral administration of Strontium (Sr) ranelate has shown effectiveness in the prevention of both vertebral and non-vertebral osteoporotic fractures [11, 12]. Unlike other anti-osteoporotic agents widely used in clinical practice, such as bisphosphonates, estrogen, selective estrogen-receptor modulators (SERMs) and calcitonin, which inhibit bone resorption [9], Sr ranelate also promotes bone formation [13-16]. Several *in vitro* studies show that Sr ranelate decreases bone resorption, by reducing osteoclast activity [13, 14, 17], decreasing functional osteoclast markers expression [13], disrupting osteoclasts cytoskeleton [14], and increasing osteoclast apoptosis [18]. Simultaneously, it induces positive effects on osteoblastogenesis and osteoblast activity in different *in vitro* models [19], namely by enhancing replication of

preosteoblastic cells [14, 20-23], increasing osteogenesis [14, 20, 24-26], decreasing osteoblast apoptosis [21, 27], and promoting terminal differentiation of osteoblasts into osteocytes [20]. Some pre-clinical studies performed in both normal and osteopenic/osteoporotic animal models confirmed these *in vitro* results, showing the beneficial effects of Sr ranelate on bone formation and remodeling [28-32]. Despite these important effects, cardiovascular safety of orally administered Sr ranelate has been questioned due to a small but significant increase in non-fatal myocardial infarctions [12, 33, 34]. Currently, there are strict indications and restrictions to its use [12].

Nevertheless, Sr incorporation into biomaterials for bone regeneration may improve their regeneration potential. *In vivo* studies showed that doping calcium phosphate cements and other ceramics with Sr promotes bone repair [35-37]. A sustained delivery system for local release of Sr ions can obviate systemic complications with similar rates of bone formation at the site of implantation.

Current injectable bone defect methacrylate-based fillers have compression strengths much higher than that of cancellous bone, and the brittleness of calcium phosphate cements is a limitation [38, 39]. We have previously developed various types of injectable biomaterials for bone regeneration, namely calcium phosphate [40-42] and calcium phosphate/alginate [43] microspheres, as well as different types of bio-functional alginate hydrogels [44-47]. When combined, alginate can act as an appropriate vehicle for ceramic microspheres delivery and immobilization at the injury site. Alginate is a natural linear polysaccharide, biodegradable and biocompatible, extensively studied for biomedical applications [48, 49]. Although generally regarded as a bioinert material, since it does not elicit specific cell-matrix interactions, grafting of alginate with arginine-glycine-aspartic acid (RGD) peptides is an effective strategy to provide appropriate guidance signals to promote cell adhesion and facilitate cell colonization [50]. Alginate forms hydrogels under mild chemical conditions, in the presence of divalent cations, such as Ca and Sr, through a cytocompatible physical

gelation process. These cations bind homoguluronic blocks in adjacent alginate chains in a cooperative manner (egg-box model) producing a crosslinked hydrogel network [51, 52].

Recently, we developed an injectable hybrid system that consists of ~500 μm diameter hydroxyapatite (HAp) microspheres doped with Sr, embedded in a functionalized alginate matrix crosslinked *in situ* with Sr [53]. As a vehicle for the microspheres delivery, functionalized alginate with RGD peptides was used, providing a scaffold for cell adhesion and migration and allowing for the injectability of the system. However, the use of hydrogels in bone tissue engineering is limited by low mechanical properties and the non-applicability in load-bearing conditions [54]. The packing of the microspheres upon delivery raises the compression strength of the material [53], and alginate creates an interconnected 3D network adequate for the invasion of blood vessels and cells [55]. Moreover, the presence of Sr in both components of the system provides two different release routes upon degradation of the materials. This system presents a clinically relevant compromise between adequate injectability and gelation time and final compression strength [53]. Moreover, *in vitro* studies showed that this Sr-hybrid scaffold promotes sustained release of Sr^{2+}, supports human mesenchymal stem cells adhesion, survival and osteogenic differentiation, and inhibits osteoclasts differentiation and activity, as compared to a similar Sr-free system [56].

In the current study we aim to evaluate the *in vivo* response to the designed Sr-rich hybrid system and its influence on new bone formation using a rat metaphyseal femoral critical-sized defect model, compared to a similar Sr-free material. The proposed system is expected to provide an adequate therapeutic approach to fill-in bone defects by minimally invasive surgery, while acting as a scaffold for local Sr^{2+} release to promote bone regeneration.

Materials and Methods

Preparation of the injectable hybrid materials

For the preparation of the hybrid system, RGD-alginate was combined with Sr-doped hydroxyapatite (HAp) or HAp microspheres and crosslinked by internal gelation with Sr or Ca carbonate, respectively (hereafter designated as Sr-hybrid or Ca-hybrid). These formulations and methodologies were adapted and optimized from previous works using Ca-crosslinked alginate hydrogels [47, 48, 57, 58].

Ultra-pure (UP) LVG Alginate (Pronova FMC Biopolymers, G content ≥60%, MW 131±13 kDa) was functionalized with RGD peptides as previously described [57], filtered in 0.22 μm Steriflip units (Millipore), lyophilized and stored at -20 °C until further use. Endotoxin levels were measured in RGD-modified and non-modified UP alginate using the Food and Drug Administration (FDA) approved Endosafe™-PTS system (Charles River). The analysis was performed and certified by an external entity (Analytical Services Unit, IBET/ITQB) revealing endotoxin levels below 0.1 EU/mL (EU - unit of measurement for endotoxin activity), respecting the US Department of Health and Human Services guidelines for implantable devices.

Sterile RGD-Alginate was dissolved in 0.9% (w/v) NaCl solution under sterile conditions to yield a 4% (w/v) solution, which was thoroughly mixed with an aqueous suspension of $SrCO_3$ (Sigma) or $CaCO_3$ (Fluka) at $SrCO_3$/COOH or $CaCO_3$/COOH molar ratio of 1.6. A fresh solution of glucone delta-lactone (GDL, Sigma) was added to trigger gel formation at a final polymer concentration of 3.5% (w/v) and a carbonate/GDL molar ratio of 0.125.

HAp microspheres were prepared as described elsewhere [42]. Briefly, HAp powder (Plasma Biotal) was dispersed in a 3% (w/v) alginate solution (FMC Biopolymers) with a ceramic-to-polymer solution ratio of 0.25. The paste was extruded dropwise into 0.1 M $SrCl_2$ (Merck) or 0.1 M $CaCl_2$ (Merck) crosslinking solution, to produce Sr-HAp or HAp microspheres, respectively. Microspheres were allowed to reticulate for 30 min in the crosslinking solution, and were then washed in deionized water, dried and sintered

at 1200 °C. Upon sintering, the polymer phase is burned out giving rise to a porous network where Sr or Ca ions are incorporate in the ceramic particles. Microspheres with spherical shape and diameter of 500-560 μm were retrieved by sieving and autoclave sterilized for further use. Sterile microspheres were promptly added to the gelling alginate solution to yield 35% in weight of the total mixture, thoroughly homogenized and placed in a 1 mL syringe (Terumo) ready for extrusion of the material.

Animal surgical procedure

All animal experiments were conducted following protocols approved by the Ethics Committee of the Portuguese Official Authority on Animal Welfare and Experimentation (DGAV) – reference no. 0420/000/000/2012. We used a critical size metaphyseal bone defect model adapted from Le Guehennec *et al* [59], as previously described [60]. Three months old Wistar Han male rats (Charles River Laboratories) with weight ranging from 300 to 400 g were used. Two different experimental groups (n=5 animals/group) were analysed: bone defect filled with Sr-hybrid material and bone defect filled with Ca-hybrid material (control material). Animals with empty defects (n=5) were used as a critical-sized defect model control. Two different time-points were used, 15 days and 60 days, to evaluate the relationship of inflammation and early bone formation, and new bone formation, respectively. Non-operated animals (n=2, 60 days) and animas with empty defects were used as control for serum Sr quantification and organ histological analysis. The analgesic buprenorphine (0.05 mg per kg), was administrated subcutaneously, 30 minutes before surgery. The animals were then subjected to volatile anesthesia with isofluorane, in a chamber, according to standard procedures of the animal facility (inducing anesthesia with 900 cc O_2 /min, 5% Isofluorane), confirmed by loss of posture and reflexes. Animals were then moved to a clean surgery area and anesthesia was maintained along all time of surgery with a face mask (300 cc O_2 /min, 2.5% Isofluorane). The right knee of each animal was shaved

and skin cleaned and disinfected with 70% ethanol. A lateral incision was performed and both skin and muscles were retracted to expose the articular capsule. After arthrotomy, a cylindrical defect with 3 mm diameter and depth of approximately 4 mm was drilled in the anterolateral wall of the lateral condyle of the femur. The defect was washed with physiological saline solution and either filled with a biomaterial or left empty. All materials were prepared in sterile conditions and injected in the femur's critical defect using a 1 mL syringe. Skin and muscle were sutured and the animal was placed back in its cage. Animals were observed until regaining consciousness. Post-operative care was carried out for 48 hours, where analgesics were given (Buprenorphine) in the same dose as before surgery, every 12 hours, with a subcutaneous injection. Behavior and wound healing were examined along time.

Sample collection

Fifteen and sixty days post-surgery animals were sacrificed. Animals were kept under volatile anesthesia (Isofluorane) and blood collection was performed by cardiac puncture. Pentobarbital (Eutasil) was administered for euthanizing animals, and femurs and organs (liver, left and right kidneys and spleen) were retrieved. Blood was centrifuged and serum collected and stored at -80 °C until further use. Femurs were cleaned from surrounding soft tissue and immediately placed in 10% (v/v) formalin neutral solution for 4 days, rinsed in phosphate buffered saline (PBS) solution and dehydrated in serial ethanol solutions (50-70%) for 3 days each. Femurs were maintained in 70% ethanol at 4ºC until further use. Organs were also placed in 10% (v/v) formalin solution for 24h and further processed for paraffin embedding.

Radiographic analysis

Lateral X-ray of femurs retrieved from animals sacrificed at 15 days post-surgery were obtained using a radiographic system (Owandy). For the remaining animals, an *in vivo*

lateral X-ray was also performed at 30 days post-surgery, to allow for a follow-up of defects and materials.

Micro-computed tomography (micro-CT) analysis

Bone defects and adjacent areas were analyzed using a high-resolution micro-CT (Skyscan 1072 scanner). Specimens (n=5, 60 days post-implantation) were scanned in high resolution mode, using a pixel size of 19.13 μm and an integration time of 1.7 ms. The X-ray source was set at 91 keV of energy and 110 μA of current. A 1-mm-thick aluminum filter and a beam hardening correction algorithm were employed to minimize beam-hardening artefacts (SkyScan hardware/software).

For all scanned specimens, representative datasets of 1023 slices were used for morphometric analysis. To quantify new bone formation, a volume of interest (VOI), corresponding to the femoral defect volume, was delineated using CTAn software (Skyscan Ltd), to enable quantitative analysis to be performed. Binary images were created using two different thresholds, 50-255 (corresponding to particles and new bone) and 90-255 (just particles), and the respective TV (Total volume) determined. The difference between both TV corresponds to the volume of new bone formed (Bone volume, BV). Additionally, 3D virtual models were generated using an image processing software (ANT 3D Creator v 2.4, SkyScan). The micro-CT threshold was first calibrated from a backscattered image with primarily determined quantitative histological measurements, which was then applied equally to all samples.

Histological Analysis

Femurs were dehydrated in 100% ethanol for 3 days, at 4°C, followed by immersion in xylol for 24 h and further embedding in methylmethacrylate and processed for histological analysis as described elsewhere [61, 62].

Serial 7 μm coronal slides were retrieved and the intermediate region of the defect (1200-1500 μm) was stained with Hematoxylin and Eosin (H&E), Masson’s Trichrome

(MT), Picrosirius Red (PSR) and Tartarate-resistant acid phosphatase (TRAP)-light green (LG) staining. Briefly, for H&E, undeplastified sections were re-hydrated in deionized water and incubated in Gill's Hematoxylin for 6 min and counterstained with alcoholic Eosin Y for 1 min. For MT staining, an MT kit (Sigma-Aldrich) was used according to manufacturer's instructions in undeplastified sections. TRAP staining was performed according to manufacturer using a TRAP kit (Sigma) and counterstained with LG 0.1% (v/v) in deplastified section with xylol overnight. Sections were visualized under a light microscope (DP25, Olympus) and imaged. For PSR staining, sections were deplastified, hydrated in decreasing ethanol gradient to de-ionized water, stained for 6 min in Celestine blue and another 6 min in Gill's Hematoxylin. After a 10 min washing step in water, sections were stained with Sirius Red for 1 h, washed with acidified water, dehydrated and mounted. Sections were imaged through polarization lens under a light microscope (Axiovert 200M, Zeiss) using MosaiX software.

Regarding the retrieved organs, paraffin sections of 3 μm thickness were sequentially obtained and stained with H&E.

Peripheral bone thickness was determined as the average thickness of twenty different random locations (arrow in Fig.4A c'' and d'') of bone found around the defect area using MT stained sections. AxioVision software was used for the measurements (n=5 animals/group). The area of residual material found within the defect was measured by the same user, manually delimiting the area of the hybrid (microspheres and alginate) in MT stained sections. Alginate and microspheres retain staining and have a different texture, allowing for the easy identification of the material. MosaicJ (ImageJ software, n=5 animals/group, 3 sections/animal) was used for the assembly of microscopic images at 20x magnification and area values were obtained in ImageJ.

Birefrigent green and red fibers were quantified as the percentage of thin/type III and thicker/type I collagen fibers, respectively [63, 64]. The collagen area within the central region of the defect (diameter=2.4 mm) was quantified in ImageJ software (n=5

animals/group, 3 images/animal). Sections were stained simultaneously and images acquired in the same day with the same parameters.

Serial 7 µm coronal slides were also analysed by Scanning Electron Microscopy/Energy-dispersive X-ray spectroscopy (SEM/EDS) using a High Resolution (Schottky) Environmental Scanning Electron Microscope with X-Ray Microanalysis and Electron Backscattered Diffraction analysis: Quanta 400 FEG ESEM / EDAX Genesis X4M. Samples were coated with an Au/Pd thin film, by sputtering, using the SPI Module Sputter Coater equipment.

Systemic Sr quantification by Inductively Coupled Plasma - Atomic Emission Spectroscopy (ICP-AES)

Sr levels in serum and organs (spleen, liver and kidneys) were quantified by ICP-AES (Horiba Jobin-Yvon, Ultima spectrometer, generator RF of 40,68 MHz). Serum samples (n=6 samples/group/time point and n=2 non-operated) were diluted 5 times in 1% Suprapur nitric acid (Fluka) as described elsewhere [65]. Spleen, liver and kidneys were digested in Suprapure nitric acid (n=4 samples/group/time point). Before use, all glass materials were washed and then immersed in a 20% (v/v) nitric acid solution for at least 1 day in order to eliminate possible contaminations with Sr or other impurities from the vessels walls. Organs (~300 mg) were dried in a microwave (MARS-X 1500 W, CEM) configured with a 14 position carousel. An aliquot of 10 mL of Suprapur nitric acid was added and microwave digestion proceeded during 55 min, according to microwave digestion program (Supplementary - Table 1). The solutions were concentrated until 1 mL and preserved at −20 °C until Sr determination. The limit of detection (LOD – 1 µg/L) and limit of quantification (LOQ – 5 µg/L) for Sr were adequate for the expected concentration range of the samples.

Statistical Analysis

Statistical analysis was performed using non-parametric Mann–Whitney test with GraphPad Prism Program. A value of $p<0.05$ was considered statistically significant: *$p<0.05$; **$p<0.01$; *** $p<0.001$.

Results

Radiographical analysis of bone and biomaterial

A cylindrical defect with 3 mm diameter and depth of approximately 4 mm was drilled in the lateral condyle of the right femur (Figure 1A). The defect was filled with the biomaterial, injected using a 1 mL syringe (Figure 1B, C). A picture of the Sr-hybrid material used is shown in Figure 1D, where spherical particles (Sr-HAp microspheres) are embedded within a transparent hydrogel (Sr crosslinked RGD-alginate).

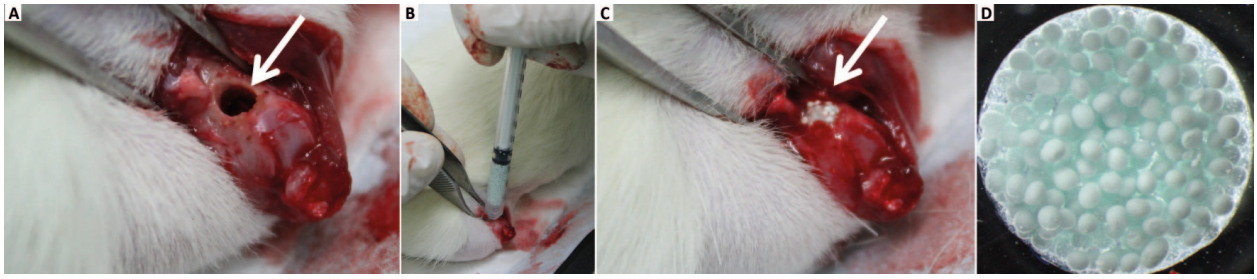

Figure 1. *In vivo* intraoperative setting. Critical sized defect created in the distal femur (A). Injection of the hybrid material using a 1 mL syringe (B) and filled defect (C). Detail of the hybrid system, composed of HAp microspheres embedded in a RGD-alginate hydrogel (D).

Rat femurs were imaged by X-ray along the experimental period allowing for a follow-up at 15 and 30 days. Representative images of defects filled with materials (Sr-hybrid or Ca-hybrid) or empty defects are shown in Fig. 2. In hybrid-filled defects (Fig. 2A to D), microspheres are located inside the created bone defect (arrows in the images), where the higher radiopacity of the HAp microspheres allowed for the easy monitoring using X-ray. Microspheres were homogeneously distributed within the defects (Fig. 2A to D) and were still detected at day 30, a non-invasive mid-term follow-up (Fig. 2B and D). Empty defects were also imaged (Fig. 2E and F) and the defect could still be observed after 30 days, confirming it to be of a critical size.

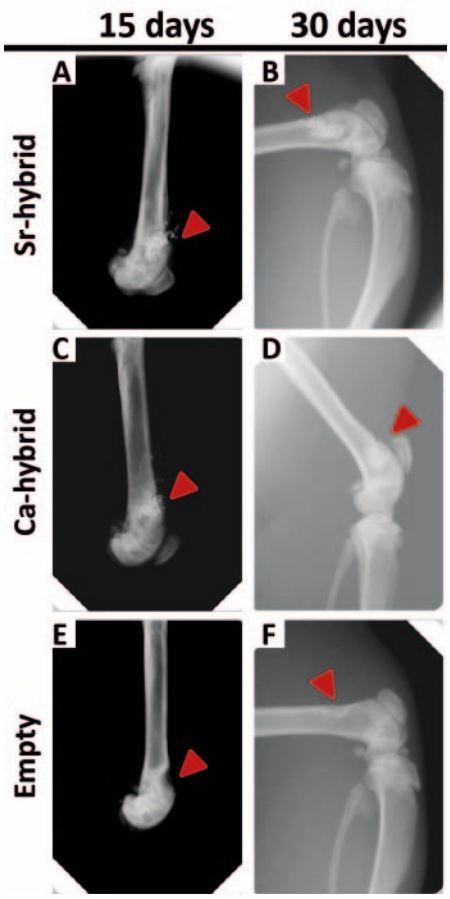

Figure 2. Radiographic imaging follow-up. Representative lateral X-Ray images from right rat femurs of Sr-hybrid (A and B) or Ca-hybrid-filled (C and D) and empty (E and F) defects at 15 days (A, C and E) and 30 days (B ,D and F) post-surgery. Arrows pinpoint site of created defect, filled or empty. Microspheres can be observed as circular objects more radiopaque than bone.

Micro-CT morphometric 3D evaluation

Micro-CT analysis was performed 60 days post-implantation (Fig. 3) to evaluate new bone formation at the defect site and to assess the spatial distribution of ceramic microspheres within the lesion. In Sr-hybrid filled defects (Fig. 3A), microspheres were homogeneously distributed inside the defect with no apparent degradation, with preserved size and without modifications in shape. Similar results were found in Ca-hybrid filled defects. Furthermore, and particularly in Sr-hybrid samples, centripetal bone colonization could be observed by new bone formation surrounding the ceramic microspheres and with the development of new bone trabeculae in the periphery of the defect. 3D morphometric analysis was performed using five femurs per group, where

the ROI was defined in binary images (Fig. 3B) and the percentage of new bone formed (bone volume fraction, BV/TV) was calculated. Values of (31.5±1.7) % and (28.6±1.1) % (BV/TV (%), mean±SE) of new bone was measured in animals that received the Sr-hybrid and Ca-hybrid materials, respectively (Fig. 3C).

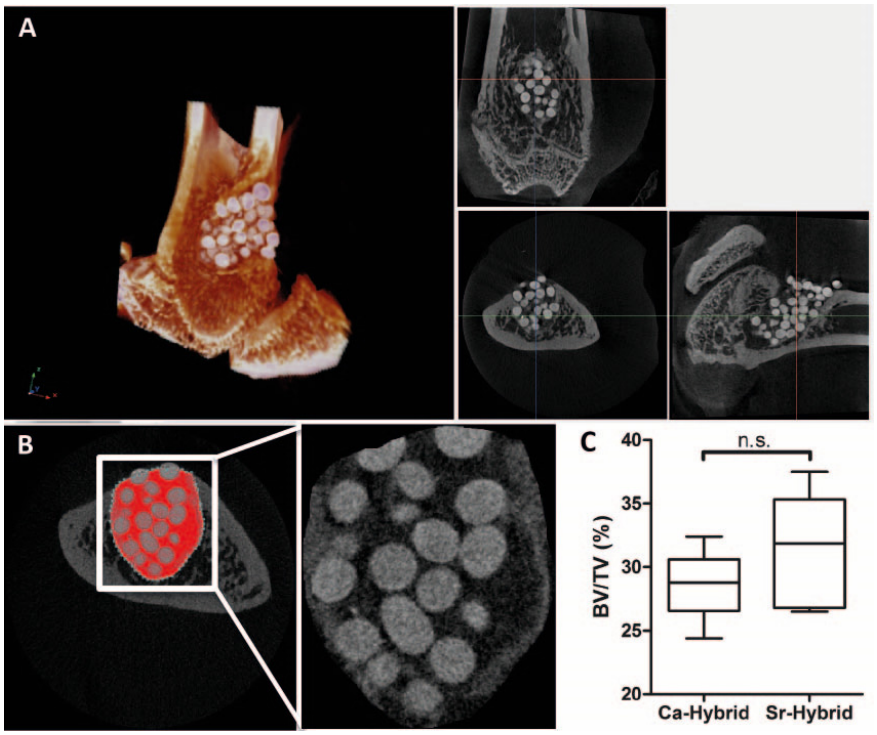

Figure 3. Micro-CT analysis of distal femur after 60 days of implantation. 3D reconstructed image and respective orthogonal slices of micro-CT acquisition of the femur with Sr-hybrid filled defect (A). Morphometric analysis approach used to quantify new bone formation: transversal micro-CT slice of a femur injected with Sr-hybrid after 60 days of implantation highlighting ROI (B). C - New bone formed (BV/TV, %) after 60 days of implantation of Sr-hybrid and Ca-hybrid materials. Data presented as box-plot with median and min to max whiskers of n = 5 samples (n.s. – statistically non-significant).

Histological evaluation of bone/biomaterial interface

In Fig. 4A representative images of femurs with defects filled with Sr-hybrid or Ca-hybrid materials, at days 15 and 60, are portrayed. A global view of the defects and materials (Fig. 4A a to d), as well as a more detailed view of the periphery of the defect (Fig. 4A a' to d' and magnifications a'' to d''), are given. Histological analysis at day 15 post-implantation showed that the created defects exhibited similar diameter and were filled with approximately 15 to 18 microspheres (Fig. 4A a, b). As early as 15 days post-

implantation, all animals showed, to some extent, newly formed bone at the periphery of the defect (Fig 4A a', b'). Sr-hybrid implanted defects also showed new bone formation in close contact with the microspheres, distant from the periphery of native bone (Fig. 4A b'', arrow). SEM images and EDS analysis of this newly formed bone in close vicinity of the microspheres is shown in Fig. 4B. The results confirmed the high content of calcium and phosphate, and a Ca/P ratio in accordance with normal bone composition (Z1 in Fig. 4B), and different from the elemental analysis of the microspheres (Z2 in Fig. 4B), where Sr was also identified.

After 60 days, new bone formation at the periphery was observed in both materials. Sr-hybrid implanted defects exhibited a thicker trabecular bone structure at the periphery of the defect (Fig 4A d', d''), when compared to the Ca-hybrid group (Fig. 4A c', c''). The quantification of new bone formed at the periphery of the defect revealed a statistically significant thicker bone structure in Sr-hybrid group (662.4±48 μm) in contrast to a thinner bone formation (381.1±29 μm) in the Ca-hybrid group (mean±SE, $p<0.001$, Fig. 4C).

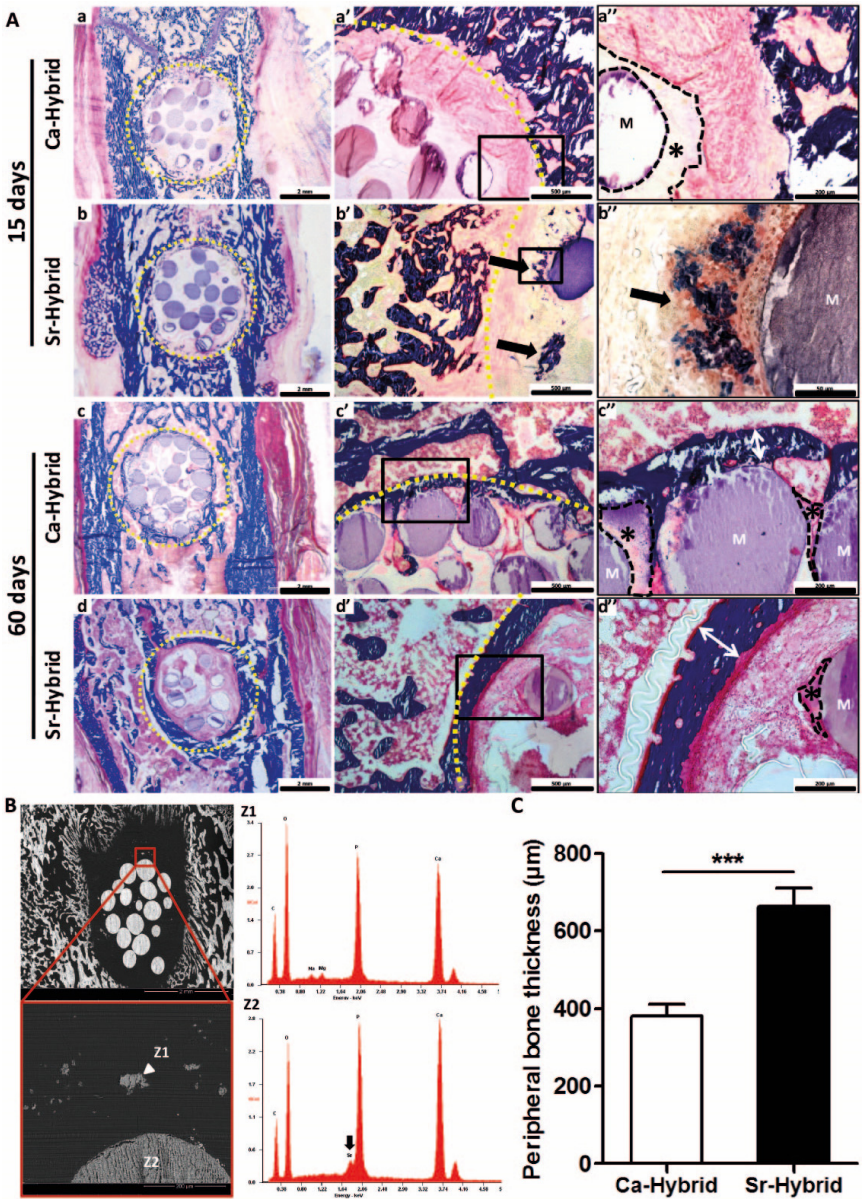

Figure 4. Histological evaluation of bone/biomaterial interface in femurs implanted with Sr-hybrid and Ca-hybrid systems. Coronal histological sections of critical sized defect created in the distal femur, 15 and 60 days post-implantation (A). Global view of the created defects filled with Ca-hybrid (a and c) and Sr-hybrid (b and d) materials, at 15 (a and b) or 60 days (c and d) post-implantation, stained with MT (a to d, dashed yellow line circling the created defect area). Interface bone/biomaterial, 15 days (a' and b') and 60 days (c' and d') post-implantation, with Ca-hybrid (a' and c') and Sr-hybrid (b' and d') systems, and higher magnification of square (a'' to d'', collagen/bone in blue, yellow dashed line – bone/biomaterial interface, * – alginate, M – microspheres, black arrows – new bone). B - SEM image of histological section of Sr-hybrid filled defect 15 days post-implantation with EDS spectra of new bone (Z1) found near the microsphere and microsphere (Z2). C - Thickness of peripheral bone found around the defect (as represented with arrows in A c'' and A d''), 60 days post-implantation of Sr-hybrid and Ca-hybrid systems. Data presented as mean±SEM of 20 different random locations of trabecular bone found around the defect of n=5 animals/group, 3 sections/animal, Asterisks show statistically significant differences (*** $p<0.001$).

Histological evaluation of the center of the defect

Representative images of the center of the defect in both groups are shown in Fig. 5A. Although no evident differences were observed in the diameter of the microspheres with time of implantation, alginate showed different behavior between groups. After 15 days, some alginate was observed surrounding microspheres in both experimental groups (Fig 5A, a and b). In Sr-hybrid group, higher cell invasion at the center was observed, mainly of polymorphonuclear neutrophils (PMN) (Fig 5A, b and b').

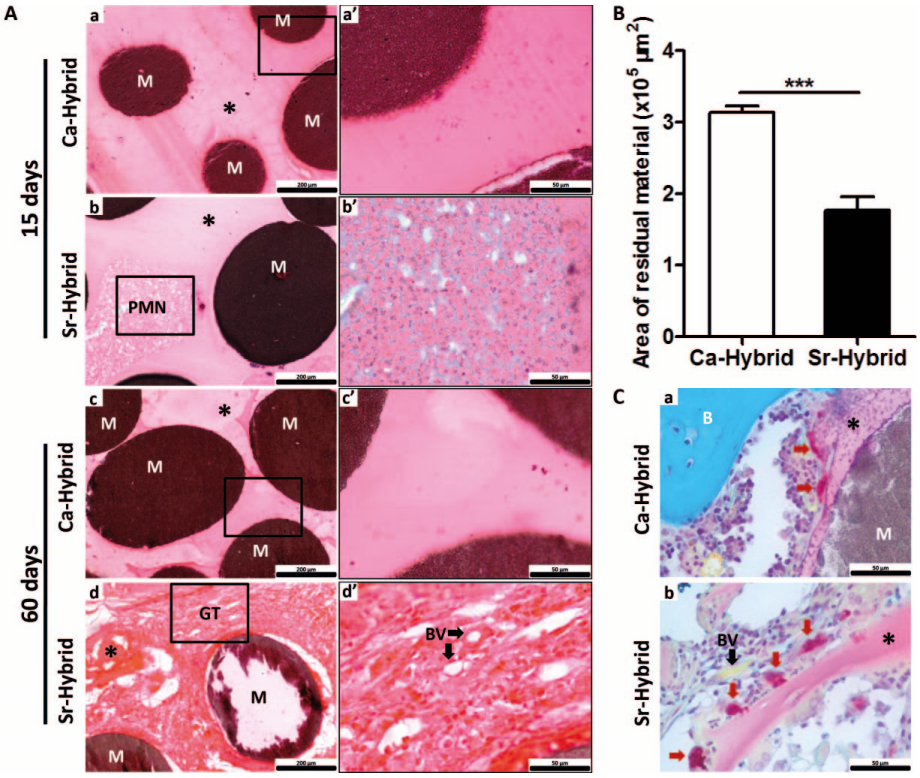

Figure 5. Histological analysis of the center of the defect in femurs implanted with Sr-hybrid and Ca-hybrid systems. Detailed view of the center of the defect implanted with Ca-hybrid (a and c) and Sr-hybrid (b and d) materials, stained with H&E, after 15 (a and b) and 60 days (c and d) of implantation, with higher magnification of square (a' to d', A). B - Area of residual material (microspheres and alginate) found within the defect area, 60 days post-implantation of Sr-hybrid and Ca-hybrid systems. Measurements were performed by delimiting the area of material in MT stained sections using ImageJ software, n=5 animals/group, 3 sections/animal. Data presented as mean±SE and asterisks show statistically significant differences (*** $p<0.001$). C – TRAP-LG staining images of Ca-hybrid (a) and Sr-hybrid (b) systems filled defects, 60 days post-implantation. (M – microspheres, * – alginate, PMN – Polymorphonuclear neutrophils, GT – Granulation Tissue, BV – blood vessels, red arrows – Osteoclasts).

After 60 days, alginate was still present in both groups (Fig. 5A, c and d), although higher degradation was observed in Sr-hybrid filled defects. A statistically significant decrease in the area of residual material (alginate + microspheres) present on the defect site was observed in Sr-hybrid group with an area of 1.77±0.2 $x10^5$ μm^2 compared to 3.14± 0.1 $x10^5$ μm^2 in Ca-hybrid group (mean±SE, $p<0.001$, Fig. 5B). In a detailed microscopic analysis of the center of the Sr-hybrid filled defects (Fig. 5A, d and d') granulation tissue could be observed, with the presence of blood vessels (Fig. 5A d') and osteoclasts (Fig. 5C b). In contrast, in Ca-hybrid group osteoclasts were found only at the periphery of the defect (Fig. 5C a). Furthermore, PSR staining images under conventional light (Fig. 6A a and c) showed the presence of collagen (in red) within the area of the defect in Sr-hybrid (Fig. 6A c) at a higher extent than in Ca-hybrid filled defect after 60 days (Fig. 6A a). The use of PSR-polarization method (Fig. 6A b and d) allowed for the quantification of different types of collagen fibrils, i.e. green and red, which are associated with thin/immature/type III and thick/mature/type I collagen, respectively. The quantification was performed within the central area of the defect using a fixed ROI (diameter=2.4 mm, yellow circle in Fig. 6A b and d) and results are shown in Fig. 6B. As expected, an increase in the percentage of red/type I collagen was observed from day 15 to day 60 in both groups. However, 60 days post-implantation, a slightly higher percentage of red/type I collagen was measured in the central defect region in Sr-hybrid group ((3.3±1.3) %, mean±SE) compared to Ca-hybrid group ((1.9±0.3) %, mean±SE).

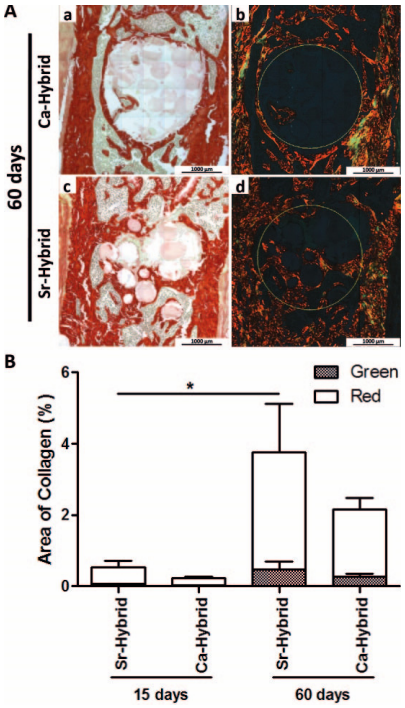

Figure 6. Quantification of birefringent collagen fibers by PSR-polarization method in the center of the defect. PSR staining visualized under conventional light (a and c) and polarized light (b and d) to identify different collagen fiber types, 60 days post-implantation of Ca-hybrid (a and b) and Sr-hybrid (c and d) systems (A). PSR stains collagen in red (conventional light) and collagen fibers are specifically birefringent in polarized light (green - thin fibers/type III; red - thick fibers/type I, MosaicX image, original magnification 20x). Fixed region of interest (ROI) used for quantification is demonstrated in b and d. B - Quantification of area of green or red birefringent collagen fibers in the center of the defect in Sr-hybrid and Ca-hybrid filled defects, 15 and 60 days post-implantation. Data presented as mean±SE of n=5 animals/group, 3 images/animal. Asterisks show statistically significant differences ($p<0.05$) between groups for red collagen data.

Evaluation of Sr systemic effect

Sr levels were quantified in serum (Fig. 7A) and organs (Fig. 7B) associated with excretory/filtration functions, such as liver, spleen and kidneys, by ICP-AES analysis, to evaluate the safety of the designed Sr-hybrid system. The Sr levels in serum of animals that were subjected to Sr-hybrid implantation (27.05±2.7 µg/L after 15 days and 20.61±1.3 µg/L after 60 days) were not statistically different from those in empty defect animals (27.26±3.9 µg/L after 15 days and 23.31±1.9 µg/L after 60 days) or non-operated animals (28.59±0.8 µg/L, mean±SD). Even after 60 days of implantation, no increase in Sr was found in serum (Limit of quantification, LOQ – 5 µg/L).

Sr quantification in organs at 60 days post-implantation supports results from measurements in serum. No statistical significant differences were observed between empty defect animals (0.44±0.1 µg/g kidney, 0.50±0.1 µg/g spleen, 0.48±0.3 µg/g liver, mean±SD) and Sr-hybrid group (0.69±0.3 µg/g kidney, 0.59±0.2 µg/g spleen, 0.36±0.1 µg/g liver, mean±SD). Moreover, histomorphological analyses were also performed in histological sections of organs after 60 days (Fig. 7C). In Sr-hybrid implanted group no morphological alterations at macro or microscopic level were observed, when compared to non-operated animals. Analysis of Ca-hybrid group presented similar results, with no alterations observed.

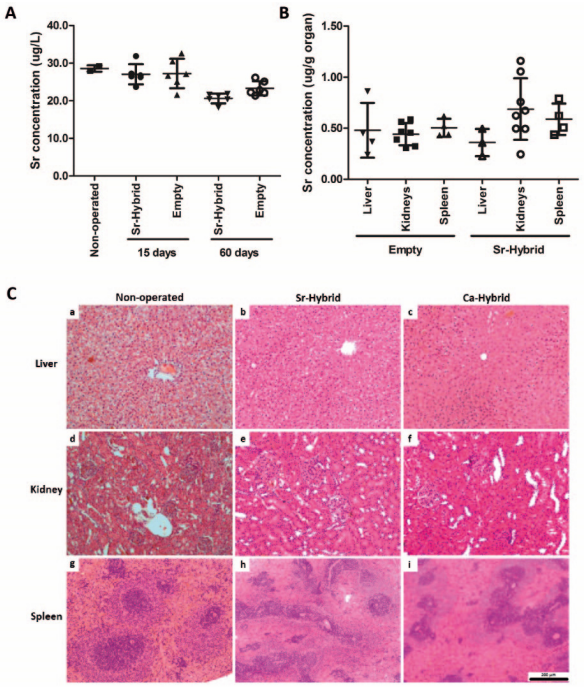

Figure 7. Strontium systemic evaluation. Strontium concentration found in serum in non-operated, empty and Sr-hybrid implanted animals at days 15 and 60 post-surgery (A). Data presented as mean±SD of 6 samples/group/time point and 2 samples non-operated. Strontium concentration found in the liver, kidneys and spleen of animals implanted with Sr-hybrid and empty defect, 60 days post-surgery (B). Data presented as mean±SD of 4 samples/group/time point. Representative histological sections from liver (a to c), kidney (d to f) and spleen (g to i) of non-operated (a, d and g), Sr-hybrid (b, e and h) and Ca-hybrid implanted (c, f, and i) animals, 60 days post-surgery (C).

Discussion

In this study the *in vivo* response to an injectable Sr-rich hybrid system, composed of Sr-doped HAp microspheres embedded in an Sr-crosslinked RGD-alginate hydrogel, as compared to a similar Sr-free system (Ca-hybrid material), using a rat metaphyseal femoral critical size defect model, is presented.

The designed hybrid system aims at providing adequate mechanical support in the early phases of bone formation and gradual replacement of the artificial scaffold by newly-formed bone with adequate function and mechanical properties. The use of hydrogels is a promising approach in skeletal regenerative medicine [49, 66-68]. Alginate has been used due to its biocompatibility, low toxicity, and mild gelation in the presence of divalent cations. Therefore alginate gels act as a natural extracellular matrix mimic which can be tuned to deliver bioactive agents and cells to the desired site, creating space for new tissue formation and control the structure and function of the engineered tissue [49]. Other works have incorporated alginate in self-setting cements, for improving injectability, cohesion and compression strength [69-71]. In the present study, the ability of alginate to form hydrogels *in situ* acting as a carrier for HAp microspheres under cytocompatible conditions, was explored. In agreement with our previous results [53], the system showed to be adequate for minimally invasive implantation. A conventional syringe can be used to manually inject the material, perfectly filling complex defects and, once set, creating a 3D matrix with homogeneous distribution of microspheres. Furthermore, alginate was modified with RGD peptides to provide biological cues for promoting cell adhesion and colonization [50, 57]. The main disadvantage regarding load-bearing application is alginate low mechanical properties which can be overcome through the reinforcement with ceramic components, application in non load-bearing areas, and the concomitant use of fixation devices [54]. With an alginate-to-microspheres weight ratio of 0.35, and microspheres with average diameter of 530 μm, the hybrid system allows for a good compromise between mechanical resistance and adequate space between

particles (approximately 220 μm), which is expected to facilitate *in situ* cell colonization and invasion by blood vessels [53, 55].

Deficient bone healing is expected to occur, especially in osteoporotic conditions. The use of crystalline HAp in the microspheres, with low degradation rate, ensures its permanency at the injury site for longer periods post-implantation, therefore allowing for a mechanical reinforcement of the defect. In this work, the high radiopacity of microspheres allowed for an easy follow-up *in vivo* of the material using conventional radiological imaging. In clinical practice, this comes as highly advantageous since regular X-rays are required to assess bone healing.

In this system we used alginate crosslinked by internal gelation with Sr^{2+} as a vehicle for the Sr-doped HAp microspheres. Sr was incorporated both in the hydrogel and the microspheres, which present different release kinetic profiles resulting in sustained Sr^{2+} release for long periods of time (AH Lourenço *et al*, unpublished results). In other *in vivo* studies, Sr has been found to enhance bone formation [35, 37, 72, 73]. For example, Banerjee et al. studied the effect of doping ß-TCP with MgO/SrO on bone formation in Sprague-Dawley rats [72]. Doped ß-TCP promoted more osteogenesis and faster bone formation than pure ß-TCP. In critical calvaria defects of an ovariectomized rat model, macroporous Sr-substituted scaffolds showed superior osteoinductive activity to enhance early bone formation, and could also stimulate angiogenesis compared with calcium silicate scaffolds [73]. The current study showed that Sr-hybrid system presents bioactive properties, promoting cell migration, implant vascularization and supports bone ingrowth. Newly formed bone developed in close contact with the material, without any fibrous interface, growing in a centripetal manner, in continuity with the surrounding host trabecular bone, indicates a good integration with the host tissue. Newly formed bone percentages is in agreement to those observed in other works testing similar materials [74, 75] and a trend towards greater new bone formation was observed in Sr-hybrid filled defects.

Major histological differences were observed between the two groups. Higher cell invasion was seen at the center of the Sr-hybrid filled defects at 15 days post-implantation, with the presence of polymorphonuclear neutrophils (PMN). Bone injury elicits an inflammatory response that is beneficial to healing when acute and highly regulated. Inflammatory cells are recruited to the site of injury for clearance of pathogens and maintenance of bone homeostasis [76]. This higher cell invasion correlates with higher material degradation and bone tissue formation seen after 60 days. We may assume that Sr induces faster bone healing, possibly due to a faster resolution of inflammation, tissue repair and remodeling. This can be appealing since the presence of Sr may be modulating the inflammatory response, a current trend in bone regeneration strategies regarding the development of biomaterials [77-79].

Earlier bone formation was identified in close contact with the microspheres in Sr-hybrid system, highlighting higher osteoinductivity when compared to Ca-hybrid system which was evidenced by the thicker trabecular bone structure at the periphery of the defect observed in Sr-hybrid group 60 days post-implantation. Cardemill *et al* have also found major differences in the topological distribution of the formed bone in association with Sr-doped calcium phosphate or HAp granules, although both materials showed comparable overall bone formation, when implanted in ovariectomized and non-ovariectomized rats [80]. A larger amount of mineralized bone was observed in the center of the defect in HAp group, mainly in ovariectomized rats, whereas at the periphery of the defect the bone area was higher using Sr-doped granules, irrespective of ovariectomy.

Granulation tissue with blood vessels and increased collagen deposition were observed at 60 days post-implantation in Sr-hybrid filled defects. Several studies have correlated the color of birefringent collagen fibers under polarized light with different collagen types [63, 64]. Our results show an increase in thicker red collagen fibers in Sr-hybrid group. These fibers are associated with type I collagen, the main type found in bone tissue. It has been shown that the incorporation of Sr in biomaterials may

decrease the number of osteoclasts significantly, but these were nevertheless closely associated with newly formed trabeculae, indicating activated bone remodeling [81]. A quantitative analysis of TRAP positive cells was not performed. However, the presence of osteoclasts in the center of the defect supports the higher bone remodeling found in the Sr-hybrid group. Although the microCT calculations did not reveal a statistically different bone volume, these histological findings sustain the evidence of an improved response with the Sr enriched material.

The use of methylmethacrylate embedding histological technique allowed for the study of both bone and material without decalcification. The technique was optimized in our lab [61] using an exothermic process. One of the disadvantages of the procedure is the inability to perform immunohistochemistry studies due to loss of antigenicity, which is worth exploring in future works.

With the use of Sr releasing systems, cardiovascular safety is of concern. Current guidelines indicate that orally administered Sr ranelate should be avoided in patients with past or present history of ischemic heart disease, peripheral arterial disease and/or cerebrovascular disease or uncontrolled hypertension, due to an observed increase of cardiovascular events [12]. Although previous reports have shown that ionic Sr can be added to calcium phosphates and ceramics, potentially stimulating bone formation locally, the risk of systemic adverse effects has been rarely reported. Baier *et al* studied the addition of Sr to calcium-phosphate cement in a distal methaphyseal femoral defect in ovariectomized rat model. Results have shown faster osteointegration of the implant with the addition of Sr, and Sr serum concentrations of 10.87 ± 4.16 μg/l were found 1 month post-implantation [35]. The systemic Sr levels were very low when compared to those found upon oral Sr ranelate treatment [82]. In the present study, Sr concentration was assessed both in the serum and organs with excretory/filtration functions, as well as the histology of these organs. Serum Sr concentration in operated animals was found to be similar to non-operated and in the same range as previously reported [35]. No statistically significant difference was observed between Sr-hybrid

implanted and empty defects, both in serum and organs. Similarly, Sr concentration levels do not seem to be increased compared to normal levels found in the liver of Wistar rats (~0.2 ug/g of dry weight [83]) . These results, together with the absence of morphological changes in histological sections of the organs suggest that Sr release is restricted to the defect site, corroborating the safety of this osteoinductive hybrid system.

Conclusions

We evaluated the *in vivo* response of an injectable Sr-rich hybrid system composed of Sr-doped HAp microspheres embedded in Sr-crosslinked RGD-alginate hydrogel intended for bone regeneration. Sr-hybrid system led to an increased bone formation in both center and periphery of a critical size defect compared to a non Sr–doped similar system, where new bone formation was restricted to the periphery. Besides promoting earlier new bone formation, Sr-hybrid system was also found to stimulate higher cell colonization with increased deposition of thick collagen fibers in the center of the defect. Importantly, our results suggest that only local release of Sr from the material was obtained, since no statistically significant differences on Sr concentration were detected in retrieved organs or serum. Together, these data demonstrate that the incorporation of Sr improved the osteoinductive properties of the hybrid system leading to higher bone regeneration without inducing detrimental side effects currently associated with other Sr-based therapeutic strategies. The Sr-hybrid material stands as a promising approach for bone regeneration strategies through minimally invasive procedures.

Acknowledgements

The authors thankfully acknowledge the use of Micro-CT in the 3B's Research Group facilities at University of Minho, the use of microscopy services at Centro de Materiais da Universidade do Porto (CEMUP) and the technicians responsible for the experimental techniques mentioned, Vitor Correlo and Daniela Silva, respectively; Carla Rodrigues from Requimte at FCT-UNL for the help with ICP-AES analysis. This work was financed by FEDER - Fundo Europeu de Desenvolvimento Regional funds through the COMPETE 2020 - Operacional Programme for Competitiveness and Internationalisation (POCI), Portugal 2020, and by Portuguese funds through FCT - Fundação para a Ciência e a Tecnologia/ Ministério da Ciência, Tecnologia e Inovação in the framework of the project "Institute for Research and Innovation in Health Sciences" (POCI-01-0145-FEDER-007274) and project PTDC/CTM/103181/2008. AHL acknowledges FCT for PhD grant: SFRH/BD/87192/2012, CCB acknowledges FCT for research position Investigator FCT (IF2013).

Author Contributions

Study design: AHL, NN, ML, CR. Preparation of materials: AHL, CR. Surgical procedures: AHL, NN. Animal follow-up and data collection: AHL, CR-M. Preparation for elemental ICP-AES analysis and interpretation: AHL, SRS. Histological analysis and interpretation: AHL, CR-M, ML, CR. Discussion and interpretation of the results: AHL, NN, CR-M, SRS, ML, CB, ATC, MB, CR. Drafting manuscript: AHL, NN, CR. All authors critically revised manuscript content and approved final version of manuscript.

Disclosures: The authors declare no conflict of interest.

References

[1] J. Goldhahn, W.H. Scheele, B.H. Mitlak, E. Abadie, P. Aspenberg, P. Augat, M.-L. Brandi, N. Burlet, A. Chines, P.D. Delmas, I. Dupin-Roger, D. Ethgen, B. Hanson, F. Hartl, J.A. Kanis, R. Kewalramani, A. Laslop, D. Marsh, S. Ormarsdottir, R. Rizzoli, A. Santora, G. Schmidmaier, M. Wagener, J.-Y. Reginster, Clinical evaluation of medicinal products for acceleration of fracture healing in patients with osteoporosis, Bone 43(2) (2008) 343-347.
[2] V. Campana, G. Milano, E. Pagano, M. Barba, C. Cicione, G. Salonna, W. Lattanzi, G. Logroscino, Bone substitutes in orthopaedic surgery: from basic science to clinical practice, Journal of Materials Science: Materials in Medicine 25(10) (2014) 2445-2461.
[3] A. Dupraz, T.P. Nguyen, M. Richard, G. Daculsi, N. Passuti, Influence of a cellulosic ether carrier on the structure of biphasic calcium phosphate ceramic particles in an injectable composite material, Biomaterials 20(7) (1999) 663-673.
[4] L.R.A. looss P, Grimandi G, Daculsi G, Merle C. , A new injectable bone substitute combining poly(epsilon-caprolactone) microparticles with biphasic calcium phosphate granules., Biomaterials. (22) (2001) 2785-94.
[5] S. Larsson, Calcium Phosphates: What Is the Evidence?, Journal of Orthopaedic Trauma 24 (2010) S41-S45.
[6] K.L. Low, S.H. Tan, S.H.S. Zein, J.A. Roether, V. Mouriño, A.R. Boccaccini, Calcium phosphate-based composites as injectable bone substitute materials, Journal of Biomedical Materials Research Part B: Applied Biomaterials 94B(1) (2010) 273-286.
[7] L. Cao, G. Liu, Y. Gan, Q. Fan, F. Yang, X. Zhang, T. Tang, K. Dai, The use of autologous enriched bone marrow MSCs to enhance osteoporotic bone defect repair in long-term estrogen deficient goats, Biomaterials 33(20) (2012) 5076-5084.
[8] S.W. Cho, H.J. Sun, J.-Y. Yang, J.Y. Jung, H.J. Choi, J.H. An, S.W. Kim, S.Y. Kim, K.-J. Park, C.S. Shin, Human Adipose Tissue-Derived Stromal Cell Therapy Prevents Bone Loss in Ovariectomized Nude Mouse, Tissue Engineering Part A 18(9-10) (2012) 1067-1078.
[9] H.-Y. Liu, A.T.H. Wu, C.-Y. Tsai, K.-R. Chou, R. Zeng, M.-F. Wang, W.-C. Chang, S.-M. Hwang, C.-H. Su, W.-P. Deng, The balance between adipogenesis and osteogenesis in bone regeneration by platelet-rich plasma for age-related osteoporosis, Biomaterials 32(28) (2011) 6773-6780.
[10] Z. Wang, J. Goh, S.D. De, Z. Ge, H. Ouyang, J.S.W. Chong, S.L. Low, E.H. Lee, Efficacy of bone marrow-derived stem cells in strengthening osteoporotic bone in a rabbit model., Tissue engineering. (12(7)) (2006) 1753-1761. .
[11] P.J. Meunier , C. Roux , E. Seeman , S. Ortolani , J.E. Badurski , T.D. Spector , J. Cannata , A. Balogh , E.-M. Lemmel , S. Pors-Nielsen , R. Rizzoli , H.K. Genant , J.-Y. Reginster The Effects of Strontium Ranelate on the Risk of Vertebral Fracture in Women with Postmenopausal Osteoporosis, New England Journal of Medicine 350(5) (2004) 459-468.
[12] J.Y. Reginster, A. Neuprez, N. Dardenne, C. Beaudart, P. Emonts, O. Bruyere, Efficacy and safety of currently marketed anti-osteoporosis medications, Best Practice & Research Clinical Endocrinology & Metabolism 28(6) (2014) 809-834.
[13] R. Baron, Y. Tsouderos, In vitro effects of S12911-2 on osteoclast function and bone marrow macrophage differentiation, European Journal of Pharmacology 450(1) (2002) 11-17.
[14] E. Bonnelye, A. Chabadel, F. Saltel, P. Jurdic, Dual effect of strontium ranelate: Stimulation of osteoblast differentiation and inhibition of osteoclast formation and resorption in vitro, Bone 42(1) (2008) 129-138.
[15] M.D. Grynpas, E. Hamilton, R. Cheung, Y. Tsouderos, P. Deloffre, M. Hott, P.J. Marie, Strontium increases vertebral bone volume in rats at a low dose that does not induce detectable mineralization defect, Bone 18(3) (1996) 253-259.

[16] F. Yang, D. Yang, J. Tu, Q. Zheng, L. Cai, L. Wang, Strontium Enhances Osteogenic Differentiation of Mesenchymal Stem Cells and In Vivo Bone Formation by Activating Wnt/Catenin Signaling, STEM CELLS 29(6) (2011) 981-991.
[17] N. Takahashi, T. Sasaki, Y. Tsouderos, T. Suda, S 12911-2 Inhibits Osteoclastic Bone Resorption In Vitro, Journal of Bone and Mineral Research 18(6) (2003) 1082-1087.
[18] A.S. Hurtel-Lemaire, R. Mentaverri, A. Caudrillier, F. Cournarie, A. Wattel, S. Kamel, E.F. Terwilliger, E.M. Brown, M. Brazier, The Calcium-sensing Receptor Is Involved in Strontium Ranelate-induced Osteoclast Apoptosis: NEW INSIGHTS INTO THE ASSOCIATED SIGNALING PATHWAYS, Journal of Biological Chemistry 284(1) (2009) 575-584.
[19] P.J. Marie, D. Felsenberg, M.L. Brandi, How strontium ranelate, via opposite effects on bone resorption and formation, prevents osteoporosis, Osteoporosis International 22(6) (2011) 1659-1667.
[20] G.J. Atkins, K.J. Welldon, P. Halbout, D.M. Findlay, Strontium ranelate treatment of human primary osteoblasts promotes an osteocyte-like phenotype while eliciting an osteoprotegerin response, Osteoporosis International 20(4) (2009) 653-664.
[21] T.C. Brennan, M.S. Rybchyn, W. Green, S. Atwa, A.D. Conigrave, R.S. Mason, Osteoblasts play key roles in the mechanisms of action of strontium ranelate, British Journal of Pharmacology 157(7) (2009) 1291-1300.
[22] J. Caverzasio, Strontium ranelate promotes osteoblastic cell replication through at least two different mechanisms, Bone 42(6) (2008) 1131-1136.
[23] N. Chattopadhyay, S.J. Quinn, O. Kifor, C. Ye, E.M. Brown, The calcium-sensing receptor (CaR) is involved in strontium ranelate-induced osteoblast proliferation, Biochemical Pharmacology 74(3) (2007) 438-447.
[24] A. Barbara, P. Delannoy, B.G. Denis, P.J. Marie, Normal matrix mineralization induced by strontium ranelate in MC3T3-E1 osteogenic cells, Metabolism 53(4) (2004) 532-537.
[25] S. Choudhary, P. Halbout, C. Alander, L. Raisz, C. Pilbeam, Strontium Ranelate Promotes Osteoblastic Differentiation and Mineralization of Murine Bone Marrow Stromal Cells: Involvement of Prostaglandins, Journal of Bone and Mineral Research 22(7) (2007) 1002-1010.
[26] L.-L. Zhu, S. Zaidi, Y. Peng, H. Zhou, B.S. Moonga, A. Blesius, I. Dupin-Roger, M. Zaidi, L. Sun, Induction of a program gene expression during osteoblast differentiation with strontium ranelate, Biochemical and Biophysical Research Communications 355(2) (2007) 307-311.
[27] O. Fromigué, E. Haÿ, A. Barbara, P.J. Marie, Essential Role of Nuclear Factor of Activated T Cells (NFAT)-mediated Wnt Signaling in Osteoblast Differentiation Induced by Strontium Ranelate, Journal of Biological Chemistry 285(33) (2010) 25251-25258.
[28] P. Ammann, I. Badoud, S. Barraud, R. Dayer, R. Rizzoli, Strontium Ranelate Treatment Improves Trabecular and Cortical Intrinsic Bone Tissue Quality, a Determinant of Bone Strength, Journal of Bone and Mineral Research 22(9) (2007) 1419-1425.
[29] P. Ammann, V. Shen, B. Robin, Y. Mauras, J.-P. Bonjour, R. Rizzoli, Strontium Ranelate Improves Bone Resistance by Increasing Bone Mass and Improving Architecture in Intact Female Rats, Journal of Bone and Mineral Research 19(12) (2004) 2012-2020.
[30] S.D. Bain, C. Jerome, V. Shen, I. Dupin-Roger, P. Ammann, Strontium ranelate improves bone strength in ovariectomized rat by positively influencing bone resistance determinants, Osteoporosis International 20(8) (2009) 1417-1428.
[31] J. Buehler, P. Chappuis, J.L. Saffar, Y. Tsouderos, A. Vignery, Strontium ranelate inhibits bone resorption while maintaining bone formation in alveolar bone in monkeys (Macaca fascicularis), Bone 29(2) (2001) 176-179.

[32] P. Delannoy, D. Bazot, P.J. Marie, Long-term treatment with strontium ranelate increases vertebral bone mass without deleterious effect in mice, Metabolism 51(7) (2002) 906-911.
[33] B. Abrahamsen, E.L. Grove, P. Vestergaard, Nationwide registry-based analysis of cardiovascular risk factors and adverse outcomes in patients treated with strontium ranelate, Osteoporosis International 25(2) (2014) 757-762.
[34] C. Cooper, K.M. Fox, J.S. Borer, Ischaemic cardiac events and use of strontium ranelate in postmenopausal osteoporosis: a nested case–control study in the CPRD, Osteoporosis International 25(2) (2014) 737-745.
[35] M. Baier, P. Staudt, R. Klein, U. Sommer, R. Wenz, I. Grafe, P.J. Meeder, P.P. Nawroth, C. Kasperk, Strontium enhances osseointegration of calcium phosphate cement: a histomorphometric pilot study in ovariectomized rats, Journal of Orthopaedic Surgery and Research 8(1) (2013) 1-8.
[36] G. Hulsart-Billström, W. Xia, E. Pankotai, M. Weszl, E. Carlsson, C. Forster-Horváth, S. Larsson, H. Engqvist, Z. Lacza, Osteogenic potential of Sr-doped calcium phosphate hollow spheres in vitro and in vivo, Journal of Biomedical Materials Research Part A 101A(8) (2013) 2322-2331.
[37] U. Thormann, S. Ray, U. Sommer, T. ElKhassawna, T. Rehling, M. Hundgeburth, A. Henß, M. Rohnke, J. Janek, K.S. Lips, C. Heiss, G. Schlewitz, G. Szalay, M. Schumacher, M. Gelinsky, R. Schnettler, V. Alt, Bone formation induced by strontium modified calcium phosphate cement in critical-size metaphyseal fracture defects in ovariectomized rats, Biomaterials 34(34) (2013) 8589-8598.
[38] C.P. Friedman CD, Takagi S, Chow LC., BoneSource hydroxyapatite cement: a novel biomaterial for craniofacial skeletal tissue engineering and reconstruction., J Biomed Mater Res (43:428-32.) (1998).
[39] Q.J. Xu HH, Calcium phosphate cement containing resorbable fibers for short-term reinforcement and macroporosity., Biomaterials (23:193-202.) (2002).
[40] C.C. Barrias, C.C. Ribeiro, M. Lamghari, C.S. Miranda, M.A. Barbosa, Proliferation, activity, and osteogenic differentiation of bone marrow stromal cells cultured on calcium titanium phosphate microspheres, Journal of Biomedical Materials Research Part A 72A(1) (2005) 57-66.
[41] S.M. Oliveira, C.C. Barrias, I.F. Almeida, P.C. Costa, M.R.P. Ferreira, M.F. Bahia, M.A. Barbosa, Injectability of a bone filler system based on hydroxyapatite microspheres and a vehicle with in situ gel-forming ability, Journal of Biomedical Materials Research Part B: Applied Biomaterials 87B(1) (2008) 49-58.
[42] C.C. Ribeiro, C.C. Barrias, M.A. Barbosa, Preparation and characterisation of calcium-phosphate porous microspheres with a uniform size for biomedical applications, Journal of Materials Science: Materials in Medicine 17(5) (2006) 455-463.
[43] C.C. Ribeiro, C.C. Barrias, M.A. Barbosa, Calcium phosphate-alginate microspheres as enzyme delivery matrices, Biomaterials 25(18) (2004) 4363-4373.
[44] C.C. Barrias, M. Lamghari, P.L. Granja, M.C. Sá Miranda, M.A. Barbosa, Biological evaluation of calcium alginate microspheres as a vehicle for the localized delivery of a therapeutic enzyme, Journal of Biomedical Materials Research Part A 74A(4) (2005) 545-552.
[45] K.B. Fonseca, D.B. Gomes, K. Lee, S.G. Santos, A. Sousa, E.A. Silva, D.J. Mooney, P.L. Granja, C.C. Barrias, Injectable MMP-Sensitive Alginate Hydrogels as hMSC Delivery Systems, Biomacromolecules 15(1) (2014) 380-390.
[46] F.R. Maia, M. Barbosa, D.B. Gomes, N. Vale, P. Gomes, P.L. Granja, C.C. Barrias, Hydrogel depots for local co-delivery of osteoinductive peptides and mesenchymal stem cells, Journal of Controlled Release 189 (2014) 158-168.
[47] F.R. Maia, A.H. Lourenço, P.L. Granja, R.M. Gonçalves, C.C. Barrias, Effect of Cell Density on Mesenchymal Stem Cells Aggregation in RGD-Alginate 3D Matrices under Osteoinductive Conditions, Macromolecular Bioscience 14(6) (2014) 759-771.
[48] M.B. Evangelista, S.X. Hsiong, R. Fernandes, P. Sampaio, H.-J. Kong, C.C. Barrias, R. Salema, M.A. Barbosa, D.J. Mooney, P.L. Granja, Upregulation of bone cell

differentiation through immobilization within a synthetic extracellular matrix, Biomaterials 28(25) (2007) 3644-3655.
[49] K.Y. Lee, D.J. Mooney, Alginate: properties and biomedical applications, Progress in polymer science 37(1) (2012) 106-126.
[50] S. Sakiyama-Elbert, J. Hubbell, Functional Biomaterials: Design of Novel Biomaterials, Annual Review of Materials Research 31(1) (2001) 183-201.
[51] T. Andersen, B.L. Strand, K. Formo, E. Alsberg, B.E. Christensen, Alginates as biomaterials in tissue engineering, Carbohydrate Chemistry: Volume 37, The Royal Society of Chemistry2012, pp. 227-258.
[52] Ý.A. Mørch, I. Donati, B.L. Strand, Effect of Ca2+, Ba2+, and Sr2+ on Alginate Microbeads, Biomacromolecules 7(5) (2006) 1471-1480.
[53] N. Neves, B.B. Campos, I.F. Almeida, P.C. Costa, A.T. Cabral, M.A. Barbosa, C.C. Ribeiro, Strontium-rich injectable hybrid system for bone regeneration, Materials Science and Engineering: C 59 (2016) 818-827.
[54] E.D. D'Este M, Hydrogels in calcium phosphate moldable and injectable bone substitutes: Sticky excipients or advanced 3-D carriers?, Acta Biomater (9:5421-30.) (2013).
[55] M. Bohner, S. Tadier, N. van Garderen, A. de Gasparo, N. Dobelin, G. Baroud, Synthesis of spherical calcium phosphate particles for dental and orthopedic applications, Biomatter 3(2) (2013).
[56] A. Lourenço, A. Torres, S. Santos, M. Barbosa, C. Barrias, C. Ribeiro, Sr-Hybrid system for bone regeneration: an in vitro study, 4th Interrogations at the Biointerface Advanced Summer School, Barcelona, 2014.
[57] S.J. Bidarra, C.C. Barrias, K.B. Fonseca, M.A. Barbosa, R.A. Soares, P.L. Granja, Injectable in situ crosslinkable RGD-modified alginate matrix for endothelial cells delivery, Biomaterials 32(31) (2011) 7897-7904.
[58] K.B. Fonseca, S.J. Bidarra, M.J. Oliveira, P.L. Granja, C.C. Barrias, Molecularly designed alginate hydrogels susceptible to local proteolysis as three-dimensional cellular microenvironments, Acta Biomaterialia 7(4) (2011) 1674-1682.
[59] L. Le Guehennec, E. Goyenvalle, E. Aguado, M. Houchmand-Cuny, B. Enkel, P. Pilet, G. Daculsi, P. Layrolle, Small-animal models for testing macroporous ceramic bone substitutes, Journal of Biomedical Materials Research Part B: Applied Biomaterials 72B(1) (2005) 69-78.
[60] S.G. Santos, M. Lamghari, C.R. Almeida, M.I. Oliveira, N. Neves, A.C. Ribeiro, J.N. Barbosa, R. Barros, J. Maciel, M.C.L. Martins, R.M. Gonçalves, M.A. Barbosa, Adsorbed fibrinogen leads to improved bone regeneration and correlates with differences in the systemic immune response, Acta Biomaterialia 9(7) (2013) 7209-7217.
[61] C. Carvalho, J. Magalhães, L. Pereira, L. Simões-Silva, I. Castro-Ferreira, J.M. Frazão, Evolution of bone disease after kidney transplantation: A prospective histomorphometric analysis of trabecular and cortical bone, Nephrology 21(1) (2016) 55-61.
[62] D.M. Sousa, P.A. Baldock, R.F. Enriquez, L. Zhang, A. Sainsbury, M. Lamghari, H. Herzog, Neuropeptide Y Y1 receptor antagonism increases bone mass in mice, Bone 51(1) (2012) 8-16.
[63] G.S. Montes, L.C.U. Junqueira, The use of the Picrosirius-polarization method for the study of the biopathology of collagen, Memórias do Instituto Oswaldo Cruz 86 (1991) 1-11.
[64] A.E. Vieira, C.E. Repeke, S.d.B. Ferreira Junior, P.M. Colavite, C.C. Biguetti, R.C. Oliveira, G.F. Assis, R. Taga, A.P.F. Trombone, G.P. Garlet, Intramembranous Bone Healing Process Subsequent to Tooth Extraction in Mice: Micro-Computed Tomography, Histomorphometric and Molecular Characterization, PLoS ONE 10(5) (2015) e0128021.

[65] R.K. Fuchs, M.R. Allen, K.W. Condon, S. Reinwald, L.M. Miller, D. McClenathan, B. Keck, R.J. Phipps, D.B. Burr, Strontium ranelate does not stimulate bone formation in ovariectomized rats, Osteoporosis International 19(9) (2008) 1331-1341.
[66] N.E. Fedorovich, J. Alblas, J.R. de Wijn, W.E. Hennink, A.J. Verbout, W.J. Dhert, Hydrogels as extracellular matrices for skeletal tissue engineering: state-of-the-art and novel application in organ printing, Tissue Eng 13(8) (2007) 1905-25.
[67] A. Khademhosseini, R. Langer, Microengineered hydrogels for tissue engineering, Biomaterials 28(34) (2007) 5087-5092.
[68] M. Patenaude, N.M.B. Smeets, T. Hoare, Designing Injectable, Covalently Cross-Linked Hydrogels for Biomedical Applications, Macromolecular Rapid Communications 35(6) (2014) 598-617.
[69] G.-S. Lee, J.-H. Park, J.-E. Won, U.S. Shin, H.-W. Kim, Alginate combined calcium phosphate cements: mechanical properties and in vitro rat bone marrow stromal cell responses, Journal of Materials Science: Materials in Medicine 22(5) (2011) 1257-1268.
[70] C. Xu, X. Wang, J. Zhou, Z. Huan, J. Chang, Bioactive tricalcium silicate/alginate composite bone cements with enhanced physicochemical properties, Journal of Biomedical Materials Research Part B: Applied Biomaterials (2017) n/a-n/a.
[71] S. Sprio, M. Dapporto, M. Montesi, S. Panseri, W. Lattanzi, E. Pola, G. Logroscino, A. Tampieri, Novel Osteointegrative Sr-Substituted Apatitic Cements Enriched with Alginate, Materials 9(9) (2016) 763.
[72] S.S. Banerjee, S. Tarafder, N.M. Davies, A. Bandyopadhyay, S. Bose, Understanding the influence of MgO and SrO binary doping on the mechanical and biological properties of β-TCP ceramics, Acta Biomaterialia 6(10) (2010) 4167-4174.
[73] K. Lin, L. Xia, H. Li, X. Jiang, H. Pan, Y. Xu, W.W. Lu, Z. Zhang, J. Chang, Enhanced osteoporotic bone regeneration by strontium-substituted calcium silicate bioactive ceramics, Biomaterials 34(38) (2013) 10028-10042.
[74] G. Daculsi, A.P. Uzel, P. Weiss, E. Goyenvalle, E. Aguado, Developments in injectable multiphasic biomaterials. The performance of microporous biphasic calcium phosphate granules and hydrogels, Journal of Materials Science: Materials in Medicine 21(3) (2010) 855-861.
[75] O. Gauthier, R. Müller, D. von Stechow, B. Lamy, P. Weiss, J.-M. Bouler, E. Aguado, G. Daculsi, In vivo bone regeneration with injectable calcium phosphate biomaterial: A three-dimensional micro-computed tomographic, biomechanical and SEM study, Biomaterials 26(27) (2005) 5444-5453.
[76] F. Loi, L.A. Córdova, J. Pajarinen, T.-h. Lin, Z. Yao, S.B. Goodman, Inflammation, fracture and bone repair, Bone 86 (2016) 119-130.
[77] D.P. Vasconcelos, M. Costa, I.F. Amaral, M.A. Barbosa, A.P. Águas, J.N. Barbosa, Modulation of the inflammatory response to chitosan through M2 macrophage polarization using pro-resolution mediators, Biomaterials 37 (2015) 116-123.
[78] D.P. Vasconcelos, M. Costa, I.F. Amaral, M.A. Barbosa, A.P. Águas, J.N. Barbosa, Development of an immunomodulatory biomaterial: Using resolvin D1 to modulate inflammation, Biomaterials 53 (2015) 566-573.
[79] D.M. Vasconcelos, R.M. Gonçalves, C.R. Almeida, I.O. Pereira, M.I. Oliveira, N. Neves, A.M. Silva, A.C. Ribeiro, C. Cunha, A.R. Almeida, C.C. Ribeiro, A.M. Gil, E. Seebach, K.L. Kynast, W. Richter, M. Lamghari, S.G. Santos, M.A. Barbosa, Fibrinogen scaffolds with immunomodulatory properties promote in vivo bone regeneration, Biomaterials 111 (2016) 163-178.
[80] C. Cardemil, I. Elgali, W. Xia, L. Emanuelsson, B. Norlindh, O. Omar, P. Thomsen, Strontium-Doped Calcium Phosphate and Hydroxyapatite Granules Promote Different Inflammatory and Bone Remodelling Responses in Normal and Ovariectomised Rats, PLoS ONE 8(12) (2013) e84932.
[81] L. Wei, J. Ke, I. Prasadam, R.J. Miron, S. Lin, Y. Xiao, J. Chang, C. Wu, Y. Zhang, A comparative study of Sr-incorporated mesoporous bioactive glass scaffolds for

regeneration of osteopenic bone defects, Osteoporosis International 25(8) (2014) 2089-2096.
[82] P.J. Marie, M. Hott, D. Modrowski, C. De Pollak, J. Guillemain, P. Deloffre, Y. Tsouderos, An uncoupling agent containing strontium prevents bone loss by depressing bone resorption and maintaining bone formation in estrogen-deficient rats, Journal of Bone and Mineral Research 8(5) (1993) 607-615.
[83] S. Takahashi, I. Takahashi, H. Sato, Y. Kubota, S. Yoshida, Y. Muramatsu, Determination of major and trace elements in the liver of Wistar rats by inductively coupled plasma-atomic emission spectrometry and mass spectrometry, Laboratory Animals 34(1) (2000) 97-105.

Supplementary Data

Table 1 - Microwave digestion program.

Stages	1	2	3
Power (W)	600	600	600
Time (min.)	5	10	10
Temperature (control, °C)	50	100	175
Hold (min.)	10	10	15

Chapter V

General discussion and future perspectives

The use of injectable biomaterials that support and stimulate bone repair/regeneration are highly attractive options for the clinical management of bone lesions. These can be implanted through minimally invasive surgery, to efficiently fill-in cavities of non-uniform shapes, with less tissue damage and limited exposure to infectious agents, thus reducing patient discomfort and procedure-associated health costs. The addition of osteoinductive factors may improve bone repair, particularly in osteoporotic conditions, characterized by an impaired healing response [1-4].

In this context, the aim of this PhD thesis was to evaluate the *in vitro* and *in vivo* response to a Sr-hybrid injectable system for bone regeneration, designed by our group [5], consisting of hydroxyapatite microspheres doped with Sr and an alginate vehicle crosslinked *in situ* with Sr.

The composite nature of bone has inspired the combination of polymeric hydrogels and calcium phosphates [6]. In a biomimetic approach, RGD-alginate hydrogel was used, creating a 3D matrix with homogeneous distribution of microspheres. The incorporation of RGD was important to promote cell anchorage, in otherwise non-adhesive hydrogels, and to improve cell survival and function, as we previously demonstrated [7-9]. The alginate hydrogel could be crosslinked *in situ*, using a previously described internal gelation strategy [7-11], allowing for the injectability of the system, an important feature for clinical use, as already discussed. The HAp microspheres, embedded within the hydrogel, acted as mechanical reinforcement of the system [5]. Microspheres with a diameter of around 500 μm were used, as this size results in sufficient interstitial space within packed microspheres (approximately 220 μm), which is expected to provide an adequate porosity for new tissue ingrowth upon implantation. Therefore, the hybrid system allows for a good compromise between mechanical resistance and available space for tissue formation and neo-vascularization to meet the growing tissue nutrient supply and clearance needs. Under osteoporotic conditions, bone healing is compromised. Therefore, microspheres were produced with crystalline HAp, which presents a low degradation rate. This is expected to ensure the permanency of the microspheres at the injury site for longer periods post-implantation, thus allowing for mechanical reinforcement of the defect for sufficient time. The viscosity and gelation time of the hydrogel reinforced with microspheres where also shown to be adequate for injectable purposes in orthopedic surgery [5].

A similar Sr-free system, using HAp microspheres and Ca-crosslinked alginate was used as a control (Ca-hybrid), to evaluate the specific effect of Sr incorporation in the designed materials, throughout all this work.

On Chapter III, we aimed at studying the Sr^{2+} release profile from the material. The hybrid system has two Sr^{2+} sources, the hydrogel and the microspheres, providing a sustained release of Sr^{2+} over long periods of time, which is very appealing for clinical applications. Sr-HAp microspheres were shown to release Sr^{2+} at a slower rate, presumably due to the rather stable nature of Sr-HAp, while the hydrogel released Sr^{2+} at a faster rate, mainly due to ionic exchange with non-gelling ions present in the medium. The magnitude of the values observed (ca. 0.3 mM released after 15 days) were in the same range of clinically relevant Sr concentrations, since upon oral administration of SrRan therapeutic (2 g per day/3 years), average serum concentrations of 0.12 mM Sr were found [12]. Importantly, the designed system is able to reach such values locally whereas in a SrRan therapeutic, the administered dosage is much higher.

Taken into account these concentrations, and considering that the amount released was only 0.3% of the total amount available, we studied *in vitro* the effect of Sr^{2+} on MSC proliferation and osteogenic differentiation and on OC formation and functionality for Sr^{2+} concentrations of 0.5, 1 and 3 mM. Although higher than the values obtained in the release studies, we believe these values would be easily achieved after implantation.

Some controversy can be found in the literature regarding the effect of different Sr^{2+} concentrations on different cell types. Although it has been generally shown that Sr^{2+} promotes MSC differentiation towards the osteoblastic lineage [13-19] and inhibits OC formation and activity [13, 19-23], the range of concentrations tested in the different studies significantly varied, ranging from 0.00625 mM up to 10 mM of Sr^{2+}. Dose-dependent effects in osteoblastic cells have been commonly reported [15, 17], however some studies showed a multiphasic effect of Sr^{2+} on osteoblastic differentiation and even deleterious effects on osteoblast mineralization for low Sr^{2+} concentrations (from 0.00625 mM to 1 mM) [16, 19]. Other studies showed a deleterious effect in human MSC osteogenic differentiation for Sr^{2+} concentrations higher than 0.1 mM [21]. Regarding OC formation and functionality, the studies performed have also used broad ranges of Sr^{2+} concentrations (from 0.1 mM to 10 mM). In some studies only higher Sr^{2+} concentrations (5 mM and 10 mM) where shown to decrease the number of adherent cells [21], while other studies have shown that at 1 mM Sr^{2+} decreased the expression of integrin $\alpha_V\beta_3$ [20] and decreased the ability of OC to resorb mineralized substrates [22]. Here the effect of Sr^{2+} amounts within the range of concentrations released from the materials was tested (0.5, 1 and 3 mM), confirming the effectiveness of such concentrations, especially 3 mM, in promoting MSC osteogenic differentiation

(ALP activity increase and mineralization,) while inhibiting PBMC adherence and OC formation and activity (decrease nuclei number, TRAP activity and mineralized substrates resorption). Importantly, the Sr-hybrid presented similar features, showing ability to promote MSC osteogenic differentiation and inhibit OC differentiation, which shows that the osteoanabolic and anti-osteoclastic activities of Sr were preserved in the system. Additional studies of gene expression would help confirming the MSC differentiation towards osteogenic lineage, as well as immunohistochemistry analysis of OC enzyme, Cathepsin K, would also further validate these results.

Another question addressed in this chapter was the *in vivo* inflammatory response to the developed material. Very few studies described in the literature address the immunomodulatory properties of Sr and consequently the information is scarce. One concern that cannot be overlooked is the fact that upon implantation of any biomaterial an inflammatory response is expected to occur. Furthermore, one promising emergent strategy in the field of tissue engineering and regenerative medicine is the development of immunomodulatory biomaterials. These should be able to modulate the immune response, for example by altering macrophage polarization, from a M1 pro-inflammatory profile to a M2 pro-regenerative one. In our work we aimed at understanding, in particular, the effect of incorporated Sr on the inflammatory response, since little information is currently available, especially regarding *in vivo* models of inflammation. Our results have shown a decrease in the number of inflammatory cells recruited to the implant site in both systems (Sr-hybrid and Ca-hybrid), as compared to sham-operated animals, but, most importantly, an increase in the number of M2 macrophages was observed in the Sr-hybrid group. These results are in agreement with other studies reported in the literature, where Sr has been shown to promote M2 polarization of macrophages [24-26]. The histological analysis revealed a thin fibrous capsule, with a non-significant difference between groups, and low numbers of inflammatory cells were observed in the implanted materials groups. In summary, although none of the systems induced a massive M1-like inflammatory response, our results indicate that Sr-hybrid system was able to promote an M2 regenerative response, when compared to the Ca-hybrid system. These results bring new insights into the emerging field of immunomodulatory biomaterials, and highlight the promising use of Sr. Future studies of the interaction of these materials with other immune cell populations would be very interesting, allowing to further understanding the immune response to this system.

On Chapter IV we aimed at evaluating the *in vivo* bone regeneration response of the developed Sr-hybrid system. For this purpose, a rat femoral critical sized defect model

was used. The material was manually injected with a conventional syringe within the created bone defect, perfectly filling it, while allowing a homogeneous distribution of the microspheres, in agreement with our previous results [5]. An advantage of our material and of major importance in clinical practice was the *in vivo* traceability using radiological imaging. In this work, microCT evaluation of new bone formation showed growth rates that are in agreement with other similar works [27, 28], with a trend to increased bone formation in Sr-hybrid materials. Histologic analysis revealed higher cell invasion at the center of the Sr-hybrid filled defects at 15 days post-implantation, with the presence of polymorphonuclear neutrophils, correlating with higher material degradation and bone tissue formation after 60 days. These results correlate with the previous ones (Chapter III), where the Sr-hybrid system promoted M2 macrophage polarization leading to a pro-regenerative milieu, which ultimately may have resulted in higher and earlier bone formation observed at the center of the Sr-hybrid filled defects. The newly formed bone developed in close contact with the material, without any fibrous interface, growing in a centripetal manner in continuity with the surrounding host trabecular bone, indicating a good integration with the host tissue. Granulation tissue with blood vessels and increased collagen deposition were observed at 60 days post-implantation in Sr-hybrid filled defects. Along this work, one of the main technical limitations was the use of exothermic methylmethacrylate embedding of bone and biomaterial samples, which allowed for the adequate sectioning, but limited immunohistochemical analysis of the samples due to the loss of immunogenicity. The use of other hard resins or endothermic methylmethacrylate embedding should be further explored in future studies.

With the use of Sr releasing systems, cardiovascular safety is of concern. Current guidelines indicate that orally administered SrRan should be avoided in patients with past or present history of ischemic heart disease, peripheral arterial disease and/or cerebrovascular disease or uncontrolled hypertension, due to an observed increase of cardiovascular events [29]. In this work, a thoroughly evaluation of Sr in excretory organs and serum samples, as well as histological evaluation of organs, including the heart, was performed. No increase in Sr levels in Sr-hybrid implanted animals was observed, at any time point in none of the studies. Serum Sr concentration in operated animals was found to be similar to non-operated and in the same range, as previously reported [30] (Chapter IV). The absence of morphological changes in histological sections of the organs suggests that Sr release was restricted to the defect site. Moreover, careful histological analysis of hearts of animals (Chapter III) did not reveal

any alteration when comparing to Ca-hybrid or non-operated animals, corroborating the safety of this osteoinductive hybrid system.

We were able to provide evidence of the promising features of this system both *in vitro* and in two different *in vivo* models. Further testing using an osteoporotic model would also bring important insights regarding the effectiveness of the material in a more clinically relevant scenario, and should be considered in future studies. However, the applicability of this material was also studied in a large animal model (Merino Branco sheep, C. Ribeiro-Machado *et al*, manuscript in preparation) where favorable results were also obtained when using the Sr-hybrid material, with functional new bone formed inside the defect.

Additionally, in another work of the group the advantages of Sr^{2+} as an antimicrobial agent have also been explored. The antimicrobial properties of Sr and the Sr-rich microspheres were evidenced towards *Staphylococcus aureus* and *Staphylococcus epidermidis* (L.M. Baptista *et al*, manuscript in preparation) highlighting the potential of the hybrid material in preventing bone surgery related infections, besides enhancing bone repair.

The developed Sr-hybrid system brings also the opportunity to incorporate other bioactive compounds. In particular, the embedding of MSC within the hydrogel is highly relevant in the field, increasing the osteogenic capacity of the material while increasing grafting of the cells to be delivered. Another very interesting possibility would be the use of co-cultures, for instance using endothelial cells cultured on top of the microspheres and MSC embedded within the hydrogel. Ideally this combination could favor the neo-vascularization of the implanted material. The versatility of the Sr-hybrid system, however, allows for the incorporation of other bioactive agents, such as growth factors, especially within the hydrogel.

One of the largest challenges facing bone tissue engineering is developing mechanically strong porous scaffolds that retain proper vascularization and host integration properties. The elastic modulus of the hybrid system is below that of cancellous bone [5]. Preliminary results of the group (ongoing studies) show that the incorporation of graphene nanoplatelets in the material significantly increases its compression strength, a strategy that is being explored in order to increase mechanical strength.

Overall our results have broadened current knowledge regarding the effect of Sr^{2+} on human MSC and human OC, along with its potential immunomodulatory properties.

The study highlights several advantages of the developed system as a potential biomaterial to be used in clinics, in bone regeneration applications. Besides providing a scaffold capable of supporting tissue ingrowth into a porous structure adequate for cell migration, the hybrid system has the ability to drive the differentiation of MSC towards the osteoblastic lineage, while inhibiting OC adhesion/fusion, activity and resorptive behaviour. This dual effect of Sr is of major interest for the therapeutic management of bone pathologies characterized by abnormal bone remodelling such as osteoporosis. The Sr-hybrid also showed to be able to modulate the immune response, inducing macrophage polarization towards a pro-regenerative phenotype. A significant advantage of the hybrid system is that it can constitute an alternative to the oral administration of Sr in the form of SrRan, providing the Sr delivery locally, surpassing systemic effects. Another innovative property of this particular injectable system is that it provides two different Sr release kinetics (from the alginate and from the microspheres) for double stimulus of bone regeneration, a feature that can be especially useful in osteoporotic conditions. Also the bactericide properties of the Sr-rich microspheres constitute an additional advantage of the hybrid, highlighting its potential to contribute to bone surgery related infections reduction. Moreover, the system can also act as a delivery system for biological agents including cells, and its degradation properties can be tuned according to the application, age of the patient and health condition, by changing the ceramic composition and the alginate characteristics, namely its functionalization.

In conclusion, this work opens excellent perspectives for the application of the Sr-hybrid system in the field of bone regeneration, both as injectable bone filling materials and drug/cell delivery matrices.

References

[1] L. Cao, G. Liu, Y. Gan, Q. Fan, F. Yang, X. Zhang, T. Tang, K. Dai, The use of autologous enriched bone marrow MSCs to enhance osteoporotic bone defect repair in long-term estrogen deficient goats, Biomaterials 33(20) (2012) 5076-5084.

[2] S.W. Cho, H.J. Sun, J.-Y. Yang, J.Y. Jung, H.J. Choi, J.H. An, S.W. Kim, S.Y. Kim, K.-J. Park, C.S. Shin, Human Adipose Tissue-Derived Stromal Cell Therapy Prevents Bone Loss in Ovariectomized Nude Mouse, Tissue Engineering Part A 18(9-10) (2012) 1067-1078.

[3] H.-Y. Liu, A.T.H. Wu, C.-Y. Tsai, K.-R. Chou, R. Zeng, M.-F. Wang, W.-C. Chang, S.-M. Hwang, C.-H. Su, W.-P. Deng, The balance between adipogenesis and osteogenesis in bone regeneration by platelet-rich plasma for age-related osteoporosis, Biomaterials 32(28) (2011) 6773-6780.

[4] Z. Wang, J. Goh, S.D. De, Z. Ge, H. Ouyang, J.S.W. Chong, S.L. Low, E.H. Lee, Efficacy of bone marrow-derived stem cells in strengthening osteoporotic bone in a rabbit model., Tissue engineering. (12(7)) (2006) 1753-1761. .

[5] N. Neves, B.B. Campos, I.F. Almeida, P.C. Costa, A.T. Cabral, M.A. Barbosa, C.C. Ribeiro, Strontium-rich injectable hybrid system for bone regeneration, Materials Science and Engineering: C 59 (2016) 818-827.

[6] M. D'Este, D. Eglin, Hydrogels in calcium phosphate moldable and injectable bone substitutes: Sticky excipients or advanced 3-D carriers?, Acta Biomaterialia 9(3) (2013) 5421-5430.

[7] S.I.J. Bidarra, C.C. Barrias, M.r.A. Barbosa, R. Soares, P.L. Granja, Immobilization of Human Mesenchymal Stem Cells within RGD-Grafted Alginate Microspheres and Assessment of Their Angiogenic Potential, Biomacromolecules 11(8) (2010) 1956-1964.

[8] S.J. Bidarra, C.C. Barrias, K.B. Fonseca, M.A. Barbosa, R.A. Soares, P.L. Granja, Injectable in situ crosslinkable RGD-modified alginate matrix for endothelial cells delivery, Biomaterials 32(31) (2011) 7897-7904.

[9] M.B. Evangelista, S.X. Hsiong, R. Fernandes, P. Sampaio, H.J. Kong, C.C. Barrias, R. Salema, M.A. Barbosa, D.J. Mooney, P.L. Granja, Upregulation of bone cell differentiation through immobilization within a synthetic extracellular matrix, Biomaterials 28(25) (2007) 3644-3655.

[10] F.R. Maia, A.H. Lourenço, P.L. Granja, R.M. Gonçalves, C.C. Barrias, Effect of Cell Density on Mesenchymal Stem Cells Aggregation in RGD-Alginate 3D Matrices under Osteoinductive Conditions, Macromolecular Bioscience (2014) n/a-n/a.

[11] K.B. Fonseca, S.J. Bidarra, M.J. Oliveira, P.L. Granja, C.C. Barrias, Molecularly designed alginate hydrogels susceptible to local proteolysis as three-dimensional cellular microenvironments, Acta Biomaterialia 7(4) (2011) 1674-1682.

[12] P.J. Meunier, C. Roux, E. Seeman, S. Ortolani, J.E. Badurski, T.D. Spector, J. Cannata, A. Balogh, E.M. Lemmel, S. Pors-Nielsen, R. Rizzoli, H.K. Genant, J.Y. Reginster, The effects of strontium ranelate on the risk of vertebral fracture in women with postmenopausal osteoporosis, N Engl J Med 350 (2004).

[13] E. Bonnelye, A. Chabadel, F. Saltel, P. Jurdic, Dual effect of strontium ranelate: Stimulation of osteoblast differentiation and inhibition of osteoclast formation and resorption in vitro, Bone 42(1) (2008) 129-138.

[14] Y. Li, J. Li, S. Zhu, E. Luo, G. Feng, Q. Chen, J. Hu, Effects of strontium on proliferation and differentiation of rat bone marrow mesenchymal stem cells, Biochemical and Biophysical Research Communications 418(4) (2012) 725-730.

[15] S. Peng, G. Zhou, K.D.K. Luk, K.M.C. Cheung, Z. Li, W.M. Lam, Z. Zhou, W.W. Lu, Strontium Promotes Osteogenic Differentiation of Mesenchymal Stem Cells Through the Ras/MAPK Signaling Pathway, Cellular Physiology and Biochemistry 23(1-3) (2009) 165-174.

[16] S.C. Verberckmoes, M.E. De Broe, P.C. D'Haese, Dose-dependent effects of strontium on osteoblast function and mineralization, Kidney Int 64(2) (2003) 534-543.

[17] F. Yang, D. Yang, J. Tu, Q. Zheng, L. Cai, L. Wang, Strontium Enhances Osteogenic Differentiation of Mesenchymal Stem Cells and In Vivo Bone Formation by Activating Wnt/Catenin Signaling, STEM CELLS 29(6) (2011) 981-991.

[18] M. Schumacher, A. Lode, A. Helth, M. Gelinsky, A novel strontium(II)-modified calcium phosphate bone cement stimulates human-bone-marrow-derived mesenchymal stem cell proliferation and osteogenic differentiation in vitro, Acta Biomaterialia 9(12) (2013) 9547-9557.

[19] D.P. Wornham, M.O. Hajjawi, I.R. Orriss, T.R. Arnett, Strontium potently inhibits mineralisation in bone-forming primary rat osteoblast cultures and reduces numbers of osteoclasts in mouse marrow cultures, Osteoporosis International 25(10) (2014) 2477-2484.

[20] R. Baron, Y. Tsouderos, In vitro effects of S12911-2 on osteoclast function and bone marrow macrophage differentiation, European Journal of Pharmacology 450(1) (2002) 11-17.

[21] M. Schumacher, A.S. Wagner, J. Kokesch-Himmelreich, A. Bernhardt, M. Rohnke, S. Wenisch, M. Gelinsky, Strontium substitution in apatitic CaP cements effectively attenuates osteoclastic resorption but does not inhibit osteoclastogenesis, Acta Biomaterialia 37 (2016) 184-194.

[22] N. Takahashi, T. Sasaki, Y. Tsouderos, T. Suda, S 12911-2 Inhibits Osteoclastic Bone Resorption In Vitro, Journal of Bone and Mineral Research 18(6) (2003) 1082-1087.

[23] S. Zhu, X. Hu, Y. Tao, Z. Ping, L. Wang, J. Shi, X. Wu, W. Zhang, H. Yang, Z. Nie, Y. Xu, Z. Wang, D. Geng, Strontium inhibits titanium particle-induced osteoclast activation and chronic inflammation via suppression of NF-κB pathway, Scientific Reports 6 (2016) 36251.

[24] X. Yuan, H. Cao, J. Wang, K. Tang, B. Li, Y. Zhao, M. Cheng, H. Qin, X. Liu, X. Zhang, Immunomodulatory Effects of Calcium and Strontium Co-Doped Titanium Oxides on Osteogenesis, Frontiers in Immunology 8 (2017) 1196.

[25] W. Zhang, F. Zhao, D. Huang, X. Fu, X. Li, X. Chen, Strontium-Substituted Submicrometer Bioactive Glasses Modulate Macrophage Responses for Improved Bone Regeneration, ACS Applied Materials & Interfaces 8(45) (2016) 30747-30758.

[26] F. Zhao, B. Lei, X. Li, Y. Mo, R. Wang, D. Chen, X. Chen, Promoting in vivo early angiogenesis with sub-micrometer strontium-contained bioactive microspheres through modulating macrophage phenotypes, Biomaterials 178 (2018) 36-47.

[27] G. Daculsi, A.P. Uzel, P. Weiss, E. Goyenvalle, E. Aguado, Developments in injectable multiphasic biomaterials. The performance of microporous biphasic calcium

phosphate granules and hydrogels, Journal of Materials Science: Materials in Medicine 21(3) (2010) 855-861.

[28] O. Gauthier, R. Müller, D. von Stechow, B. Lamy, P. Weiss, J.-M. Bouler, E. Aguado, G. Daculsi, In vivo bone regeneration with injectable calcium phosphate biomaterial: A three-dimensional micro-computed tomographic, biomechanical and SEM study, Biomaterials 26(27) (2005) 5444-5453.

[29] J.Y. Reginster, A. Neuprez, N. Dardenne, C. Beaudart, P. Emonts, O. Bruyere, Efficacy and safety of currently marketed anti-osteoporosis medications, Best Practice & Research Clinical Endocrinology & Metabolism 28(6) (2014) 809-834.

[30] M. Baier, P. Staudt, R. Klein, U. Sommer, R. Wenz, I. Grafe, P. Meeder, P. Nawroth, C. Kasperk, Strontium enhances osseointegration of calcium phosphate cement: a histomorphometric pilot study in ovariectomized rats, Journal of Orthopaedic Surgery and Research 8(1) (2013) 16.

Appendix

Licence to publish

Manuscript id:	SREP-16-45995B
Proposed title:	Injectable hybrid system for strontium local delivery promotes bone regeneration in a rat critical-sized defect model
The "Author(s)":	Ana Henriques Lourenço, Nuno Neves, Cláudia Ribeiro-Machado, Susana R Sousa, Meriem Lamghari, Cristina Barrias, Abel Trigo Cabral, Mário Barbosa, Maria Cristina Castro Ribeiro
The "Article":	All content of the article, with the Proposed title listed above, including but not limited to all text, supplementary information, tables, graphs and images.
The "Journal":	Scientific Reports

Purpose

NPG will consider publishing the Contribution pursuant to the terms set forth herein, including granting readers rights to use the Contribution on an open access basis identified below.

Open access licence

Licence is preferred by many research funding bodies. We support use of this licence as it is recommended for maximum dissemination and use of open access materials.

Grant of rights

In consideration of NPG evaluating the Contribution for publication (and publishing the Contribution if NPG so decides) the Author(s) grant to NPG for the full term of copyright and any extensions thereto, except as set out in the Author rights below, the right and irrevocable licence:

a. to edit, adapt, publish, reproduce, distribute, display and store the Contribution in all forms, formats and media whether now known or hereafter developed (including without limitation in print, digital and electronic form) throughout the world;
b. to translate the Contribution into other languages, create adaptations, summaries or extracts of the Contribution or other derivative works based on the Contribution and exercise all of the rights set forth (a) above in the translations, adaptations, summaries, extracts and derivative works;
c. to licence others to do any or all of the above, including but not limited to the right to grant readers the right to use the Contribution under the Creative Commons licence listed above; and
d. to re-licence article metadata without restriction (including but not limited to author name, title, abstract, citation, references, keywords and any additional information, as determined by NPG).

Author rights

Ownership of the copyright in the Contribution remains with the Author(s).

However, the Author(s)' re-use rights in the Contribution are subject to the rights and restrictions set forth in this Section, and in the Pre-print services and Warranties a) Section. After the Author(s) have submitted the Contribution to NPG hereunder, the Author(s)' rights to re-use the Contribution shall be the same as those set forth in the Creative Commons licence listed above, with the following additional re-use rights:

a. to reproduce the Contribution in whole or in part in any printed volume (book or thesis) of which they are the Author(s); and
b. to reuse figures or tables created by the Author(s) and contained in the Contribution in oral presentations and other works created by them.

Pre-print services

NPG acknowledges that an earlier version of the Contribution may have been submitted to a pre-print service (in accordance with that service's standard licence terms).

Warranties

The Author(s) warrant and represent that:

a. the Author(s) are the sole Author(s) of and sole owners of the copyright in the Contribution and the Contribution is the original work of the Author(s) and not copied (in whole or part)

from another work. If however the Contribution includes materials from other sources, the Author(s) warrant they have obtained the necessary rights from the owners of the copyright in all such materials and hereby license to NPG the rights to use such materials in accordance with the Grant of rights Section above. Copies of all such grant of rights from third parties have been submitted.

b. all of the facts contained in the Contribution are true and accurate;
c. the signatory (the Author or the employer) who has signed this Agreement below has full right, power and authority to enter into this Agreement and grant the rights herein on behalf of all of the Authors;
d. nothing in the Contribution is obscene, defamatory, libelous, violates any right of privacy or publicity, infringes any intellectual property rights (including without limitation copyright, patent, database or trademark rights) or any other human, personal or other rights of any person or entity or is otherwise unlawful; and
e. nothing in the Contribution infringes any duty of confidentiality which any of the Author(s) may owe to anyone else or violates any contract, express or implied, of any of the Author(s), and all of the institutions in which work recorded in the Contribution was created or carried out, have authorized such publication.

Dispute resolution

The Author(s) authorise NPG to take such steps as it considers necessary at its own expense in the Author(s) name and on their behalf if NPG believes that a third party is infringing or is likely to infringe copyright in the Contribution including but not

limited to initiating legal proceedings.

The Author(s) grant NPG the perpetual right to edit, correct, or retract the Contribution if NPG considers (in its reasonable opinion) that such actions are required. The Author(s) hereby agree that they shall not object to NPG carrying out any such actions.

The Author(s) shall cooperate fully with NPG in relation to any legal action that might arise from the publication of the Contribution and the Author(s) shall give NPG access at reasonable times to any relevant accounts, documents and records within the power or control of the Author(s).

Reversion of rights

If the Contribution is rejected by NPG and not published, all rights under this licence shall revert to the Author(s).

Law & jurisdiction

This Agreement shall be governed by and construed in accordance with the laws of England and Wales. The parties irrevocably agree that the courts of England and Wales shall have exclusive jurisdiction to settle any dispute or claim that arises out of or in connection with this Agreement or its subject matter or formation.

Macmillan Publishers Limited (trading as Nature Publishing Group), registered office: Brunel Road, Houndmills, Basingstoke, Hampshire, RG21 6XS, UK. Company number 785998.